Multi-Continental Multimedia Model of Pollutant Intake and Application to Impacts of Global Emissions and Globally Traded Goods

by

Shanna Shaked

A dissertation submitted in partial fulfillment
of the requirements for the degree of
Doctor of Philosophy
(Applied Physics)
in The University of Michigan
2011

Doctoral Committee:

Associate Professor Olivier J. Jolliet, Chair
Professor Gregory A. Keoleian
Professor Mark E. Newman
Professor Richard B. Rood
Research Scientist Manuele Margni, Polytechnique Montreal

2011

To my givers of life and partner in life

For planting the seed and helping it flourish

ACKNOWLEDGEMENTS

This work inspired passion in me because of its application of science in the direct interest of people, and I have many people to thank for inspiring, educating, and enhancing those passions.

This is my chance to permanently acknowledge and thank all the people that have taught me, classmates that have helped me learn, and friends that have made the process along the way so enjoyable. So I have to begin by giving my most sincere thanks to the person who has been all three of these to me, my partner in life, Jasper Shok. As my graduate instructor, he had a lot to teach me despite only being two months older. As my classmate, we had the perfect level of collaboration (with just a little competition). And as my partner, he always expressed his overarching confidence in my ability to complete this work. He is truly mijn rots in de branding.

I always have the sincerest of gratitude for my advisor, Olivier Jolliet. When I first met Olivier the physicist, he had a colorful tie and he talked quantitively about how to maximize happiness through sustainable consumption – how could I not work with such a man? His level of energy, enthusiasm and constant stream of ideas is unmatched in anyone else I've ever met, and even while ill he easily outlasted our entire group during a particularly long group meeting. He is extremely driven, and yet recognizes that life is here to be enjoyed. I am so grateful just to have been able to spend so much time working and interacting with such an admirable presence.

Of course, sometimes Olivier's enthusiasm gets the better of him, so I would also like to thank my committee members, Manuele Margni, Greg Keoleian, Ricky Rood, and Mark Newman, for sometimes bringing things back down to Earth.

I would also like to thank all the previous professors who have mentored me as I developed research and scientific skills. Bill Currie, in particular, helped me achieve my initial dream of combining physics with environmental studies, and forests will never

look the same after our work together. In addition, I would like to thank John Bieging and Brian Talbot.

In working with Olivier, I soon discovered that he had a knack for attracting other people as idealistic (and quirky) as himself, so I need to thank my many collaborators and colleagues that I have met through him. First, I always have to remind myself that I've only met Damien Friot once in person, since our regular skype conversations always make me feel otherwise. I am very grateful to him for patiently spending endless hours explaining the economic aspects of his models and never seeming to get frustrated. (I'm sure he did sometimes, but he hid it well over skype.)

I thought that Olivier's energy was unmatched… until I met Sebastien Humbert. His tireless passion for life cycle assessment (and everything else actually) make him a joy to work with. Manuele Margni is another 'Jolliet groupie' with his very own form of passionate dedication (it generally involves a lot of smiling, not sleeping, and working on his laptop in hotel lobbies). In addition to teaching me about carbon offsets for kids, he also explained the many ins and outs of the IMPACT model. Finally, Ralph Rosenbaum who rounds out the core IMPACT crew, taught me about bioaccumulation, and always demonstrated his commitment to the environment by getting every last drop out of any container.

I'd also like to thank Rima Manneh, Julia Steinberger, and (the delightful) Cecille Bulle for their fruitful interactions.

The local iMod squad was also a great group of people to work with. Cedric Wannaz was always happy to explain how to invert a sparse matrix (even if not asked), and we had much fun insulting one another. He has been a true friend and a fun(ny) officemate. I have also greatly enjoyed collaborating and sharing the office with Gabrielle Soucy, Roel Helmes, Peter Fantke, Anne Asselin, and Andrew Henderson, who always provided thought-provoking research questions and wonderful lunch conversations. Meghan Milbrath (a CLW) was one of the original iMod members, and she has injected fun throughout my grad school time, and most importantly, taught me the wonderfulness of Nichols Arboretum.

The Applied Physics program is an amazing program that has been wonderful and perhaps essential for me to complete my degree. Their flexibility in research and

coursework and recognition of the benefits of applying physics backgrounds to unconventional topics is so rare that I have never regretted my decision to come here. Brad Orr was an approachable program head, while Cyndi and Charles were happy to help at any point and always welcomed you to the office.

Applied Physics also had this wonderful ability to bring together amazingly smart and fun people. Chris Kelly, Katherine Truex, Divine Kumah, Jeff Herbstman, Abigail Mechtenberg, Craig Tenney and Nicole Campbell were all interesting and thought-provoking officemates (as well as great ping pong combatants!). But I also strayed into the 'real' physics realm and had the pleasure of working (and playing) with Brian Nord, Alejandra Castro, and Brian MacFarland. I'm especially grateful to Brian and Jeff for their extra encouragement (and bad jokes).

I am lucky to have had many peers that turned out to be great friends. And I consider these friendships made in graduate school comparable (if not greater) in value to the scientific endeavor known as a dissertation. Fun times with Chris Kelly, Katie Kelly (honorable applied physics-er), Pascale Leroueil (wishes she could be an applied-physicser), Shokelleroueil, Brian, Alejandra, Katherine and Beau Truex, and Leon Webster will never be forgotten, and neither will the fun times shared at Barton, Eberwhite, Kraushaus, playgrounds, Euchre nights, buckyballing, camping trips, climbing walls, and pretty much anywhere we found ourselves. Whether trying to figure out the science behind a natural phenomenon or debating things we knew nothing about, these were the funnest physicists I know.

Fortunately, I managed to form a few non-nerdy friendships and cling to those for dear life. Yes, we had to sometimes explain what "an n of 1" means in general conversation, but we also got to learn all about art, social work, 'institutionalized heterosexuality', the fact that people can get a whole degree in musicology, and much more. Eva Leventer was the swing dancing seed from which sprouted the friendships with Lydia Hanson, Sarah Gerk, and Elaine Denny (with some help from Leon), who are all amazing people that do such admirable work (even if they're not scientists…).

In my time as a graduate student, I got to share housing with many different people (often paying with not much more than work and smiles). Thanks so much to Rima, Ralph, Pablo Tirado, Manuele, and CIRAIG for 'housing' me in Montreal for two

months. Thanks to Sebastien and his wonderful family for hosting me as we worked in the Swiss mountains with beautiful (if rare) views of Mont Blanc. And thanks to Pascale, Jessie, Paul, Brian, Nicholas, Le, and Ajay for hosting me during my homeless year in Ann Arbor. The ‘quaint’ basements you provided offered strong motivation to go to my clean, warm, spider-free office.

Also, I need to thank a local Boulder doctor who reassured me that I was in fact NOT getting carpal tunnel two weeks before my thesis was due.

To wrap up the wonderful set of collaborator/friends/great people, I would like to thank Sherri (what-the-)Heck for so much more than I often remember. She was an original inspiration for combining science with concerns for people, and trying to be as silly as possible along the way. She made me a more confident, colorful, confiding, and most importantly, happier person. And she brought me hand sanitizer and chapstick when I needed it most. Sherri’s work was continued by Pascale Catherine Raymond Marie Leroueil, who is precious in far too many ways than can be listed here. She has given me so much in all aspects of my life – food, shelter, conversation, advice, comfort, and of course lots of fun. Finally, thanks to Topher for always being surprising.

My life was further enriched by managing to find a wonderful adopted family in the blunt, teasing, easily-excited Koks – Marijke, Peter, Diederik, Wouter, Evelien, Inge, Gerwin, Kalle and Sverre. They are truly a super-leuk family and I’m so lucky to have married into them. I’d also like to thank them for letting me keep their son over Christmas 2010. Jullie zijn allemaal super geweldig! Donderdag!

I will end where it all started – with my family and its perfect representation of the dual aspects of this thesis. My dad encouraged me in math and science for as long as I can remember, with regular dinner conversations about the probability of having two people with the same birthday in a classroom. He once spent a whole summer going with me to the mall just to teach me math – and I thought it was a blast! But my mom provided the human element to everything. She has an unending passion for all her kids and an enthusiasm that cannot be stopped. Analagous to my parents, my brother provided regular intellectual stimulation, perfect rationality, and someone to always try to live up to when my teachers would say “Oh, you’re Tal Shaked’s sister. Wow, he was an amazing student.” Thanks Tal, that was great… He also never tried to hide his nerdiness or ‘fit in’

for arbitrary reasons, which is a quality I always admire (and which managed to help him snag a wonderful and caring wife, Carrie Gomez Shaked). Although my brother is amazingly smart, my sister Lila has more street smarts than everyone in my family combined. Anywhere in the world that you drop her, she will find her way out and she will have a blast along the way. She taught me how much you can learn by operating a boat in Maui, and she is a constant reminder that the present is something to be enjoyed. And now she can finally stop asking “Wait – you’re STILL not done with school?!”

TABLE OF CONTENTS

LIST OF FIGURES

LIST OF TABLES

LIST OF APPENDICES

GLOSSARY OF IMPORTANT TERMS

Characterization factor (CF): expresses the impact of an emitted pollutant (in kg of the category's reference substance per kg of substance emitted).

DALYs: disability-adjusted life years, equivalent to the sum of years of life lost and years of life disabled.

Endpoint damage category: midpoint impact categories can be grouped by area of protection (human health, ecosystems health, resources, climate change) into endpoint damage categories, which are easier to interpret but more uncertain than midpoint impacts.

Effect factor: relates the quantity taken in by a population to the adverse effects of the pollutant.

Exposure: concentration or quantity of a substance taken in by a person or population.

Fate: links the pollutant emission to its resulting mass in the environment.

Functional unit: the common unit representing the function of the system (the offered service), serving as the basis for scenario comparison

Human toxicity: measure of the damage to human health to to intake of toxic pollutants, a midpoint impact category in life cycle impact assessment

Impact assessment: general term referring to the evaluation of the environmental impacts of emissions.

Input-output LCA: LCA based on sector spending and emissions associated with monetary flows.

Intake fraction: population intake of a given substance as a fraction of total mass of substance emitted.

Life Cycle Inventory analysis: phase of life cycle assessment involving the compilation and quantification of inputs and outputs for a product throughout its life cycle (ISO, 2006)

Life Cycle Assessment (LCA): compilation and evaluation of the inputs, outputs and the potential environmental impacts of a product system throughout its life cycle (ISO, 2006).

Life Cycle Impact Assessment (LCIA): phase of life cycle assessment aimed at understanding and

evaluating the magnitude and significance of the potential environmental impacts for a product system throughout the life cycle of the product (ISO, 2006).

Midpoint impact category: groups the impacts of different chemicals according to their effects in 10-15 different categories, such as global warming, human toxicity, and eutrophication. Cause-effect modeling is used to estimate the contribution of each chemical emission to each impact category. These midpoint impacts are usually expressed as equivalent emissions of a selected reference chemical for each category.

Multimedia model: model describing pollutant fate in multiple environmental media.

Process LCA: LCA based on individual processes over entire life cycle.

Risk assessment: evaluates the hazard, exposure and dose-response of an emission in a systematic approach to estimate the probability of specific harm to an exposed individual or population.

ABSTRACT

Decision-makers seeking to more comprehensively assess and mitigate the environmental health impacts of products and chemicals require a tool to quantify the impacts associated with global emissions, global supply chains, and global food trade. To be effective, this tool needs to include pollutant fate in multiple environmental media, cover multiple exposure pathways accounting for trade of pollutant through food, and account for high exposure intensity areas and transboundary transport, all while minimizing computational needs.

This thesis thus develops IMPACTWorld, the adaptation of a multimedia model to a global scale that accounts for trans-boundary transport and urban exposure. I use IMPACTWorld to calculate the regional intakes of ingestion-dominant polychlorinated biphenyl-118 (PCB-118) and inhalation-dominant fine particulate matter ($PM_{2.5}$). I then analyze spatial differences in the intake fraction (iF), which is the fractional population intake of each regional emission. $PM_{2.5}$ iFs are dominated by local urban exposure, whereas transboundary transport of the more persistent PCB-118 leads to substantial portions of the pollutant ingested outside the region of emission. This model helps to further bridge the fields of life cycle assessment and risk assessment by calculating impacts from both the emitter and receiver perspectives.

I then add a component to IMPACTWorld that accounts for pollutant economic fate through trade of food and feed. By applying the expanded model to two pollutants that bioconcentrate differently in food and have different global emissions patterns, I find that food exports can substantially alter the absolute pollutant regional intake

Finally, IMPACTWorld is combined with an economic model of global trade to yield the first spatially-explicit integrated model describing the full causal chain from consumption to impacts. The results for $PM_{2.5}$ suggest that the majority of the PM-related health impacts induced by consumption in developed countries occur outside their borders, mainly in Asia.

In summary, this thesis reveals new insights into impacts associated with environmental pollutant transport, pollutant transport through food, and “virtual” export of pollution through global trade. It thus provides a motivation and foundation for further exploration of the significance and contribution of these impact mechanisms in the assessment of a product or emission.

CHAPTER 1

Introduction

1.1 Motivation: the need to understand globally-distributed impacts of pollutants

1.1.1 Health impacts of pollutants

The release of chemicals and pollutants into air, water and soil has substantial and detrimental impacts on human health. Exposure to such pollutants can substantially increase the risk of a variety of health impacts, including cancer, neuropsychiatric disorders, perinatal conditions, and cardiovascular disease (Mattison, 2010; Pruss-Ustun and Corvalan, 2006; Schantz et al., 2003). Outdoor air pollution, for example, is estimated to be responsible for 800,000 deaths per year, causing 1% of respiratory infections, 5% of the lung cancer disease burden, and 2% of the global cardiopulmonary disease burden, as well as exacerbating asthma and increasing the rates of low-birth-weight infants and congenital anomalies (Ostro, 2004). Currently, more than 100,000 species of harmful chemicals and pollutants have been documented in the environment, which range over 12 orders of magnitude in their toxicity (Rosenbaum et al., 2008). Yet the resulting impacts on human health are difficult to compare between pollutants due to the differences in environmental fate, intake, and toxicity mechanisms.

1.1.2 Emissions associated with goods and global trade

The manufacturing, use and disposal of goods and services result in many substance emissions that cause adverse health effects (e.g., Breivik et al., 2002a; Buzby, 2003; Ruchirawat et al., 2008; WHO, 2008). When seeking more environmentally benign products, analytical tools are needed to consider the many ramifications of the different

options. In particular, tools are needed to quantify differences in environmental health impacts and identify the key parameters influencing these impacts.

With increasing globalization, any such analytical tool to quantify the impacts of products needs to cover impacts over the entire global supply chain, since many goods are produced outside the region where they are consumed (Bolisani and Scarso, 1996; Hammami et al., 2008; van den Bergh and Verbruggen, 1999). As a consequence of these increasingly global supply chains, emissions associated with manufacturing are "virtually" exported to other regions, and result in as yet unquantified impacts that can be disproportionate to economic compensation in producing versus consuming nations (Peters and Hertwich, 2006; Streets et al., 2003; Tisdell, 2001). The environmental situation in Western countries has generally improved since the 1960s, whereas it has worsened in much of Asia (Streets et al., 2003), which generally has higher population densities at risk of exposure to the pollution. This has contributed to such phenomena as the Asian brown cloud, which is estimated to cause 180,000-490,000 excess deaths per year (Ruchirawat et al., 2008).

1.1.3 Characterizing the impacts of globally distributed products and emissions

Addressing these health impacts due to global emissions and products requires accounting for the following three factors.

(i) First, emission intensities for different industrial processes vary by the location of emission (Friot, 2010a; Steinberger et al., 2009) due to differences, for example, in filtering technology, electricity mix, or technological efficiency. This, combined with many other regional variations in industrial, use and disposal activities, leads to varying emissions by region (Breivik et al., 2007; Kazerouni et al., 2001).

(ii) Second, health impacts due to toxic emissions often depend on the region of emission and subsequent environmental transport. For an emission that does not live long enough to become uniformly globally distributed, the fate and impacts can vary widely with the location of emission, due to such factors as varying wind speeds, agricultural intensities and population densities exposed (Rochat et al., 2006). Moreover, through long-range transport, these and other emissions can result in impacts distant from the pollutant source (Liang et al., 2007; Macleod et al., 2005).

(iii) Third, food trade can transport pollutants between regions. The "virtual" export of manufacturing emissions and the long-range transport of pollutants are not the only methods of pollutant transboundary transport. Since food is a dominant exposure pathway for many persistent pollutants (Liem et al., 2000; UNEP, 2003; Wang and Needham, 2007), the increase in global food trade (FAO, 2000) can act to increase pollutant transport through food. The FAO estimates that approximately 11% of food is exported from the country of production, thus food trade can provide a vector for long-range transport of pollutants comparable to that of long-range atmospheric transport.

1.1.4 A tool is needed to quantify all of these impacts

In summary, to address the increasingly global distribution of pollutants, decision-makers aiming to minimize health impacts need a tool to quantify and better understand the impacts associated with global emissions, global supply chains, and global food trade. Due to the potentially large number of pollutants involved in pollutant regulation, this tool should be easily and quickly applicable to a range of pollutants and scenarios to perform a screening or comparative assessment. After reviewing existing tools below, I outline the main objective of this thesis: to address deficiencies in current tools and thereby create and apply a tool that quantifies globally-distributed impacts.

1.2 Current tools available to estimate impacts of pollutants

1.2.1 Broad overview of tools

Several different tools are used to assess impacts for policy and decision making based on the breadth of impacts, pollutants, and spatial and time scales desired (Wrisberg and Udo de Haes, 2002). For example, preliminary evaluations of technological systems can be based on concepts such as life cycle thinking (qualitative consideration of the whole life cycle of a good), or environmental design (consideration of environmental parameters when designing a good). However, the drawback of these tools is that they generally provide qualitative, not quantitative assessments. To overcome this problem,

different end-users are increasingly using more quantitative procedures and tools to support decision-making.

Many end-user tools rely on quantified analytical methods such as substance flow analysis, risk assessment, and Life Cycle Assessment (LCA), which differ mainly in the focus of the analysis. Substance flow analysis quantifies flows and reservoirs of a given substance (e.g., lead) or of a group of substances (e.g., inorganic nitrogen compounds) for a given region and time duration (Brunner and Rechberger, 2004). In contrast, risk assessment, which evaluates the hazard, exposure and dose-response of an emission, is a systematic approach to estimate the probability of specific harm to an exposed individual or population (NRC, 1994). Finally, the focus of LCA is to relate environmental and health impacts to the function of a product over its whole life cycle, from cradle to grave, considering a wide range of pollutants and impacts. In this way, the environmental burden of a product can be minimized by ensuring that problems are not shifted between life cycle stages and pollutant impacts. Because of this broad application, the results are more comprehensive but with higher uncertainties (discussed in more detail below). As these analytical tools are all based on common elements, such as mass balance and multimedia modeling, LCA developments are generally performed in collaboration with specialists from the other domains described above.

In the context of global products and emissions, LCA is the tool with the most potential for estimating global impacts of multiple pollutants over multiple types of impacts. It can be applied to spatial scales greater than those intended for risk assessment and environmental impact assessment, which are more site or application specific, and it considers the impacts of all parts of the life cycle and production chain. To perform a comprehensive assessment, an LCA considers impacts from a large number of pollutants (in contrast to, for example, a carbon footprint calculation), allowing the consideration of local air pollution impacts as well as global indirect impacts such as climate change.

Thus, LCA has the potential to be applied over the entire global production chain and life cycle, in a manner that allows policy-makers and industries to determine how to meet consumer and population demands most environmentally sustainably. However, several adaptations are still necessary to perform life cycle assessment on a global scale, and these are described below.

1.3 Life cycle assessment from emissions to impacts in a global context

Having reviewed above the potential of the life cycle approach to quantify globally distributed health impacts, this section summarizes the basic stages of a life cycle assessment, focusing on the specific methods relevant to assessing human health and global impacts. An LCA is usually performed in four iterative stages: goal definition, inventory, impact assessment, and interpretation (ISO, 2006). The first stage, goal definition, defines the product or system function and the functional unit to which emissions will be related, as well as the boundary of the system that meets this function. The next stage in LCA is the inventory, which lists the resources extracted and pollutant emissions to air, water, and soil for all the processes needed to achieve this functional unit. The third stage, impact assessment, estimates the environmental impacts of these emissions. And finally, the interpretation identifies key processes and pollutants, performs sensitivity, uncertainty and cost-benefit analyses, and can assess the improvement potential.

The calculation of globally-distributed impacts requires global emissions inventories (addressed by the second stage) followed by adaptation of the impact assessment methodology for global application (third stage and main focus of the this thesis). Thus, we review the inventory and impact assessment stages in more detail below, focusing on the potential application in a global context.

1.3.1 Inventory of emissions, resource use and extractions in a global context

The system boundary of an LCA encompasses all processes needed to achieve the desired function, and the inventory stage aims to quantify all emissions associated with these processes (ISO, 2006). This latter stage/step can be achieved using one of two approaches, both of which are used in this thesis. The first approach is the the process-based approach, which accounts for all direct processes involved. For example, the process-based inventory of a T-shirt would include not only the emissions associated with the energy used to sew the T-shirt, but also the emissions associated with energy use to wash and dry the shirt. Moreover, when data is available, the process-based approach also accounts for so-called background processes necessary to the direct processes, such as

manufacturing the sewing machine used to sew the T-shirt. To estimate the inventories associated with such such background processes, LCA experts have created large inventory databases, such as the ecoinvent database (Weidema et al., 2009), but these databases still miss many background processes that may ultimately contribute a large portion of emissions.

For many applications, especially services, it is difficult to assess which processes are negligible and which processes produce substantial impacts. For example, what are the main causes of impacts for hotels or banks? One way to ensure that all relevant processes are included is to use a method known as Economic Input-Output Life Cycle Assessment (IO LCA**)** (Hendrickson et al., 2005). Rather than using physical fluxes, IO LCA inventories the monetary fluxes between different economic sectors involved in the production chain for a given product, process or activity. Each sector is then studied to determine the resource extraction and pollutant emissions associated with each dollar spent in this sector. This method accounts for the entire economy of a country or region by dividing it into sectors or products. Since the expenditure of each sector on all other sectors is included, it is possible to exhaustively describe the chain of suppliers needed for a given service, and therefore the associated emissions and environmental impacts (Matthews et al., 2002). The disadvantage compared to process-based LCA is that IO-LCA is not able to differentiate products from the same sector (e.g., it is not able to distinguish a shirt from a pair of jeans), and it has little spatial resolution. As an indicator of the uncertainty in these values, the US Toxic Release Inventory data shows that certain pollutant discharges can vary by more than a factor of 10 among US oil refineries (Matthews et al., 2002), but this uncertainty will vary greatly depending on the substance and industry considered. Both methods of inventorying emissions have the limitation of depending on the allocation method and functional unit chosen (Bare, 2006).

The concept of inventorying emissions throughout the life cycle of a product is essential to consistently capturing impacts of many products and services (Norris et al. (2002) find that far-removed background processes can account for roughly half of total supply-chain emissions for many products), and this deserves particular attention for items with global supply chains. Since pollutants are emitted in many different phases of a product's life cycle, some supposed improvements may merely displace the impacts to

another part of the product's life cycle. For example, a building constructed using less insulation than average will have lower emissions during its manufacturing phase, but the additional air conditioning and heating required would shift emissions to the use phase, which could lead to an overall higher impact. With global trade, such displacements can occur not only between different phases, but also between different countries and continents. This changes not only the location but also the quantity of emissions due to the wide ranges in environmental standards and implementation of emission reduction technologies.

Despite the importance of global emissions data, there are currently no comprehensive global databases that inventory location-specific processes. Indeed, most processes in existing databases are based on emissions data from Europe, although databases are beginning to incorporate processes from other countries, such as the U.S. However, potential steps are available to globalize inventories, including adapting the large existing European-based databases to the country of interest by introducing the appropriate electricity grid mix and possibly substituting this mix for all background processes. A second option is to use generic data to first identify the key processes and then gather site-specific data for these key processes. A third option is to apply region-specific linked Input-Output matrices that characterize trade between countries related to the supply chain of products. In the context of the present work, both process LCA databases (for the specific case of a globally traded T-shirt in Chapter 2) and regionalized Input-Output databases (Chapter 4) have been applied.

1.3.2 Life cycle impact assessment in a global human health context

Inventories are useful for comparing the environmental emissions of different products, but are not sufficient to compare, for example, one product that has more lead emissions to another with more formaldehyde emissions. In contrast, impact assessment estimates the environmental and human health impacts associated with multiple emissions, such that the impacts can then be compared among different pollutants. Quantifying these impacts can aid regulators in deciding among options that have very different pollutant emissions.

Many different methods of impact assessment exist (the main methods are listed in Table 1.1), all of which share a common design. They divide impacts into so-called midpoint impact categories (e.g., global warming, human toxicity, and other categories listed as rows in Table 1.1) and use models to estimate the contribution of each chemical emission to each of these midpoint impact categories. The midpoint impact categories can be grouped by "areas of protection" into endpoint damage categories (human health, ecosystem health, resource consumption, climate change) (Jolliet et al., 2003; Pennington et al., 2004).

Table 1.1 Summary of the main life cycle impact assessment methodologies and the midpoint and endpoint categories addressed by each one.

	LCIA METHODOLOGIES[a]					
	EU LCIA[b]	**CML-IA Handbook**	**IMPACT 2002(+)**	**ReCiPe**	**SWISS ECO-SCARCITY**	**TRACI**
Midpoint Impact Categories						
Human toxicity (listing model used in methodology)	USEtox 1.0	USES-LCA version 2.0	IMPACT 2002	USES-LCA version 2.0	Policy targets	CalTOX 4.0
Global warming, Ozone depletion, Photochemical ozone creation, Acidification, Eutrophication, Ecotoxicity, Resource consumption	x	x	x	x	x	x
Ionizing radiation, Land Use	x	x	x	x	x	
Endpoint Damage Categories						
Human health, ecosystem health, and natural resources	x		x	x		
Source of methodology	(Hauschild)	(Guinee et al., 2002)	(Jolliet et al., 2003)	(De Schryver et al., 2009)	(Brand et al., 1998)	(Bare et al.)

[a]The following website describes all methodologies in greater detail, http://www.netzwerk-lebenszyklusdaten.de/cms/content/site/lca/Home/Aktivitaeten/LCIAcorner/LCIAmethods, except EU LCIA, which is described at http://lct.jrc.ec.europa.eu/international-reference-life-cycle-data-system-pre-version-1/documents-preversion/ILCD-Handbook-Requirements-for-LCIA-models-Pre-version-of-Draft-for-public-consultation.pdf/view. For a detailed description of each impact category, see the corresponding source of methodology (listed on last row).
[b]EU LCIA is not actually an LCIA methodology, but is a compilation of recommended best practices per impact category.

Two of the main midpoint impact categories contributing to human health damage are the human toxicity and respiratory effects categories, which comprise the main focus of the impacts discussed in this thesis. As described in more detail below, the framework

to calculate human toxicity and respiratory effects estimates the damage to human health due to intake of toxic pollutants. This framework thus has the potential to address my goal of quantifying the health impacts associated with emissions and trade. A given emission can have varying levels and spatial distributions of human toxicity and respiratory effects, depending on the emission region, substance persistence and environmental transfer (Rochat et al., 2006). This has led to the development of spatialized human toxicity impact assessment models (e.g., Humbert et al. (2009)), but no established global model is available[*].

The other midpoint impact categories often related to human health damage are global warming, ozone depletion, photochemical ozone creation, and ionizing radiation, all of which are not addressed here for the following reasons. First, the objective here is to quantify the link between globally-distributed emissions and globally-distributed impacts, which is not relevant for the case of global warming or ozone depletion. These categories have impacts that vary by region (De Schryver et al., 2009; Struijs et al., 2010) but that are independent of the emission location. The impacts from photochemical ozone creation do vary by region and depend on the emission location, but are beyond the scope of the present work (due to the complications with background concentrations). Finally, ionizing radiation, caused by high radioactive waste and radionuclide emissions from nuclear power plants, has primarily local emissions and is not considered here.

Human toxicity models use a cause-effect framework capable of linking a large set of emissions (often covering thousands of pollutants) to their ultimate impacts in a consistent manner. The simplest versions are one-box models with a few key environmental parameters defined (Rosenbaum et al., 2008), but other factors such as background concentrations (in the case of eutrophication) and spatial differentiation can also be considered (Pennington et al., 2005). Fig. 1.1 shows a schematic of the cause-effect steps modeled to estimate the impacts of a given emission on human health and aquatic ecosystems (shown to demonstrate the consistent manner in which different types of impacts are calculated). To assess the human toxicity resulting from eventual intake of a given pollutant emission, a pollutant "fate factor" links the quantity released into the environment to the chemical masses or concentrations in a given compartment (i.e., air,

[*] Spatial impact assessment models are reviewed in more detail in Section 1.5

water, or soil), followed by an "exposure factor" that relates the amount found in a given environmental compartment to the chemical intake by humans (Jolliet et al., 2003; Rosenbaum et al., 2007). The intake fraction is the fraction of the total emitted pollutant mass that is eventually inhaled or ingested by a population, and it is commonly used to describe the emissions-to-intake relationship (Bennett et al., 2002a):

$$iF = \frac{\sum_{\text{people, time}} \text{intake of pollutant by an individual } (\text{kg}_{\text{in}})}{\text{mass released into environment } (\text{kg}_{\text{emit}})} \qquad 1\text{-}1$$

To complete the cause-effect model, the intake fraction can be multiplied by an "effect factor" to result in a "characterization factor" which estimates the resulting disease severity or years of life lost per kg emission. It is important to note that, because life cycle assessment is applied to marginal increases in emissions associated with products or services, each link in the cause-effect chain is assumed to have a corresponding marginal increase (i.e., all responses in the models are linear) (Pennington et al., 2004).

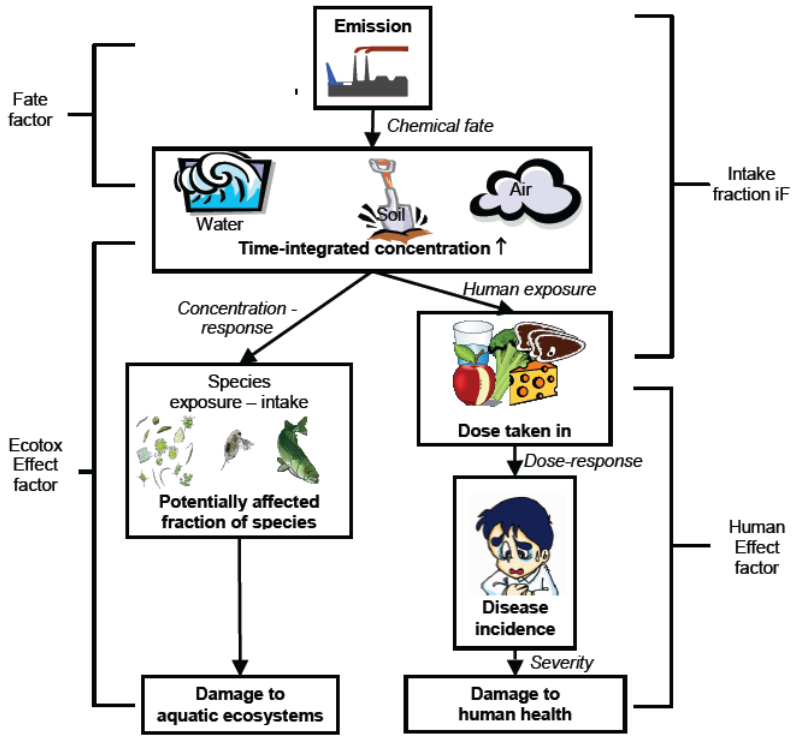

Fig. 1.1 Chain showing the cause-effect steps for human and eco-toxicity in life cycle impact assessment (adapted from Jolliet et al. (2003)

The final human toxicity midpoint impact can be expressed as equivalent kg of a reference substance (e.g. IMPACT 2002+ uses equivalent kg of chloroethylene emitted to air). Some methodologies, such as IMPACT 2002+, extend this to a human health endpoint damage in units of Disability-Adjusted Life Years (DALYs), which are the sum of the years of life lost and years of life disabled (as defined by the World Health Organization (WHO, 2008)).

Life cycle impact assessment can have many limitations and uncertainties depending on the model used. Virtually none of the models include the spatial and temporal detail needed to accurately assess absolute impacts, such as accounting for background concentrations, thresholds, stack heights, or emission release timing. This particularly limits the quantification of impacts that vary by emission region and extend over large areas (Bare, 2006), as discussed above. To indicate the magnitude of this uncertainty, Pennington et al. (2006) estimate that a model predicting an average European characterization factor of a benzo[a]pyrene emission would have an uncertainty around a factor 37 (this is the sum of the factor 12 uncertainty in average intake fraction estimates from Hofstetter (1998), the factor 10 uncertainty based on the where the European emission occurs, and the factor 15 uncertainty in effect factor). Estimates of human impacts due to non-cancer effects compared to cancer effects may further increase this uncertainty (Pennington et al., 2006).

1.3.3 Pollutants relevant for the proposed tool and impact categories

Each step of the cause-effect chain in Fig. 1.1 can yield vastly different results depending on the persistence, bioaccumulation, and toxicity of the considered pollutant. Since the focus of the proposed tool is on human toxicity and respiratory effect midpoint categories, pollutants considered here are relevant to these categories on regional and global scales. To address the ingestion exposure pathway on regional to global scales, a persistent pollutant should be addressed, such as polychlorinated biphenyl-118, with relatively long degradation half-lives in air, water and soil (about 30, 320, and 790 days, respectively), and a relatively high bioconcentration in fish (described in detail in Chapter 2). This can be compared with a shorter-lived pollutant that will be less influenced by

transboundary transport, such as benzo[a]pyrene, which has half-lives of 30 minutes, 2 days, and 540 days in air, water and soil, respectively, and bioconcentrates mostly in produce (described in detail in Chapter 3). Finally, an inhalation-dominant pollutant should be examined, such as particulate matter, which remains in the air for approximately 1-20 days, and thus has the potential for transboundary transport (Liu et al., 2009a) (described in detail in Chapter 2). This model is irrelevant for very long-lived pollutants, such as carbon tetrachloride, since these will become well-mixed in the atmosphere, thus their impacts will be independent of emission location.

1.3.4 Interpretation and uncertainties in life cycle assessment

The preceding overview of life cycle assessment has referred to and roughly quantified uncertainties at each step, which are compounded with each stage of interpretation (Pennington et al., 2004). The inventory stage already has uncertainties associated with the emissions estimates for each pollutant, and models applied to estimate the midpoint and endpoint impacts of these emissions enhance the uncertainty. Yet each step helps the decision-maker better interpret the potential impacts of each option, and many of the assumptions made are consistently applied to all scenarios yielding less comparative uncertainty.

1.3.5 Advances required to enable LCA methods to quantify globally-distributed impacts

Based on the preceding overview of life cycle assessment, further development is needed to quantify impacts associated with global emissions, global supply chains, and global food trade. First, the global distribution of emissions is needed, and then a global version of an impact assessment model is needed to assess these globally-distributed emissions. Moreover, although the simple cause-effect framework accounts for intake through food and would allow for the integration of a food trade model, no operational method enables us to link the necessary steps to account for pollutant transport through food exports.

1.4 Bridging the gap between life cycle impact assessment and risk assessment

One key advance required to allow life cycle impact assessment to quantify globally-distributed impacts is to further adapt some relevant tools from risk assessment, a field which has been recognized for the potential to greatly improve life cycle assessment (Matthews et al., 2002; Russell, 2006). In this section, we provide a brief overview of risk assessment as it relates to life cycle assessment, review the differences in fate, exposure and damage between the two methods, and briefly describe the elements of risk assessment that are incorporated here to achieve the goal of quantifying globally-distributed human health impacts.

1.4.1 General overview of risk assessment in the context of life cycle assessment

As described in Section 1.2, risk assessment aims to provide a systematic approach to estimate the probability of specific harm to an exposed individual or population (NRC, 1994). Since risk assessment has been developing longer than life cycle assessment and is generally recognized as calculating more accurate impacts (Bare, 2006), life cycle assessment developers look to risk assessment for possible improvements in methodology. However, due to the differences in application and ultimate impact calculation, it is difficult and perhaps impossible to create a tool that fully integrates life cycle impact assessment with human and environmental risk assessment (Udo de Haes et al., 2006), as outlined in more detail below.

Many of the differences between LCA and RA stem from the LCA application to a functional unit and the subsequent marginal increases in impacts, whereas RA is applied to site-specific emissions in greater detail (Udo de Haes et al., 2006). Historically, life cycle assessment calculates impacts with no time or spatial element, whereas risk assessment is specific to a certain time and location (Russell, 2006), and therefore generally assesses impacts much more accurately (Bare, 2006). However, as life cycle assessment develops, it is expanding its scope from application to a product or service to the potential to support public policy and long-term decisions, a domain historically addressed by risk assessment and analysis (Hofstetter and Hammitt, 2002).

1.4.2 Comparison of fate, exposure and damage modeling between LCIA and RA

The pollutant fate modeling in both risk and life cycle assessment has a similar basis (Bare, 2006), with key differences due to the different intentions. The goal of human health risk assessment is to protect the local population from exposure above a level of acceptable protective risk (Pennington et al., 2006), thus assumptions err on the side of over-estimating damage to local populations, while LCIA attempts to best estimate and compare between scenarios the average damage to society (Bare, 2006). Thus the fate models used in risk assessments span relatively small regions (e.g., 200 x 200 km^2), whereas an LCA needs to cover a wider region to which the pollutant can be advected (Pennington et al., 2006). In addition, risk assessment generally accounts for background concentrations to allow absolute risk calculations, while LCA accounts for life cycle emissions and therefore is not site-specific, relying on default values for landscape and meteorology (Bare, 2006). Thus LCIA is better at modeling pollutant fate (and subsequent impacts) on a global or regional scale rather than site-specific (Bare, 2006).

For exposure modeling, the intake fraction concept defined in eq. 1-1 can be used in both LCA and comparative risk assessments (Bennett et al., 2002a), but the perspectives of population intake usually differ between the two. Due to the local scales considered in risk assessment, a consumption perspective is generally used, assuming that the local population has a relatively high per capita consumption rate of local food. LCA, on the other hand, is concerned with total population exposure, and thus uses a production perspective, assuming that food is consumed somewhere in the world (Pennington et al., 2006).

Finally, even after pollutant intake is estimated, the ultimate human health damage calculation differs between the two methods. There are many differences in the modeling of damage in RA and LCIA (Crettaz et al., 2002; Pennington et al., 2002; Pennington et al., 2006) due to the differing goals of avoiding exceeding a threshold rather than estimating average impacts.

1.4.3 Proposal to combine risk assessment and LCIA to estimate global impacts

By incorporating some risk assessment components, a tool can be developed for application in a traditionally life cycle assessment manner related to functional units or

goods, as well as application in a non-traditional manner to globally-distributed emissions. The finer spatial scales typical to pollutant fate in risk assessment can be partially addressed, while still including long-range advection, by accounting specifically for urban exposure. Most importantly, by accounting for changes in pollutant emissions and transport through food trade and global trade, the consumption perspective from RA will be added to the typically production-perspective life cycle impact assessment.

1.5 Key criteria for a tool to assess global human toxicity and review of relevant pollutant fate models

The preceding sections illustrate the potential for applying life cycle impact assessment methodology to create a tool to quantify globally-distributed impacts. Based on the effects described above, such a tool should include the following key criteria:

(a) Multiple environmental media – To follow the transport and intake of a pollutant through air, water and soil, it must model exchanges between these compartments, as well as entrance into food (Margni et al., 2004).

(b) Multi-pathway exposure – Exposure to pollutants can occur through inhalation, ingestion, and dermal exposure (dermal exposure not considered here, since it is not affected by global transport). The pollutant intake pathways of air, water, and different types of food are each modeled separately and then grouped into the two exposure routes of inhalation and ingestion, which are kept distinct due to their different effect factors (and therefore impacts). Exposure is commonly expressed as an intake fraction (iF), the fraction of each emission that is eventually taken in by a population (Bennett et al., 2002a). In addition to distinguishing inhalation and ingestion, the increasing global food trade pathways (FAO, 2000) should be identified to quantify impacts by both food production and food consumption region.

(c) High exposure intensity areas – Emissions in areas with higher populations or more agriculture will often have higher population intakes. Humbert et al. (2009) show that intake fractions of urban emissions can be an order of magnitude higher than non-urban emissions. It is therefore critical that models assessing the health impacts of inhalation-dominant substances account for urban emissions.

(d) Multi-continental – Rochat et al. (2006) show that regional variations in parameters such as population density and food production intensity cause the total pollutant intake to vary substantially with the region of emission and the spatial distribution of chemicals. The inclusion of multiple continents accounts for these differences and also allows for the trans-boundary transport of persistent pollutants (Liang et al., 2007; Liu et al., 2009b; Macleod et al., 2005).

(e) Minimal Data Needs – To enable linkage with life cycle assessment (LCA) and economic models, as well as to allow application of the model to a broad range of products and pollutants, the model should have limited computational cost and data requirements. In LCA, such models are applied to thousands of pollutants or tens of scenarios and thus should ideally run one pollutant on the order of minutes.

Table 1.2. Comparison of pollutant fate models and key criteria to accurately assess impacts of globally-distributed emissions; colors indicate the extent to which characteristics are met (low, medium and high suitability are indicated by red, yellow and green, respectively).

Table 1.2 shows the extent to which different types of models meet the key criteria described above. Multimedia models simulate pollutant transport through air, water and soil, with the one-box version using averaged environmental and exposure parameters to estimate concentrations and intake fractions (Huijbregts et al., 2000; Maddalena et al., 1995; Rosenbaum et al., 2008). Although one-box impact assessment

models can roughly estimate health impacts in the emission region, previous studies show that one-box models do not properly account for regional differences in emissions, substance fate (Huijbregts et al., 2003) and total global impacts (Rochat et al., 2006). Some models have utilized the increasing computing power to add spatial differentiation, predicting monitored concentrations throughout Europe (Pennington et al., 2005) and North America (Humbert et al., 2009), yet these do not cover the world. Other multimedia models have included transport between continents, but without modeling exposure (Macleod et al., 2005; Wania and Daly, 2002).

The recent development of the GLOBOX model (Wegener Sleeswijk and Heijungs, 2010) represents the first global multimedia model to include exposure; however, it does not account for urban exposure and it has not yet been compared with or evaluated against measurements. Moreover, bilateral wind flows between countries are adjusted to match one another based on 30 year averaged wind speeds within the country considered (irrespective of direction). These may be able to roughly estimate the regional loss rates of pollutants through wind, but they do not accurately represent the wind direction and therefore pollutant transport between regions.

Global circulation models provide the best estimates of long-range pollutant transport, but do not simulate concentrations in the food chain or calculate human exposure (Bey et al., 2001; Collins et al., 2006; Fox-Rabinovitz et al., 2006; Schmidt et al., 2006). Recent studies by Liu et al. (Liu et al., 2009a; Liu et al., 2009b) sought to address some of these problems by modeling emissions, transport, and concentrations of particulate matter (PM) with the MOZART-2 global circulation model, and then using epidemiological relations to estimate the PM health impacts. However, this study only accounted for impacts due to trans-boundary transport and not impacts in the region of emission. Moreover, this study required intensive computing power to run the simulation, and is not easily applied to other pollutants.

Therefore, none of the above models fully meet the criteria required for evaluating the globally-distributed health impacts associated with goods or pollutant emissions.

1.6 Objective of this thesis: create a tool to estimate globally-distributed impacts

1.6.1 Objectives and outline of the thesis

The objective of this thesis is to create a tool to estimate globally-distributed impacts for comparative assessment of global emissions and products, and then apply this tool to analyze spatial distributions of human toxicity and respiratory effects (with a framework that can be extended to other emission-related impact categories). To achieve this goal, the following specific aims are addressed to fill the gaps in existing models:

1. I aim to develop and evaluate a global impact assessment model that accounts for urban exposure and trans-continental transport, and then analyze patterns in spatial exposure of an ingestion-dominant pollutant (based on the global emissions inventory of polychlorinated biphenyl-118 introduced in Section 1.3.3) and an inhalation-dominant pollutant (based on particulate matter emissions associated with a T-shirt case study). This aim introduces the receiver perspective that is more traditionally used in comparative risk assessment to examine where impacts are taking place in addition to where they are induced.
2. I aim to expand the global impact assessment model by adding a component to account for food trade, and thus estimate the contribution of food exports to tranboundary transport of persistent pollutants. This represents a further necessary step in calculating impacts from a receiver perspective, in addition to the traditional producer perspective.
3. I aim to integrate the developed global impact assessment model with an environmentally-extended input-output model that predicts emissions throughout a product's global supply chain, and then analyze the subsequent globally-distributed health impacts induced by global consumption. This achieves one of the main goals of estimating globally-distributed health impacts associated with the manufacturing of globally produced goods.

This thesis is structured according to these three specific aims. The three chapters each contain an introduction that expands upon the specific objectives within each aim, followed by description of the methods, results and conclusions for achieving this aim.

To supplement the information that is concisely presented in each chapter (to be more consistent with a journal format), appendices are provided that mirror each chapter section and provide more detailed data and step-by-step calculations.

Chapter 2 describes the first step in creating this tool, which is the adaptation of an existing impact assessment model to a global scale, accounting for urban and continental exposure in a simple framework. The model (IMPACTWorld) is applied to two representative pollutants with different exposure pathways and lifetimes to illustrate the global variations in regional intake fractions. I also apply the model to two case studies, first analyzing the distribution of total global intake based on a global emissions inventory, and then performing a global life cycle assessment of a T-shirt made in India and shipped to Germany.

Taking advantage of the simplified framework of the global impact assessment model, Chapter 3 describes the expansion of IMPACTWorld with a component that accounts for global trade of feed and food based on an economic model of this trade. I again apply the expanded model to two representative pollutants and analyze the effects of food trade on local and exported pollutant intake. The results are used to compare for the first time the environmental fate of a pollutant with its economic fate (through food trade).

Finally in Chapter 4, the impact assessment model is integrated with an Input-Output model of global supply chains. The combined models are used to estimate and consistently allocate respiratory effects of particulate matter, thus representing the first spatially-explicit integrated model describing this full causal chain from consumption to impacts.

Chapter 5 presents general conclusions based on the model applications to global emissions inventories, food trade, and global trade, including how and where the key criteria are addressed. Chapter 5 also presents the limitations and possibilities of this integrated model, and provides recommendations for future refinement and application.

Taken together, these chapters describe the creation of a global model of human health impacts that accounts for global environmental and economic fate of toxic pollutants. This model combines environmental inter-continental transport with food trade, exposure, and impacts on continental and urban scales, while having limited

computational requirements. As such, it meets the key criteria outlined above, enabling the first calculations and allocations of impacts of globally-distributed emissions, products, foods and sectors.

In addition to the work presented here, and in collaboration with other researchers, several papers and other publications have resulted from my thesis work, and these publications are listed in Appendix 1. Among other contributions, these documents discuss the T-shirt case study of Chapter 2 in an encyclopedia chapter of globally distributed products (Shaked and Jolliet, 2011), describe the development of a spatialized North American version of the model presented in Chapter 2 (Humbert et al., 2009), provide global and region-specific damage factors for primary and secondary particulate matter emissions (Humbert et al., in review), and provide the coherent structure for a comprehensive handbook of the global impact assessment model, which is currently in development.

1.6.2 Scope of the model and its applications

In developing a global model with potential applicability to a wide variety of pollutants and scenarios of emissions and trade, many approximations are necessary, thereby introducing many uncertainties. Throughout this work, I describe many of the approximations and limitations of IMPACTWorld and its applications. Where possible, I compare predictions of the tool to measurements or more computationally-intensive or regionally-specific predictions of other models. In addition, sensitivity studies of some model applications are provided in the relevant appendices. Although uncertainties in our results are substantial, the damage factors of known pollutants range over 12 orders of magnitude (Rosenbaum et al., 2008), making these results an important step towards identifying where different pollutants fall in this range and prioritizing areas for further research. By identifying where the most interesting and substantial (shifts in) impacts are occurring, further work can be done in these areas so that uncertainties can be reduced and impacts can be better understood. Rather than provide specific impacts for a given region and pollutant, the goal of this work is thus to create a tool that can be used for comparative screening of pollutants and impacts on a global scale. Finally, as is true for any life cycle or risk assessment tool, the necessary weighting and values behind some decisions should be recognized (Anex and Focht, 2002; Cowell et al., 2002), and this model should be used in conjunction with other tools and assessments to provide information within the context of a complex decision (Bare, 2006).

CHAPTER 2

IMPACTWorld: Development and application of a multi-continental multimedia model to estimate global intake fractions and impacts of globally distributed emissions[*]

2.1 Introduction

As described in detail in Chapter 1, decision-makers seeking to assess and mitigate the environmental health impacts of globally distributed products and chemicals require a tool that accounts for the global emissions, fate, and exposure of associated emissions. To meet these needs, we aim to develop and evaluate a global impact assessment model, and then analyze patterns in spatial exposure of ingested and inhaled pollutants.

This chapter thus presents IMPACTWorld, a global multimedia model with limited computational requirements that accounts for inter-continental pollutant transport, and exposure and impact on continental and urban scales. Below, we describe IMPACTWorld's simplifying model framework for calculating intake fraction (the fraction of an emission taken in by a population) and explain the model parameterization. We evaluate the model application to a global emissions inventory of polychlorinated biphenyl-118 (PCB-118), and use the resulting intake fractions (iFs) to allocate intake by region of emission and exposure. The ingestion-dominant PCB-118 iFs are compared with those for the inhalation-dominant particulate matter (PM) to analyze global variations in intake fractions and the relative importance of inter-continental transport. We apply PCB-118 iFs to a global emissions inventory to estimate and allocate the global

[*] This chapter is being finalized for submission to *Environmental Science and Technology*, with myself as first author, and co-authored with Sébastien Humbert, Manuele Margni, Damien Friot, Stefan Schwarzer, and Olivier Jolliet.

intake, and we apply PM iFs to a sample T-shirt made in India and exported to Germany to demonstrate application of the model to a globally traded good.

2.2 Methods

2.2.1 Overview of methods section

Below we describe the spatialized matrix framework of IMPACTWorld, followed by a description of the set of subcontinental and oceanic zones to which this framework is applied, after which we discuss the model innovations in pollutant fate and exposure. We then describe the evaluation and application of the model to PCB-118 and PM, including analysis of globally-distributed emissions and a globally traded good .

2.2.2 IMPACTWorld description and parameterization

2.2.2a Regionalization and environmental compartments

IMPACTWorld divides the world into 17 sub-continental regions, 9 ocean regions, and 33 coastal regions (Fig. 2.1). As in previous IMPACT versions (Pennington et al., 2005), each continental region consists of an air zone (containing an air compartment) and a terrestrial zone (containing water, soil, vegetation, roots, and sediment), and each ocean region consists of an air zone and an ocean zone (containing surface ocean, deep ocean, and ocean sediment). Each region is characterized by environmental and demographic parameters, such as rainfall rate, vegetation fraction, and, most importantly for estimating population intake, vegetable and animal production intensity and population density. We increase the model accuracy while minimizing complexity by embedding a regionally-parameterized urban box to account for urban emissions and exposure in each region (see section on urban exposure below for detailed methods and equations).

Trans-boundary pollutant transport can occur between regions through water flows and, more importantly for the applications considered here, air flows. The regional divisions are based on a combination of geography (national boundaries), climate

(latitudinal boundaries where global circulation changes), and population (for example, the densely-populated eastern part of China is separated from the rest of China).

The 33 coastal regions, shown as the long and narrow regions between the continents and oceans in Fig. 2.1, are included to better capture pollutant transport to marine ecosystems and the resulting accumulation of pollutants within consumed fish. Due to river runoff and high coastal population density, much of the ocean pollution is concentrated in coastal areas, which are relatively shallow and contain up to 90% of the global fisheries catch (Schwartz, 2005). We use GIS to define coastal regions as the sections of ocean adjacent to land that are less than 150 m in depth, which includes most of the continental shelf (Chaudhary and Chaudhary, 2009).

Fig. 2.1. Model framework from emissions to intake, with fate factor matrix (FF) is based on the environmental fate model illustrated in the top inset. Based on pollutant transfer between the environmental compartments pictured, FF converts emissions to environmental concentrations or mass, from which the exposure factor matrix (XP) then estimates intake by region. The intake fraction matrix is a product of the fate and exposure matrices. The pink shading denotes the population density. Coastal regions are included as ocean zones that are generally long and thin and separate the terrestrial zones from the oceans. Appendix A2.2.2b provides the full list of countries in each IMPACT region and Fig. A2.1 shows all the detailed intermedia partitioning and degradation rate constants.

2.2.2b Spatialized matrix framework

For a given emission to an air, water or soil compartment, IMPACTWorld estimates the globally-distributed increases in environmental and food pollutant concentrations, and the resulting increased human intake and impacts through inhalation and ingestion. The IMPACTWorld framework builds upon the spatial version of the IMPACT2002 model, which has been implemented and evaluated for Europe (Margni et al., 2004; Pennington et al., 2005), North America (Humbert et al., 2009), and Canada (Manneh et al., 2010), but not at a global level.

We reduce the complexity of the spatialized global model by using the matrix framework presented by Rosenbaum et al. (2007), changing the emissions, intake and damage vectors to matrices to track the emitting and receiving regions. The vector $\vec{E}$ of emissions by region and environmental compartment is entered as a set of diagonal entries in the square matrix **E** (kg_{emit}/yr), which is multiplied by the spatial intake fraction matrix **iF** (kg_{in}/kg_{emit}) yielding the matrix of intake **I** (kgin/yr) (where the column and row indicate, respectively, the emitting and receiving regions). The sum over emitting regions yields the intake vector $\vec{I}$ from Rosenbaum et al. (2007). The human health damage matrix **D** (DALY/yr) is the product of **I** with a pollutant-dependent effect factor **EF** ($DALY/kg_{in}$) matrix:

$$\mathbf{D} = \mathbf{EF} \cdot \underbrace{\overbrace{\mathbf{XP} \cdot \mathbf{FF}}^{\mathbf{iF}} \cdot \mathbf{E}}_{\mathbf{I}} \qquad 2\text{-}1^{*}$$

Here, **FF** ($kg/(kg_{emit}/yr)$) is the fate factor matrix predicting environmental concentrations for a given set of emissions, and **XP** ($(kg_{in}/yr)/kg$) is the exposure matrix predicting population intake for given environmental concentrations. The fate matrix, described in detail in Rosenbaum et al. (2007), is the inverse of the matrix of steady-state rate constants that express pollutant deposition, degradation, advection, and partitioning between environmental media. The environmental compartments accounted for in our

[*] Note that to help the reader easily distinguish each matrix term, dot products are used here to indicate multiplications between matrices and vectors. Matrices are indicated by bold capitalized letters and vectors are indicated by italicized elements topped by an arrow. Elements of matrices or vectors are italicized without arrows or boldface.

fate and exposure calculation are shown in Fig. 2.1, and the detailed rate constants are depicted in Fig. A2.1.

The intake *I* for each region can be expressed from the perspective of either the emitting region *r* or the receiving region *r'*, both of which will be analyzed in the results below. The intake in the "emitting perspective", I_r^{emitter}, is the product of the emissions to environmental compartment *m* of region *r*, E_r^m, with the sum of the intake fractions in each receiving region *r'*, $iF_{r\to r'}^m$ (eq. 2-2b). For the "receiving perspective", the intake received by a single region, $I_{r'}^{\text{receiver}}$, is the sum over each emitting region that contributes to the receiving region's intake (eq. 2-2c). That is,

$$\mathbf{I} = \mathbf{iF} \cdot \mathbf{E} \qquad \text{2-2a}$$

$$I_r^{\text{emitter}} = \sum_{r'} \left(\mathbf{iF} \cdot \mathbf{E}\right)_{r\to r'} = \left(\sum_{r'} iF_{r\to r'}^m\right) E_r^m \qquad \text{2-2b}$$

$$I_{r'}^{\text{receiver}} = \sum_{r} \left(\mathbf{iF} \cdot \mathbf{E}\right)_{r\to r'} = \sum_{r} iF_{r\to r'}^m E_r^m \qquad \text{2-2c}$$

The emitter perspective intake is thus the sum over the columns of the **I** matrix, and the the receiver perspective intake is the sum over the rows. The intake fraction matrix is the product of the exposure and fate matrices, fully expressed in the "emitting perspective" in eq. A2-1.

2.2.2c Pollutant fate

IMPACTWorld calculates pollutant fate by accounting for advection, transfers between environmental media, deposition and degradation (Pennington et al., 2005). The full list of fate and exposure parameters is provided in a previous publication (Pennington et al., 2005), and we describe below the important changes made. Moreover, ranges in values for important parameters are listed in Table 2.1, and additional details on regional divisions, parameters, and values are provided in Appendix A2.2.2.

Because we adapt the model here for global application and thus need to explicitly account for inter-continental transport, we improve upon the previous atmospheric transport component in Pennington et al. (2005) and other impact assessment models. GLOBOX, the other existing global model of pollutant fate and exposure,

roughly estimates advection between countries based on average measured wind speeds (independent of direction) in capital cities (Wegener Sleeswijk and Heijungs, 2010). We aim here to better capture the directional transport between regions. As done in previous impact assessment models, we calculate atmospheric transport using an air layer with an 800 m mixing height (Hofstetter, 1998)[*]. However, we compute advective rate constants between regions using horizontal wind speeds from GEOS-Chem, a global 3-D model of tropospheric chemistry that provides 6-hour averages of wind speeds from the Goddard Earth Observing System (2005) at 2°×2.5° resolution. The north, south, east and west components of the wind speeds are each arithmetically averaged, temporally over one year, vertically over the lower three atmospheric layers in GEOS-Chem (corresponding to 800 m in height), and horizontally over continental boundaries. To conserve mass, air flows are balanced such that total flows into and out of each region are equal (see Appendix A2.2.2c for more details). Since atmospheric flows vary greatly vertically, diurnally, seasonally, and annually, these averages do not fully capture the atmospheric transport processes, but they are intended to provide an improved approximation of transboundary transport, as well as provide a framework for future refinements. We use Geographic Information Systems (GIS) data to determine many of the geographic parameters, such as soil and freshwater areas.

2.2.2d Pollutant exposure

After modeling the pollutant environmental fate, IMPACTWorld calculates human exposure through both inhalation and through ingestion of water, vegetables, dairy, meat and fish. This calculation is based on regional values of population and food production (Margni et al., 2004; Pennington et al., 2005).

To calculate human exposure due to fish consumption, we allocate sea fish production among coastal and ocean zones based on FAO FishStatPlus data by ocean section for the year 2000 (FAO, 2002). Pollutant concentrations in fruits and vegetables are based on the vegetation concentrations provided by the fate model, and animal

[*] This is an estimate used commonly in life cycle impact assessment, including the consensus USEtox model (Rosenbaum et al., 2008). No other globally averaged mixing height was available, especially considering the need to account for pollutant transport across time- and spatially-varying mixing heights; future work should determine the best mixing height for such an application.

product concentrations are based on the bioaccumulation factors between air, water or vegetation and the animal considered. Moreover, we use FAO food production and supply data by food sector and country to estimate population intake rates of food (FAO, 2000), which are grouped into IMPACT regions and exposure pathways (Table A2.2). At this point, we allocate pollutant impacts due to food intake to the food producing region. However, in Chapter 3 we estimate the effects of food trade on regional pollutant intake, and also provide more detail on the pollutant exposure through vegetable and animal food intake.

Table 2.1. Important parameters adapted for global version of IMPACT.

2.2.2e Inclusion of urban areas

Shorter-lived inhalation-dominant pollutants, such as PM, have substantially higher impacts when emitted in high population density (urban) rather than in low population density (rural) areas (Humbert et al., 2009) In many regional impact assessment models, this urban effect is not captured because the large area in each cell dilutes the total population density, thereby failing to capture the non-linear dependence of the intake on population density. A global model with high enough resolution to capture the urban effect (cells smaller than a few hundred km across) would require large computational resources that inhibit, and largely prevent, its application to multimedia fate and exposure. To overcome this limitation, the IMPACTWorld model uses population and size characteristics of the urban areas in each region to estimate generic urban exposure by region. The necessary methods were introduced by myself and colleagues in Humbert et al. (2009), but we expand these methods below for global application.

The total intake fraction of a given regional emission, iF_{tot}, is the emission-weighted average of the intake fractions due to urban and rural emissions (iF_{urb} and iF_{rur}, respectively). The IMPACTWorld model already calculates iF_{rur} as its default value (this is the default for any continental-sized box model), so we describe here the derivation of iF_{urb}.

The intake fraction due to urban emissions is the sum of the intra-urban (iF_{urb}^{urb}) and the rural iFs of the urban emissions that are advected out (almost all urban emissions advect out to rural areas (Marshall et al., 2005);–see eq A2-2 for details). We average the urban area properties in each region to calculate the effective iF_{urb}^{urb} and apply it to any substance living longer than the timescale it takes for the pollutant to be advected out of the urban area (usually a few hours). The effective iF_{urb}^{urb} is a population-weighted average over all urban areas in a region (fully derived in eqs A2-3 and A2-4):

$$\left\langle iF_{\text{urb}}^{\text{urb}} \right\rangle = \frac{Q \cdot \sum_i N_i \cdot C_i}{\sum_i \dot{E}_i} \cong \frac{a \cdot Q}{(u\,H)_{\text{eff}}} \cdot (d\,L)_{\text{eff}} \qquad \text{2-3}$$

where Q is the average person's breathing rate, 13 m^3/pers-day (NCEA, 1997); and each urban area i has a given emission rate $\dot{E}_i$ (kg/s), concentration C_i (kg/m^3), and exposed population N_i (in pers). Assuming a simple square box model, eq 2-3 rewrites the average $iF_{\text{urb}}^{\text{urb}}$ as a function of effective meteorological and population density properties for a given region, where a (unitless) is a correction factor to account for the effects that (i) a pollutant can be emitted anywhere in the urban area i and not only at the edge, and (ii) air exiting the urban area i can return with some of the pollutant. This correction factor varies between 0.5 and 1, and is approximated here as 0.75 for all urban areas (Benarie, 1980). Furthermore, $(u\,H)_{\text{eff}}$ is the effective dilution rate in m^2/s, which is a product of the typical wind speed u_i in m/s (defined below) and mixing height H_i (m). Finally, $(d\,L)_{\text{eff}}$ (pers/m) is the effective linear population density, which is a useful parameter when considering urban exposure because it has less variation than population density and is more relevant to intake fractions (Marshall, 2007). It is defined here as the emission-weighted averaged product of population density d_i (pers/m^2) and box length L_i (m), with a factor to account for differences in loss due to different-sized areas (derived in eqs A2-3 and A2-5). Thus $iF_{\text{urb}}^{\text{urb}}$ is proportional to the exposed population and inversely proportional to box volume and loss rate.

Because the relevant dependencies are non-linear, the effective dilution rate is not simply a product of arithmetic averages of the wind speed and mixing height. Since the dilution rate is in the denominator, its effective value is well approximated by a harmonic average (eq. A2-4). We use the best available value of a dilution rate of 610 m^2/s, which is the harmonic average of twice-daily measurements in 75 US urban areas (Marshall et al., 2005).

The total continental iF is the sum of the emissions-weighted urban iF and the iF calculated by IMPACTWorld for the adjusted non-urban population. Due to the lack of urban-specific emissions data for many pollutants, we use population as a proxy for

emissions as done previously by Humbert et al. (2009). Urban population (and some area) data for 3,670 urban areas (covering 2.2 billion people) are provided by the United Nations and the World Bank (Angel et al., 2005; UN, 2008), and properties of smaller urban areas are estimated based on region-specific regressions between populations and population densities. Effective linear population densities for each region are listed in Table A2.5.

2.2.3 Pollutants studied and description of model application and evaluation

Using the methodological framework described above, IMPACTWorld can be applied to a variety of substances for which the degradation rate and intermedia partitioning coefficients can be characterized (Pennington et al., 2005). Here, we select an ingestion-dominant pollutant (polychlorinated biphenyl-118, PCB-118) and an inhalation-dominant pollutant (fine particulate matter, $PM_{2.5}$) to help demonstrate the importance of the key criteria listed in Table 1.2. After explaining the reasons for these specific pollutants and detailing their important properties, we describe the methods used to apply the model.

2.2.3a PCB-118

PCBs are a set of persistent organic pollutants, many of which are hazardous due to their toxicity, bioaccumulative properties, and long-range atmospheric transport (Breivik et al., 2007). PCB-118 is a well-studied congener with relatively long half-lives in air, water and soil (32 days, 0.9 years and 2.2 years, respectively), as well as a high bioconcentration factor in fish (476,200 kg_{water}/kg_{fish}) (see Table A2.3 for full list of chemical properties). Most importantly, PCB-118 is included in the Breivik et al. (2007) global emissions inventory; this inventory includes three dioxin-like congeners that have the highest toxic equivalency factor among PCBs (0.00003) (Van den Berg et al., 2006), of which PCB-118 has the largest emission rate.

We used emissions estimated for the year 2000 at $1^{o}x1^{o}$ resolution from (Breivik et al., 2007). As recommended by other studies based on comparisons with measurements, we use the maximum emissions scenario rather than default values (Breivik et al., 2010; Hauck et al., in press; Macleod et al., 2005; Meijer et al., 2003). As

an indication of the uncertainty in emission values, the maximum emissions are 3-4 orders of magnitude higher than in the minimum scenario, and the averaged annual emissions decrease by approximately a factor of two between 2000 and 2010 (Breivik et al., 2007).

As an evaluation of the model application to PCB-118, the fate of PCB-118 emissions simulated with IMPACTWorld is compared to measured globally distributed concentrations in soil (14 regions, 188 measurements), air (5 regions, 63 measurements), water (4 regions, 14 measurements), butter (10 regions, 65 measurements), beef (1 region, 2 measurements), chicken (1 region, 2 measurements) and fish/seafood (5 regions, 39 measurements) (Borga and Di Guardo, 2005; Domingo and Bocio, 2007; Gioia et al., 2008a; Gioia et al., 2008b; Hayward et al., 2007; Kalantzi et al., 2001; Loutfy et al., 2007; Meijer et al., 2003; Perugini et al., 2004; Zhao et al., 2005). For each region, we calculate the median and 95% confidence interval of each set of measurements. The sources and locations for each measurement are provided in Table A2.4.

The predicted and measured concentrations don't represent precisely the same quantities for a few reasons. Because the global inventory includes air emissions but none of the known water emissions, water and fish/seafood concentrations are expected to be underestimated. More importantly, IMPACTWorld predicts steady state concentrations assuming continuous constant emissions (in this case, from the year 2000, with a world total emission rate of 23 tonnes/yr), but actual emissions vary seasonally and annually. Total annual emissions from 1930 until 2050 are estimated to vary between 0 and 78 tonnes/yr, with a drop from 62 to 9 tonnes/yr between 1985 and 2010 (Breivik et al., 2007) (Fig. A2.2). The longest environmental half-life of PCB-118 is 2.2 years in soil, therefore soil concentrations should reach at least 75% of their steady state value after 4.4 years of constant emissions, according to the definition of half-life (Fjeld et al., 2007). The measurements occur between 1995 and 2006. The implications of this imperfect matching are discussed in the conclusions.

We use IMPACTWorld to calculate and examine the key factors affecting the spatial intake fraction for PCB-118, and then multiply the iFs by emissions to analyze global intake from the emitters' and receivers' perspectives (eq. 2-2).

2.2.3b Particulate matter

PM is a mixture of tiny particles of solid or liquid suspended in the air. Inhalation of PM has many adverse health effects, including reduced life expectancy, pulmonary disease, heart failure, and asthma (Bascom et al., 1996; Franklin et al., 2008; Schwartz et al., 2008). For example, Pope et al. (2002) found that each 10 $\mu g/m^3$ increase in fine particulate pollution was associated with approximately a 4% increase in risk of mortality. Because of the more complex reactions involved in the formation of secondary particulates, we only consider primary particulate emissions, such as soot from combustion.

We describe below the data, methods, and models used to evaluate the IMPACTWorld application to particulate matter. To assess the trans-boundary transport and regional concentrations predicted by IMPACTWorld, we compare these to results from a study using a high-resolution ($\sim 2^o x 2^o$) atmospheric transport model. This study simulated black carbon, organic carbon and dust $PM_{2.5}$ concentrations in ten sub-continental regions (Liu et al., 2009b), and obtained results within approximately a factor of two of measurements. To best compare the resulting regional concentrations and levels of trans-boundary transport between IMPACTWorld and Liu et al. (2009b), we drive IMPACTWorld with the emissions used in Liu et al. (2009b).

The predicted urban and rural intake fractions are difficult to fully evaluate since intake fractions are not directly measurable. Moreover, IMPACTWorld is the first model to account for urban areas in calculating continental intake fractions around the world, so there are few studies available for comparison. In Section 2.3.2, we compare the US and China urban iFs to specific studies in these regions (Marshall et al., 2005; Zhou et al., 2006), and we also compare rural intake fractions to region-specific studies that don't specifically account for urban areas (Levy et al., 2003; Tainio et al., 2009).

After analyzing the key factors influencing the PM spatial intake fraction, we apply the spatial iF to estimate the globally distributed impacts of a globally traded good. Clothing items, in particular, are increasingly manufactured in India and the rest of Asia for Western consumption (Palpacuer et al., 2005). Thus, we demonstrate a life cycle application of the model by estimating the impacts due to PM emissions associated with a T-shirt manufactured in India for consumption in Germany (Steinberger et al., 2009). To

estimate the associated impacts, we use an effect factor of 57.8 DALYs (disability-adjusted life years) per kg inhaled by the population (van Zelm et al., 2008).

2.3 Results of model and case study

2.3.1 Model application to PCB-118

2.3.1a Assessment of model application to PCB-118

Based on the allocation of Breivik et al. (2007) emissions to IMPACTWorld regions (shown in Chapter 3, Fig. 3.3), we estimate approximate values of concentrations in the environment and food by region (Table A2.4) and compare these to measured concentrations (Fig. 2.2) (as explained above, note that modeled and measured values represent different quantities due to the model assumption of constant emissions based on the year 2000; the implications of this difference are further discussed in the conclusions). The model predictions are within an order of magnitude of all but three globally distributed measurements of pollutant concentrations. The model does underpredict pollutant concentrations in water; however, this is expected, since IMPACTWorld does not account for pollutant emissions to water. If no coastal zones were included in IMPACTWorld, coastal water measurements would be compared to modeled ocean concentrations, yielding the even less accurate outlined diamonds in Fig. 2.2a.

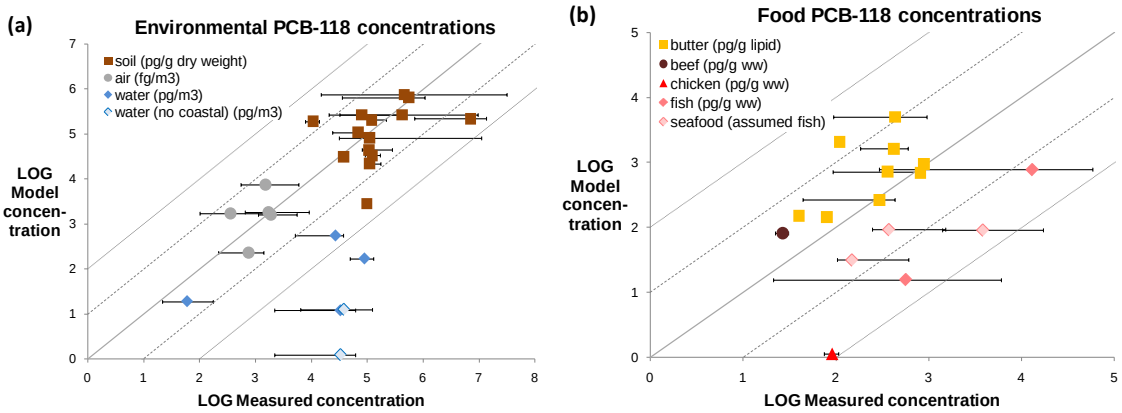

Fig. 2.2. Comparison between modeled and measured PCB-118 concentrations in soil, air, and water (a) and in food (b). Each point represents a different region, indicating the medians and 95%

confidence intervals of measured concentrations from a variety of studies (detailed values and references are provided in Table A2.4). Note that water emissions are not accounted for, therefore water and fish concentrations are shown for comparison and not to assess model performance; (a) shows an additional dataset of modeled water concentrations if no coastal zones were present (outlined diamonds); (b) uses outlined diamonds to denote seafood measurements, which are compared to modeled fish concentrations.

The model predictions are also within an order of magnitude of the beef concentration and all but two globally distributed butter concentrations. The underprediction of fish concentrations is expected from the underpredicted water concentrations. The underpredicted chicken concentration suggests that the chicken bioconcentration factor in the IMPACT model should be refined (the cow model has been much better determined and evaluated (Rosenbaum et al., 2009)).

Fig 2.2 indicates that when using constant emissions from the year 2000, IMPACTWorld calculates environmental concentrations to within an order of magnitude of measurements between 1995 and 2006, yielding differences between modeled and measured values similar to those of the much higher resolution BETR-World model (MacLeod et al., 2005).

2.3.1b PCB spatial intake fraction

Fig. 2.3 displays the PCB-118 spatial oral intake fractions predicted by IMPACTWorld, and shows that the oral intake fraction varies greatly from region to region. For example, China has a global intake a factor 12 higher than in Argentina (0.024 vs. 0.002 kg_{in}/kg_{emit}, respectively). Breaking this down by region of intake, 82% of the intake fraction from a China emission is ingested locally (i.e., intake in the region of emission), with 9% exported to Japan and India. Even though local intake dominates most iFs, trans-boundary transport accounts for more than 90% of the intake due to emissions in the West Asia and N. Europe + N. Canada regions. Note that more Indian emissions are taken in by Chinese than vice-versa due to the dominating westerly winds. Emissions in Europe and the US, which are some of the largest sources of PCB-118, have respectively 37% and 33% of the global intake fraction occurring outside their borders.

Since freshwater fish and exposed (aboveground) produce are the main exposure pathways for PCB-118, much of the regional variation in the iF is due to differences in the production intensities of these foods in the region of emission (Fig. A2.4).

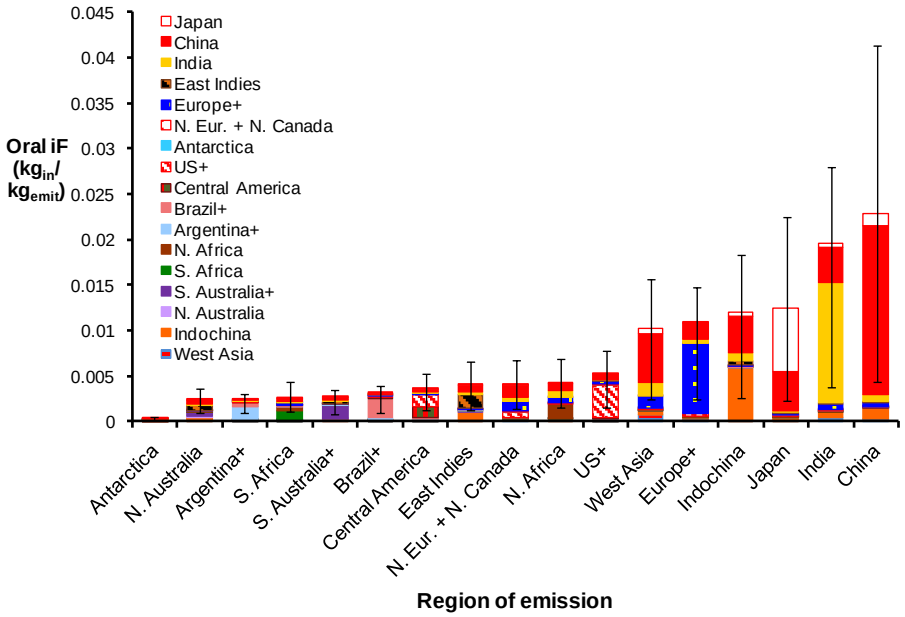

Fig. 2.3. Spatial intake fraction (iF) of PCB-18 for different regions of emission, with colored bars representing the regions of intake. Since the vertical axis denotes total global iF, this graph represents the emitter's perspective. Error bars represent total iF ranges due to variation of physical-chemical properties reported in the literature (Table A2.3), and they are thus correlated between regions, but they do not capture all sources of uncertainty, which are discussed further in section 2.4.4.

2.3.1c Application to global emissions: PCB intake in different perspectives

The total global intake as a function of emission region (shown in Appendix 3, Fig. A3.20) is a product of the PCB-118 spatial intake fraction matrix and regionally-allocated emissions (about 23 tons are emitted in the year 2000, with an estimated 213 kg taken in by the world population). Taking advantage of the matrix framework, Fig. 2.4 transposes the resulting matrix of regional intakes to show the results in the receiving region perspective, with the vertical axis representing total intake in a region differentiated by the region of emission. The intake in many regions shows a substantial contribution from emissions in Europe, US and West Asia, which emphasize the effects of trans-boundary transport. For example, Chinese emissions result in a global intake of only 11 kg, with 9.2 kg ingested in China (Fig. A3.20). Yet due to transboundary transport, Fig. 2.4 shows that global emissions lead to a 56 kg intake in China, 21 of which are due to European emissions. Thus, China has the second highest intake despite having only the 9th highest emissions.

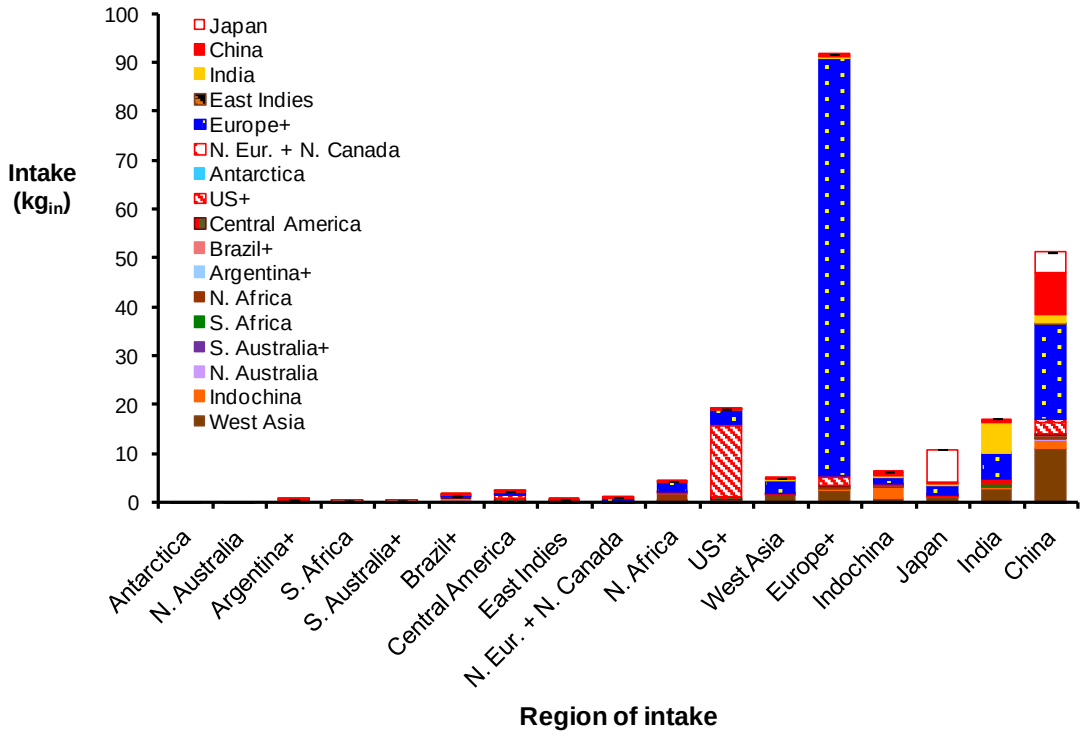

Fig. 2.4. Absolute intake of receiving regions, differentiated by the emission regions responsible for this intake. Note that colors represent region of emission, whereas in Fig. 2.3 they represent region of intake.

2.3.2 Model application to PM

After applying IMPACTWorld to the ingestion-dominant PCB-118, we now apply the model to inhalation-dominant PM. Below, we first address fate and transboundary transport by comparing the predicted concentrations to results from a high-resolution atmospheric model. We then address exposure in two parts. First, we compare the IMPACTWorld predicted intake fractions to other predictions of regional intake fractions that account for urban areas. Then, we compare the rural portion of the IMPACTWorld intake fractions to other model predictions that do not explicitly account for urban exposure. Finally, we illustrate the potential of IMPACTWorld to quantify emissions from globally traded goods and services by applying the calculated spatial intake fractions to the PM emissions generated by a globally traded T-shirt.

2.3.2a Fate: comparison of PM concentrations with high-resolution model results

We assess the PM fate predicted by IMPACTWorld by driving the model with emissions from from a high-resolution atmospheric transport study (Liu et al., 2009b), and comparing the results. Even though IMPACTWorld is much simpler than the high-resolution model used in Liu et al. (2009b), it predicts most concentrations of black carbon, organic carbon, and dust to within a factor two, three, and five, respectively, of the Liu et al. predictions (Fig. A2.5a). We also compare the IMPACTWorld concentrations due to transport with those from Liu et al. (2009b), and find that our regional black and organic carbon concentrations have similar imported shares (0-38%, with medians of 2% and 6% for black and organic carbon respectively) to those calculated by the high-resolution model (0-23%, with medians of 5% and 7% for black and organic carbon respectively) (Fig. A2.5b). However, IMPACTWorld somewhat underpredicts the trans-boundary transport of dust (0-60% with median of 25%) relative to Liu et al. (4-96% with median of 31%). Moreover, IMPACTWorld predicts transport between adjacent regions relatively well, but underestimates the longer range transport (between China and the US for example) (Fig. A2.6). However, we show below that transboundary transport has a small contribution to intake fractions of short-lived pollutants such as PM. Therefore, the inability to perfectly capture certain aspects does not greatly affect our final results.

2.3.2b Exposure: PM spatial intake fraction predicted by IMPACTWorld and comparisons with other studies

Fig. 2.5 shows that PM spatial intake fractions vary by a factor of ten, with 89-99.8% of intake occurring in the region of emission. (Table A2.5 lists the urban and continental population and size parameters, as well as intake fractions for urban and rural emissions.) The transboundary transport comparison above provides support for the level of PM transport calculated in our model, finding it to be much lower than PCB-118 due to PM's smaller lifetime, as well as its dominating effects of local urban exposure. Specifically accounting for urban area exposure leads to 72-99% of the intake, depending on the region of emission. To compare these results to other studies, we separately consider the urban iFs and non-urban iFs below.

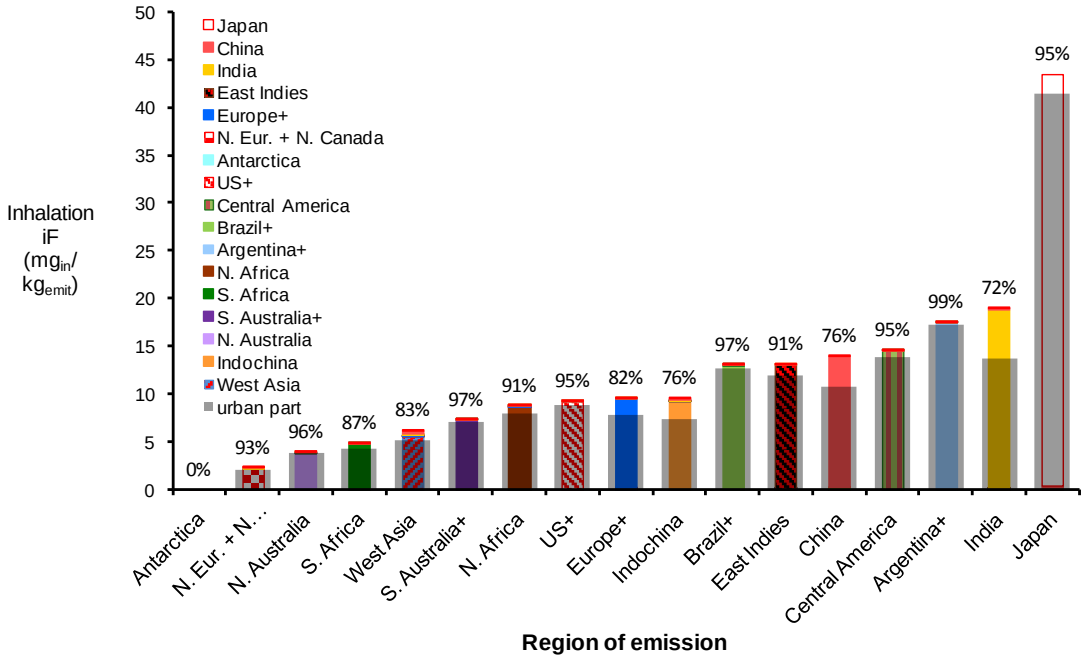

Fig. 2.5. Spatial intake fraction of particulate matter ($PM_{2.5}$), with grey shading and percentages to indicate urban intake in region of emission.

Our model predicts that emissions in the US and southern Canada (US+) have a population-weighted iF of 9.3 mg_{in}/kg_{emit} and an intra-urban iF of 17 mg_{in}/kg_{emit} (this latter figure is higher because it is not averaged with the lower iFs for rural emissions). Marshall et al. (2005) calculate intra-urban iFs for US urban areas with mean values (and 80% confidence intervals) of 21 (2.4-50), 10 (2.6-15), and 15 (11-29) mg_{in}/kg_{emit} for, respectively, a one-box model, and summer and winter values in an empirical model. The IMPACTWorld value of 17 mg_{in}/kg_{emit} is within the range of the winter empirical model and one-box model and just above the summer empirical range.

For eastern China, IMPACTWorld predicts an iF for $PM_{2.5}$ of 14 mg_{in}/kg_{emit}. Zhou et al. (2006) estimate the PM_3 (particulate matter smaller than 3 microns in diameter) intake fractions of 29 power plant emissions in eastern China, modeling PM concentrations over a grid of 28x28 km (therefore capturing urban concentrations) and population exposure at the county level. They find a mean iF of 3 mg_{in}/kg_{emit}, ranging between 1.7 and 12 mg_{in}/kg_{emit}. These values are somewhat lower than our prediction, which could be due to a variety of differences between the two studies; most importantly, the IMPACTWorld iF is a population-weighted average over urban and rural populations,

whereas Zhou et al. take the average of emissions from 29 power plants (i.e. not necessarily representative of the population distribution). Although it is inherently difficult to assess the accuracy of the calculation of iFs by IMPACTWorld since intake fractions cannot be measured, the above comparisons with the two studies of Marshall et al. (2005) and Zhou et al. (2006) suggest that our urban iFs are of the correct order of magnitude.

Fig. 2.5 indicates that models that do not account for urban intake could substantially underestimate iFs, decreasing each region's iF by more than 70%, with non-urban iF values of 1.7 and 0.4 mg_{in}/kg_{emit} for Europe+ and US+, respectively (see expanded non-urban iF in Fig. A2.7). These values are similar to US and European iFs estimated by models that also do not account for urban areas. Tainio et al. (2009) calculate an average European iF of 2.2 mg_{in}/kg_{emit}, ranging from 0.3 to 4.4. For the U.S., Levy et al. (2003) calculate an iF of 0.6 mg_{in}/kg_{emit} based on Georgia power plants, located mostly in non-urban areas. They extrapolate these values to estimate an iF of 0.5 mg_{in}/kg_{emit} for the entire US.

Although data is not available to provide a full evaluation of the model application to PM, the above comparisons support our finding that accounting for urban areas is critical in assessing iFs. Indeed, doing so results in iFs that are about an order of magnitude larger than iFs found by the non-urban treatment typically performed in impact assessment models. Moreover, accounting for urban areas not only increases intake but also changes the relative ranking of the iF by region (as shown by comparing Fig 2.5 with Fig. A2.7). This occurs because the urban population fractions and urban linear population densities, which determine the urban iF, differ from the continental population densities, which determine the non-urban iF (see Fig. A2.8 for correlations between total inhalation iF and these population densities).

2.3.2c Application of PM spatial intake fraction to globally traded T-shirt

After assessing the IMPACTWorld predictions of the fate and exposure of PM in the previous sections, we now apply the calculated spatial iF to $PM_{2.5}$ emissions associated with a T-shirt made in India for German consumption (Steinberger et al., 2009). We thus define the functional unit as a cotton T-shirt made in India and worn and

washed 50 times in Germany. The system boundary of this LCA includes: the growing of the cotton in India; the spinning, knitting, sewing and dyeing in India; the transport within India, to Germany, and within Germany; the washing and drying in Germany; and finally the disposal. A full life cycle assessment would account for all pollutants, but an initial screening of the emissions inventory estimated that PM emissions are the dominant source of human toxicity and respiratory effect impacts to human health. When we apply IMPACTWorld to the life cycle $PM_{2.5}$ emissions of a T-shirt made in India for German consumption, we find the distribution of emissions and impacts shown in Fig. 2.6.

Fig. 2.6 Regional distribution of money spent, particulate matter emissions and population impacts associated with a T-shirt made in India for German consumption. Total value for each bar shown at top.

The predicted total $PM_{2.5}$ damage to human health is $2.4 \cdot 10^{-6}$ DALYs for this T-shirt (to put this into context, smoking one cigarette incurs approximately 10^{-5} DALYs). Although 100% of the consumption occurs in Germany (where the T-shirt is bought and used), 84% of the emissions are in the densely populated India, 89% of the human health damage occurs in India, 7% occurs in Europe, and the remainder is distributed throughout the rest of the world due to trans-boundary transport. This example application demonstrates the impacts of the globalization of the supply chain, which is investigated in detail in Chapter 4.

2.4 Discussion and conclusions

2.4.1 Importance of key criteria

In the previous section, we presented the first calculations, to our knowledge, of the globally distributed impacts of global emissions. This advance was made possible by developing a new model, IMPACTWorld, that adequately addresses the five key criteria summarized in Table 1.2. First, the multimedia and multi-pathway exposure, one of the key criteria and included in IMPACTWorld, is crucial to account for transport through air, water, and into the food chain. This was demonstrated by the application of IMPACTWorld to the ingestion-dominant PCB-118. Second, the matrix framework of the model is used to estimate intake from both the emitter and receiver perspectives, bringing this beyond the typical LCA scope into the realm of risk assessment (although food trade needs to be included for a full receiver perspective, as described in Chapter 3). A third critical advance of IMPACTWorld over previous models is that it accounts for urban-specific emissions and exposure (which is added to an adjusted continental exposure). For our application to the inhalation-dominant PM, this increased iFs by about an order of magnitude relative to assuming an evenly distributed continental population density. Fourth, the regional variations in spatial iFs for PM and PCB-118, as well as the importance of trans-boundary transport for the longer-living PCB-118, are only revealed by including multiple continents linked by air flows, another advance of IMPACTWorld over previous models (e.g., Pennington et al. (2005)). And, finally, IMPACTWorld has limited computational needs, allowing the results to be applied to two case studies (global PCB-118 emissions and T-shirt) and they were easily adapted for comparison with other models and sensitivity studies. IMPACTWorld's low computational needs, combined with its applicability to any pollutant with known partitioning coefficients and degradation rates in environmental media, results in a model that can thus be applied to a wide array of other scenarios and pollutants.

2.4.2 Comparison of spatial iFs

The spatial intake fractions of particulate matter differ greatly from those of PCB-118 in terms of magnitude and trans-boundary transport. Because PM has a short lifetime

and is inhalation-dominant, more than 89% of its intake occurs in the region of emission, whereas the local intake fraction for PCB-118, which has a much longer lifetime and is ingestion-dominant, can be as low as 3%. PM iFs vary slightly more than PCB iFs mainly due to the large difference in urban population density between Japan and the other regions (PCB iFs are independent of population density, and instead depend on food production intensity).

2.4.3 Case study applications

The matrix framework in IMPACTWorld provides information on impacts from the perspectives of both the inducing and impacted populations. Thus, in addition to displaying the globally-distributed impacts due to a region, one can also display the total impacts in a region broken down by region of emission.

More specifically, the matrix framework shows that even regions with relatively low PCB-118 emissions, such as China and India, can have very high intake due to trans-boundary transport. And application to the T-shirt case study quantifies, for the dominant pollutant, how impacts can be shifted from the region of consumption.

2.4.4 Limitations and future work

2.4.4a Evaluation of IMPACTWorld for application to multiple substances

The application of IMPACTWorld to global emissions inventories and globally traded goods has many uncertainties and limitations, which future developments should address. First, future work should apply and evaluate the model for a broader range of pollutants, as has been done for previous versions of IMPACT (Humbert et al., 2009; Margni et al., 2004; Pennington et al., 2005). In addition to better evaluating the model framework, such studies would allow model application to a broader range of emissions associated with globally traded goods, thereby allowing a more comprehensive quantification of the health impacts of global supply chains. Studying different pollutants will also help determine for which pollutants and which impacts the spatialization or trans-boundary transport is important to incorporate.

2.4.4b Limitations in the pollutant fate and recommended future developments

Our model framework for pollutant fate calculation has inherent limitations as a consequence of the simplified calculations. For example, the steady state assumption requires constant emissions and constant transport rates between different regions and environmental media, which for example neglects diurnal, seasonal and annual variations in emissions, winds, and temperatures.

Specific to the application presented here, there are uncertainties in the emissions and fate that are not fully evaluated by the comparison above. The above comparison suggests that the model predictions, based on the assumption of continuous constant emissions, are mostly within one order of magnitude of measured environmental and food concentrations. However, as noted above, the inputted constant emissions do not accurately account for the changing emission rates that contributed to the measured concentrations, and it can take up to 4.4 years to reach 75% of the steady state environmental concentrations predicted by the model. Measurements occur between 1995 and 2006, and emissions are predicted by Breivik et al. (2007) to have fallen from 61 to 13 tonnes/yr between 1986 (four half-lives before 1995) and 2006, whereas we use the continuous annual value of 23 tonnes/yr from 2000. Therefore the assumption of a constant continuous emission rate based on the year 2000 value may be underestimating values by a factor of up to 2.5 (61 divided by 23) prior to 2000, and overestimating values by up to a factor of two (23 divided by 13) after approximately 2000. This comparison should thus be interpreted cautiously with additional uncertainty in predicted values due to the lack of accounting for non-constant emissions. Since toxicity among pollutants can vary by 12 orders of magnitude (Rosenbaum et al., 2008), this level of accuracy can still provide useful information toward identifying areas of further research or prioritizing regulatory actions to limit population exposure.

In terms of future developments, the model should be adapted to allow temperature-dependent pollutant degradation rates and inter-media partitioning coefficients to better account for globally varying temperatures. Future improvements in trans-boundary transport should more accurately determine the optimal height of the surface air compartment that best captures air flows. Moreover, including an upper air layer to account for the jet stream could produce more accurate calculations of long-range transport. Preliminary studies suggest that this upper air layer does not greatly affect

intake, but this will vary with pollutant lifetime and should thus be further explored. Furthermore, trans-boundary transport, particularly in the case of PCB-118, should be further evaluated against high-resolution atmospheric models as was preliminarily done here for particulate matter. And, finally, sensitivity tests using an array of test pollutants should be conducted on all regionalized parameters so that parameter refinement can be prioritized.

2.4.4c Limitations in pollutant exposure and future developments

Several improvements are also possible to improve the modeling of pollutant exposure in IMPACTWorld. First, the large regions used in IMPACTWorld simplify calculations but also tend to underestimate concentrations (and therefore exposure) near an emission. Accounting for urban areas represents an important step in addressing this problem for the inhalation pathway, but this method still approximates all the urban areas in a region with one set of parameters. Another improvement to the exposure calculations would be to obtain region-specific dilution rates. The model meteorology is currently based on dilution rates measured in the U.S. due to lack of data availability. Moreover, emissions are assumed to be proportional to population density. Thus, more meteorological and emissions data is needed to test and refine these approximations.

In a similar manner to urban exposure for inhalation-dominant pollutants, exposure to ingestion-dominant pollutants can be improved by accounting for emissions in high agricultural intensity areas. Ingestion intake can also be better understood by building upon the current intake fraction calculation based on the production perspective, where intake is allocated to the region of production rather than food consumption; future work in the integration of risk assessment concepts should account for pollutant transport through food exports such that intake based on consumption can be estimated (which is described and implemented in Chapter 3).

And, as in the case of previous IMPACT models, we do not account for a detailed food chain, differences in age structure by region, or non-linear dose-response factors when calculating intake and impacts. Finally, indoor emissions throughout the value chain should also be considered due to their potentially large health impacts, but this is out of the scope of this work (Hellweg et al., 2009).

2.4.4d Limitations in PM effect factor and future work

Regarding limitations on particulate effect factors and damage, preliminary analyses of recent epidemiological studies (Humbert et al., in review) suggest that the PM factor from Van Zelm et al. (2008) may be a factor three too low.

Despite the many uncertainties associated with the emissions, fate, advective transport, exposure, and impacts of pollutants, most of our concentration and exposure estimates are within an order of magnitude of measurements or high-resolution models. Moreover, a sensitivity study of the application of the PM spatial intake fraction to globally traded goods shows that while absolute intakes are sensitive to model parameters, regional and spatial patterns are not (see Chapter 4 for more details). The relative uncertainties greatly decrease for comparative applications, such as impacts among regions or among similar pollutants, making IMPACTWorld a potentially powerful tool for better quantifying impacts of global emissions and value chains.

Acknowledgements related to this chapter:

We thank Cedric Wannaz for averaging the GEOS-Chem wind data, and for helping with GIS analysis. We thank Jasper F. Kok for critical review of the manuscript. We thank the Graham Environmental Sustainability Institute, and the University of Michigan Rackham and Applied Physics graduate programs for financial support of S.S. We thank the Geneva International Academic Network for financial support of D.F.

CHAPTER 3
Food trade contribution to long-range transport of persistent organic pollutants*

3.1 Introduction

With increasing global trade, international food trade is also increasing, thereby providing a vector of long-range transport for pollutants that bioconcentrate in food. We present here an integrated model of impact assessment and global food trade to estimate the contribution of food exports to transboundary transport of persistent pollutants.

3.1.1 Motivation

For persistent pollutants, many studies examine the atmospheric long-range transport (Lammel et al., 2007; Macleod et al., 2005; Wania and Daly, 2002), yet no study to our knowledge has examined the contribution of food exports to this long-range transport. GLOBOX (Wegener Sleeswijk and Heijungs, 2010) is the only other global impact assessment model that partially accounts for food exports on a global scale, but it groups all food exports from every region to determine a globally averaged exported food concentration based on the concentrations in the exporting regions. Thus, although the GLOBOX method captures the total global pollutant intake, it does not properly allocate this intake to the consuming region (due to the information lost by grouping all exports together).

Since intake through food is a dominant exposure pathway of many persistent pollutants (Liem et al., 2000; UNEP, 2003; Wang and Needham, 2007), properly allocating food consumption has the potential to substantially change the calculated intake in each region. For this reason, accounting for food trade can help better inform decision-makers of the regional distribution of health impacts.

* This chapter was written in collaboration with Damien Friot and Olivier Jolliet.

Food is often the main exposure pathway for persistent organic pollutants, such as polychlorinated biphenyls (PCBs), polycyclic aromatic hydrocarbons, polybrominated diphenyl ethers, polychlorinated dibenzo- p-dioxins (PCDDs), and polychlorinated dibenzofurans (PCDFs) (Kazerouni et al., 2001; UNEP, 2003; Wang and Needham, 2007). More specifically, Liem et al. (2000) found that 90% of exposure to PCDDs, PCDFs and dioxin-like PCBs occurs through food consumption, mostly animal and fish products. Similarly, Kazerouni et al. (2001) found in their study population that grains and meat contributed more than half of the daily intake of benzo[a]pyrene (a polycyclic aromatic hydrocarbon).

The extent to which exported food transports particular pollutants depends on the types of food in which the pollutant bioconcentrates. For example, dioxin-like pollutants are lipophilic and bioconcentrate in animal fat, so their intake is largely determined by levels of animal product consumption (Wang and Needham, 2007). Thus, the influence of food trade on the transport of dioxin-like pollutants will depend more heavily on the levels of fish and meat trade. Benzo[a]pyrene however, bioconcentrates differently, often with most intake occurring through non-meat food (Sinha et al., 2005).

For such pollutants as those described above that bioconcentrate in food, the growth in global food trade provides an increasing vector for long-range pollutant transport, since a pollutant can enter fodder (animal feed) or food in one region and be shipped for consumption to another region. According to the Food and Agriculture Organization (FAO), food exports summed over all countries and sectors have increased from 20 million tons in 1961 to 126 million tons in 2008, with a similar increase in fodder exports (Fig. A3.1).

Pollutant transport through food has not yet been calculated, in part, due to the distinctions between life cycle impact assessment and risk assessment modeling, introduced in Chapter 1. Historically, life cycle assessment estimates total population impacts, whereas risk assessment estimates pollutant intake by specific population, but only covers small spatial scales (Pennington et al., 2006). Thus using food exports to estimate pollutant consumption by population requires integration of a typically risk assessment perspective with a model that covers global impacts.

In summary, accounting for the long-range transport of persistent organic pollutants (POPs) and thus better estimating specific population intake through food, has the potential to provide for the first time global impacts due to food ingestion from a consumption perspective as well as production perspective. This has not yet been quantified because such a study requires not only a global impact assessment model (developed in Chapter 2), but also a global model of food trade adapted for impact assessment.

3.1.2 Objectives and outline

A model is thus needed to account for pollutant transport and impacts through food, ideally in a manner that can be compared with environmental transport and impacts. In this chapter, we aim to address this gap by expanding the IMPACTWorld model developed in Chapter 2 with added components to account for pollutant transport through feed and food. Moreover, we aim to apply the expanded model to persistent pollutants in order to analyze the importance of its economic fate through food and compare it to the importance of the environmental fate through air.

We achieve these aims by first expanding the IMPACTWorld framework to account for feed and food trade, obtaining data from a global economic model of feed and food trade, and then implementing this data in the exposure portion of the IMPACTWorld model. We apply the resulting expanded model to the following two persistent pollutants that bioconcentrate in different types of food and have different global distributions of emissions: polychlorinated biphenyl-118 (PCB-118), a dioxin-like PCB, and benzo[a]pyrene, a polycyclic aromatic hydrocarbon (described in more detail below). For both pollutants, we examine the food trade contribution to the spatial intake fractions. We also use the global emissions inventories to estimate absolute regional intake of each pollutant and examine how this intake is altered by accounting for food trade.

3.2 Methods

3.2.1 Overview of methods

We calculate the food contribution to pollutant transport in IMPACTWorld by adding components to account for international trade in feed and food and subsequently calculating adjusted regional pollutant concentrations in consumed food. In practice, this amounts to embedding data from an economic model within the IMPACTWorld exposure matrix (introduced in eq. 2-1 of Chapter 2). Below, we give an overview of the elements that need to be included in an exposure matrix to account for feed and food trade. We then describe the use of an Input-Output model (presented in Chapter 1) to provide the needed elements. Finally, we present the matrix equation that links pollutant emissions to damage through environmental and economic fate and describe the methods for calculating each matrix step in detail.

The exposure matrix relates the environmental concentrations (or mass) of a pollutant to the population intake of a pollutant through a series of exposure pathways (Fig. 3.1). Including the effects of food and feed trade provides the pollutant three different routes from the environment to population intake. First, the pollutant can be taken in through air, water or fish, all of which the food trade matrix does not apply to (we discuss below the lack of availability of fish trade data). Second, the pollutant can be taken in through exposed or unexposed produce after accounting for food trade. Finally, the pollutant can enter feed, then enter an animal product after accounting for feed trade, and finally be ingested by a human (after accounting for food trade). Food and feed trade thus need to be implemented in the exposure matrix to allow for these three routes, and the next section describes the economic model that will provide this food and feed trade data.

Fig. 3.1. A schematic representing the pollutant pathways covered by the exposure matrix, from environmental compartments to population intake. The black boxes indicate the roles played by the food, feed, and population intake matrices in eq. 3-1 below. In total, there are twelve exposure pathways, covering air inhalation, drinking water, fish, produce and animal products (contained in the grey bold arrow boxes). Feed pathways are indicated by dashed arrows. Note that animals ingest not only feed that may be traded but also take in air, water, soil, and local roughage (pasture animal feed or feed that does not enter the market).

3.2.2 Expansion of IMPACTWorld using data from an Input-Output model

The ideal method of estimating pollutant transport through food would be to calculate food pollutant concentrations in the production region based on the impact assessment model, account for food processing and preparation, and then allocate this pollutant among regions based on the quantities of food exchanged. This is not possible for two reasons, First, global data in physical units expressing actual food exports between all food sectors and regions is not available. Second, the production of prepared

and processed food involves multiple steps that are increasingly spread over several regions (i.e., relying on international supply chains). The only known models able to adequately consider international supply chains are economic models of the multi-regional Input-Output (MRIO) family (Friot, 2010b). We thus adapt an existing MRIO economic model to adequately model international supply chains of food. In doing so, we use monetary values of food production and exports by sector and region as an approximation for physical quanties of traded food. To ensure coherence with physical data, we obtain the total amounts of food production and supply for each region from the Food and Agriculture Organization (FAO). The IO model is thus used to approximate the structure of the processing and trade of food between regions by assuming that the amount of food traded between regions is proportional to the amount of money spent.

To obtain the relevant food trade and feed trade data, we adapt an environmentally-extended Input-output (IO) model called TREI-C. Environmentally-extended IO models are based on data from the System of National Accounts[*] and represent the full monetary exchanges between economic sectors and the final demand (of households, government, investment and exports). TREI-C is a multi-regional input-output model, parameterized based on data for the year 2001, that estimates the economic flows associated with global trade among 19 regions (Friot, 2010b). The TREI-C model is used in the application of IMPACTWorld to global trade and is thus described in more detail in section 4.2, so only information relevant to the application to global food trade is described here.

In this application of TREI-C to food trade, we perform a series of modifications of the original matrix of economic flows to consider only flows relevant to feed and food production and exchange. The TREI-C model is based on data from the global trade analysis project (GTAP) (Dimaranan, 2006) and thus benefits from its large number of food-related sectors: seven agricultural crop sectors, three raw animal product sectors, and eight processed food sectors. Due to lack of data availability, fish trade is not included in this model. To adapt the data for the application of food and feed trade, the matrix of flows is modified to include only economic exchanges that effectively transfer pollutant along feed or food chains. For example, we set to zero the economic exchanges

[*] http://unstats.un.org/unsd/nationalaccount/sna2008.asp

from the cattle industry to the leather industry. For further details on application of the Input-Output model and assumptions made, see Appendix 3.2.2.

We then add the data matrices expressing economic feed trade and food trade as components of the IMPACTWorld exposure matrix. Thus IMPACTWorld calculates the environmental and crop pollutant concentrations as before, then accounts for the effects of the feed and food trade components, and finally calculates pollutant intake and impacts as before. Since IMPACTWorld and TREI-C have slightly different regions and food sectors, we use FAO food data by country and sector to perform regional and sector conversions when necessary.

3.2.3 Matrix framework spanning impact and trade models

To summarize the integration of the environmental and trade data:

(i) The impact assessment model calculates the concentration of pollutant emissions in feed and raw crops.

(ii) The adapted feed trade matrix from the TREI-C model is used to calculate the traded feed concentrations.

(iii) The animal product concentrations are calculated based on the impact model factors, taking into account the traded feed.

(iv) The adapted food matrix from the TREI-C model is combined with FAO data to estimate the concentrations in food after trade and processing.

(v) The impact model calculates the pollutant intake through all pathways, including the raw, traded and processed food.

Fig. 3.2 illustrates these different steps and expresses them through individual transfer matrices that relate a series of potential measurables (emissions, concentrations, intakes and damage). For each matrix, the columns represent the original regions and compartments, food sectors or exposure pathways, whereas the rows represent the destination regions and compartments, food sectors, or exposure pathways. First, the fate concentration matrix $\mathbf{FF}^{\mathbf{CONC}}$ determines the environmental pollutant concentrations, which the feed trade matrix $\mathbf{FEED}^{\mathbf{TR}}$ converts to pollutant concentrations in traded feed. The **BAF** matrix bioaccumulates the feed concentrations to estimate concentrations in

raw untraded food, and the $\mathbf{FOOD}^{\mathbf{TRPR}}$ matrix converts these to pollutant concentrations in traded and processed food. Finally, the population intake of the pollutant is calculated by multiplying concentrations in traded food by the population intake rates of each food type in each region $\mathbf{IR}^{\mathbf{POP}}$.

Fig. 3.2. Overview of the model steps to estimate pollutant exposure and damage accounting for feed and food trade. Matrices link the sample regions and compartments provided as measurables, where 'IMPACT' and 'IO' represent, respectively, the regions and sectors associated with the impact assessment and economic (input-output) models. Any kg unit without a subscript represents pollutant mass. Transfers between the two sets of regions and sectors in the IO and IMPACTmodels are carried out by conversion matrices.

Translating this into a matrix equation form, the pollutant intake *I* is a product of the spatial intake fraction and emissions, and the spatial intake fraction is a product of the fate and exposure matrices (section 2.2.2a and Rosenbaum et al. (2007)). As illustrated in Fig. 3.2, the pollutant intake equation and intake fraction of eq. 2-1 are expanded here as follows:*

$$\vec{I} = \overbrace{\underbrace{\mathbf{IR}^{\mathbf{POP}} \cdot \mathbf{FOOD}^{\mathbf{TRPR}} \cdot \mathbf{BAF} \cdot \mathbf{FEED}^{\mathbf{TR}}}_{\text{exposure matrix, } \mathbf{XP}} \cdot \mathbf{FF}^{\mathbf{CONC}}}^{\text{intake fraction, } \mathbf{iF}} \cdot \vec{E} \qquad 3\text{-}1$$

where the annual emissions to each region $\vec{E}$ (kg_{emit}/yr) (assumed steady state) are converted to an environmental concentration by the fate matrix $\mathbf{FF}^{\mathbf{CONC}}$ (units of $(kg/kg_{env})/(kg/yr)$). The matrix $\mathbf{FEED}^{\mathbf{TR}}$ (units of $(kg/kg_{feed\text{-}tr})/(kg/kg_{env})$) then converts environmental concentrations to feed concentrations after accounting for trade, after which the bioaccumulation factor matrix **BAF** (units of $(kg/kg_{food})/(kg/kg_{feed})$) converts the traded feed concentrations to animal product concentrations. Note that $\mathbf{FEED}^{\mathbf{TR}}$ and **BAF** only affect the feed concentrations and leave the air, water, fish and food crop concentrations unchanged. The $\mathbf{FOOD}^{\mathbf{TRPR}}$ matrix ($kg_{food\text{-}tr}/kg_{food}$) calculates the change in concentrations due to food trade and processing from production to consumption regions, and is then multiplied by the population intake rate matrix $\mathbf{IR}^{\mathbf{POP}}$ (kg_{in}/yr) to complete the spatial intake fraction matrix. ($\mathbf{FOOD}^{\mathbf{TRPR}}$ only affects the concentrations in food sectors that can be traded or processed.) The feed and food trade matrices do not affect the total global pollutant intake through food – they merely redistribute the intake to the region of consumption rather than allocating it to production region.

3.2.4 Sequence of matrices from environmental concentrations to intake

Having provided an overview of the matrix framework integrating the impact assessment and economic food trade models (Eq. 3-1), this section provides a detailed

* Note that to help the reader easily distinguish each matrix term, dot products are used here to indicate multiplications between matrices and vectors. Matrices are indicated by bold capitalized letters and vectors are indicated by italicized elements topped by an arrow. Elements of matrices or vectors are italicized.

description of the model outlined above by describing each matrix in the sequence that links environmental concentrations to population intake (Fig. 3.2).

3.2.4a Fate concentration matrix

The IMPACT model calculates pollutant fate and environmental concentrations as described in section 2.2.2c, thereby linking emissions in the region of emission to the concentration of a receiving region. The traditional fate matrix calculates pollutant mass in each environmental compartment, but we take it one step farther here to calculate pollutant concentrations. This matrix, $\mathbf{FF}^{\mathbf{CONC}}$, is simply a product of the fate matrix defined earlier and the diagonalized matrix of the inverse environmental compartment masses, thus yielding pollutant concentrations in the environment. See Appendix A3.2.4a for more details.

3.2.4b Feed trade matrix

The physical feed trade matrix, $\mathbf{FEED}^{\mathbf{TR}}$, expresses the resulting feed concentration in each receiving region as a weighted average of the feed concentrations in all imported and locally produced feed. Ideally, this average would be weighted by accurate data on physical feed exports, but these are not available. Thus we use the reliable data on economic food trade to estimate trade in feed, as described in Appendix A3.2.2. Note that feed made from animal products and trade of this feed is not currently included in the model.

The economic feed trade matrix links IO regions and sectors, so the concentrations in IMPACT regions need to first be multiplied by conversion matrices before the IO matrix can be applied. First, the pollutant concentrations in the environmental vegetation compartments (vegetation leaf, surface and stem) are multiplied by FAO production data to calculate pollutant masses in food by FAO crop. FAO data for the year 2001 is used throughout to match the economic data from the TREI-C model. IMPACT regions are then converted to IO regions based on intersecting FAO crop production. Then FAO crops are aggregated to IO feed sectors so that the economic feed trade matrix can be applied.

Finally, we approximate feed transfers between regions based on the dollars spent by each region's meat industry on every other region's raw feed sectors. Detailed descriptions of each part of the feed trade matrix calculation are provided in Appendix A3.2.4b.

3.2.4c Bioaccumulation from feed to food

Once the pollutant concentrations in traded feed are calculated, we calculate the bioaccumulation in the animals ingesting the feed. We account for this using the bioaccumulation factor matrix, **BAF**, which expresses the factors linking feed concentrations to concentrations in raw animal products derived from animals that ingest this feed (with units of $(kg/kg_{food})/(kg/kg_{feed})$). The bioaccumulation factor linking each feed sector to each food sector is the product of the animal's intake rate of feed, IR^{feed} (kg_{feed}/day), with the animal's biotransfer factor *BTF* for the considered pollutant (units of $(kg/kg_{food})/(kg/day)$) (Rosenbaum et al., 2009). Animal intake rates of feed vary widely, but previous IMPACT versions have determined average intake rates (Pennington et al., 2005). These are adjusted here for each region based on the regional feed availability and animal production (both of which are provided by FAO data). See Appendix A3.2.4c for further description of the adjusted intake rates and graphs of relevant aggregated values.

3.2.4d Food trade matrix

The physical food trade and processing matrix, $\mathbf{FOOD}^{\mathbf{TRPR}}$, calculates the adjusted pollutant concentrations in each consuming region's (raw and prepared) food due to processing and trade. It does so by expressing the food concentration after trade and processing, as a weighted average of the concentrations in food from the importing regions. As was done for the feed trade matrix above, $\mathbf{FOOD}^{\mathbf{TRPR}}$ is calculated by combining several intermediary region and sector transformation matrices with the economic food trade matrix ($\mathbf{FOOD}^{\mathbf{TRPR\text{-}IO}}$).

For a pollutant mass in a given IO region and raw food sector, $\mathbf{FOOD}^{\mathbf{TR\text{-}IO}}$ calculates the the regions and sectors to which that pollutant is distributed by food trade and processing. $\mathbf{FOOD}^{\mathbf{TRPR\text{-}IO}}$ effectively allocates food based on the monetary

exchanges between food sectors and regions, distributing raw food to two potential endpoints – domestic and foreign consumers in each region – in the form of raw or processed food items. This ultimately results in a matrix of food distribution from the production region to consumption region.

The effects of accounting for food trade are evaluated by comparing results to analogous calculations that assume no food trade. In the case of the $\mathbf{FOOD}^{\mathbf{TRPR\text{-}IO}}$ matrix, the version that doesn't account for food trade still allocates raw foods to processed sectors, but within the same region of raw food production.

The economic food trade matrix does account for food losses due to trade and processing, but does not yet account for any decreases in pollutant concentrations due to food processing (or cooking). As discussed above, the food losses between production and market are captured by adjusting the consumption data to match the FAO food supply. The global loss fractions are presented in section 3.3.1.

More detailed explanations of all methods described here are provided in Appendix A3.2.4d.

3.2.4e Population intake rate

Once the pollutant concentrations in traded and processed food are available, the intake rate matrix ($\mathbf{IR}^{\mathbf{POP}}$) calculates the actual pollutant intake for each consuming region and impact pathway. $\mathbf{IR}^{\mathbf{POP}}$ is simply a diagonal matrix of the population intake rates for each region and food pathway, based on the same FAO food supply data used in $\mathbf{FOOD}^{\mathbf{TRPR}}$ (thus the intake rates are consistent with the food consumption rates used to allocate food trade and processing). In the scenario that doesn't account for food trade, the food is assumed to be eaten somewhere, and impacts are allocated back to the region of raw food production. Losses from market to consumer intake are not considered here. See Section A3.2.4e for more details.

Thus the distribution of actual food from the production region to consumption region is the product of $\mathbf{FOOD}^{\mathbf{TRPR}}$ (the physical food trade and processing matrix which allocates producing food to consuming regions) and $\mathbf{IR}^{\mathbf{POP}}$ (the annual population intake rate of food).

3.2.5 Quantities examined and pollutants addressed

The matrices described above are used to calculate and compare pollutant spatial intake fractions for the scenarios accounting for no trade, feed trade and food trade (and combined feed and food trade). For these scenarios, we examine the transboundary transport of intake from a regional emission (i.e., the portion of the intake fraction that is ingested outside the region of emission). Moreover, we determine the portion of pollutant intake from each regional emission that travels through food export before being ingested. Finally, we calculate the change in absolute intake in each region due to global food trade.

We first apply the food export calculations to polychlorinated biphenyl-118 (PCB-118), described in detail in section 2.2.3a. PCB-118 is chosen because of its relatively high toxicity, and, most importantly, it has a published global emissions inventory (Breivik et al., 2007) that allows examination of the effects of food trade on absolute intake. Moreover, previous application of IMPACTWorld yielded globally distributed environmental and food concentrations generally within an order of magnitude of measurements (section 2.3.1).

In addition to PCB-118 application, we also apply the model to a different type of persistent pollutant, benzo[a]pyrene (B[a]P). B[a]P is a polycyclic aromatic hydrocarbon listed as carcinogenic to humans by the International Agency for Research on Cancer (Boyle et al., 2008). B[a]P is chosen because, in contrast to PCB-118, it bioconcentrates in vegetable produce more than fish. Fish trade is not currently accounted for, thus we expect food trade to shift pollutant intake for B[a]P more than for PCB-118. Moreover, a B[a]P global emissions inventory is available for the year 2004 (Zhang and Tao, 2009). Finally, the global emissions of B[a]P occur mainly in China and India, in contrast to the dominantly European and American emissions of PCB-118 (Fig. 3.3).

Application of the IMPACT framework to B[a]P has been evaluated for the North American and Great Lakes versions of the model (Humbert et al., 2009; Jolliet et al., 2008). Results for the global application, however, should be interpreted cautiously as it has not yet been evaluated on a global scale.[*] Thus, rather than provide an absolute

[*] As a preliminary check of the model predictions, the model's estimated U.S. intake is compared to a study on the intake distribution by food type (Sinha et al., 2005) to verify the basic intake pattern observed.

measure of global B[a]P intake, the objective of the model application to B[a]P is to demonstrate how food trade can shift impacts differently for different types of pollutants with different global emissions profiles.

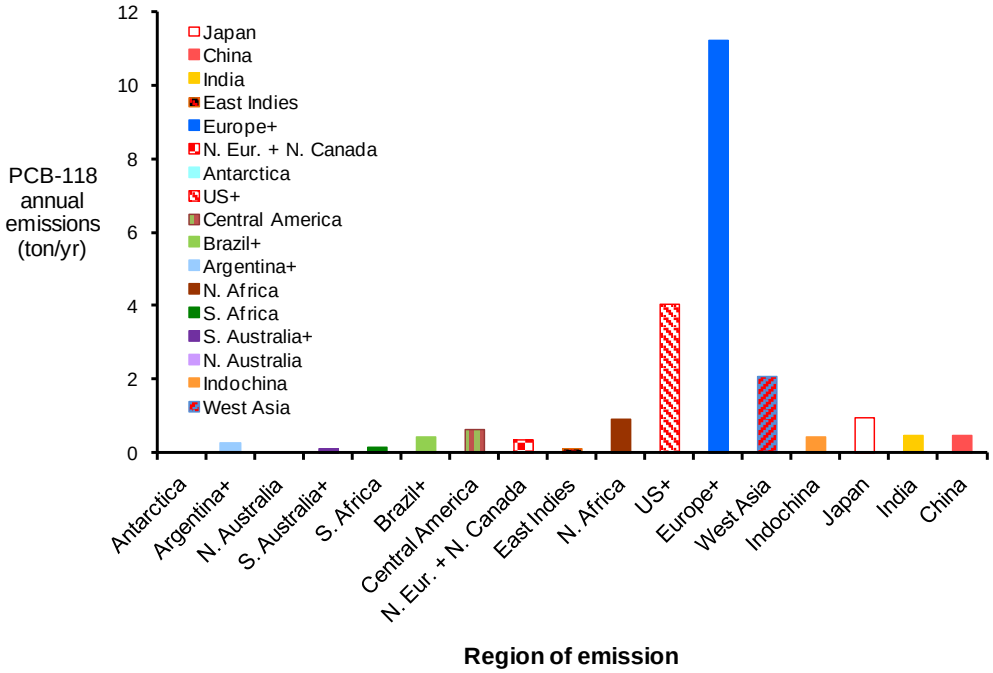

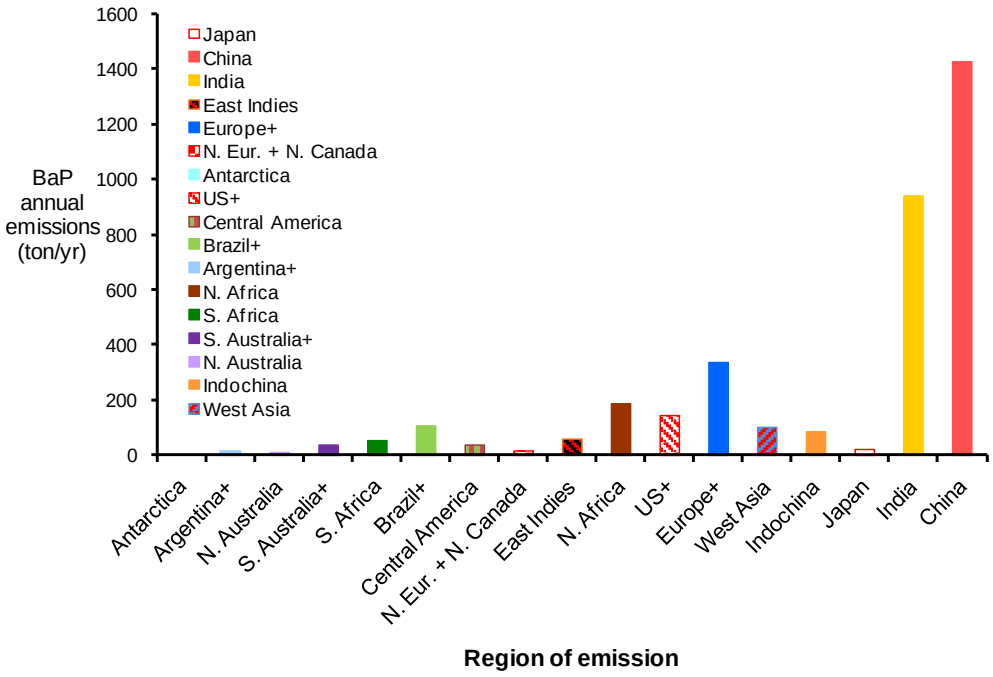

Fig. 3.3 Annual emissions for PCB-118 (year 2000 (Breivik et al., 2007)) and benzo[a]pyrene (year 2004 (Zhang and Tao, 2009)). PCB-118 emissions occur mainly in US and Europe, whereas B[a]P emissions occur mainly in China and India.[*]

3.3 Results

Results for application to PCB-118 and B[a]P are obtained for each step in the integrated model, including each measurable and transfer matrix listed in Fig. 3.2. Here we focus on the distribution of food due to food trade and the subsequent contribution of food trade to the pollutant spatial intake fraction and absolute intake. Additional intermediary results are provided in Section A3.3.1. It is important to note that in all results presented below, the contributions of feed and food trade never affect the total global intake – they merely redistribute the pollutant for intake in different regions. (In reality, food waste from market to table will differ by country, but this is not accounted for here.)

3.3.1 Distribution of food due to food trade

The amount of pollutant transported through food is of course limited by the total amount of food transport. This food distribution (summed over all food sectors) is shown in Fig. 3.4, where the total food produced in each region is allocated to all other regions based on consumption. Note that the food consumption values shown here already account for food losses from production to market, which range from 2% to 49% depending on the food pathway (Table A3.4).

Fig. 3.4 shows that Australia has the maximum fraction of food exported, with 72% of non-fish food production shipped to other regions. The U.S. also has a relatively high fraction, with 34% of food exported, in contrast to China, which exports 3% of its food by mass. An average of 12% of global food is exported. This is consistent with the FAO global estimate that 11% of produced food is exported from the region of

[*] Note that the emissions for B[a]P are based on emissions by country that are grouped into IMPACT regions. In cases where countries span IMPACT regions, emissions were allocated based on population distribution.

production (FAO, 2000). Section A3.3.2 provides additional comparisons as well as the IO trade matrix used to generate these results.

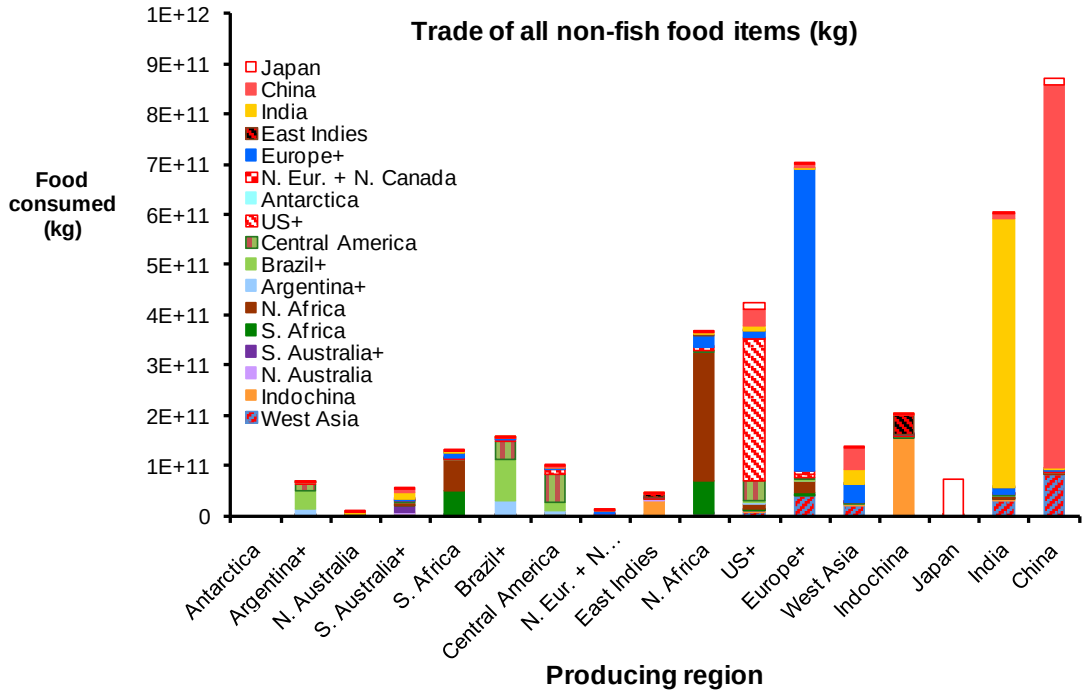

Fig. 3.4. Food distribution matrix illustrating the total amount of food produced in each region that is eventually sold as food, either in the original region or exported to a different region.[*]

3.3.2 Changes in local shares of each regional intake fraction

Having shown that a substantial portion of food is exported from the region of production on a global scale, we now aim to determine the extent to which food exports influence trans-boundary transport of pollutants. To do so, we first examine the "exported" iF portion for each region in each food trade scenario. The exported iF portion is the percentage of a region's intake that is ingested outside the region of emission. Fig. 3.5 shows the change in each region's exported iF portion for each food and feed trade scenario. Note that the exported iF portions are slightly overestimated, because the

[*] Note that the original food distribution data is provided for IO regions and implemented in the model by IO region to decrease the errors associated with conversions between sets of regions. Here, the food distribution data has been transformed to IMPACT regions to illustrate the contribution of the food trade to the intake fractions by IMPACT region (Fig. 3.6). In Fig. 3.4, exports appear slightly higher than actually calculated in the model due to the conversions between different sets of regions. Fig. A3.17 shows the actual food distribution matrix used with percentages for each IO region, which are the percentages quoted in the main text.

conversions between sets of regions cause some false exports due to imperfect overlapping (region overlap shown in Fig. A3.3). However, regional conversions are performed in all scenarios, so the relative change in exported iF portions between scenarios is a real effect due to trade.

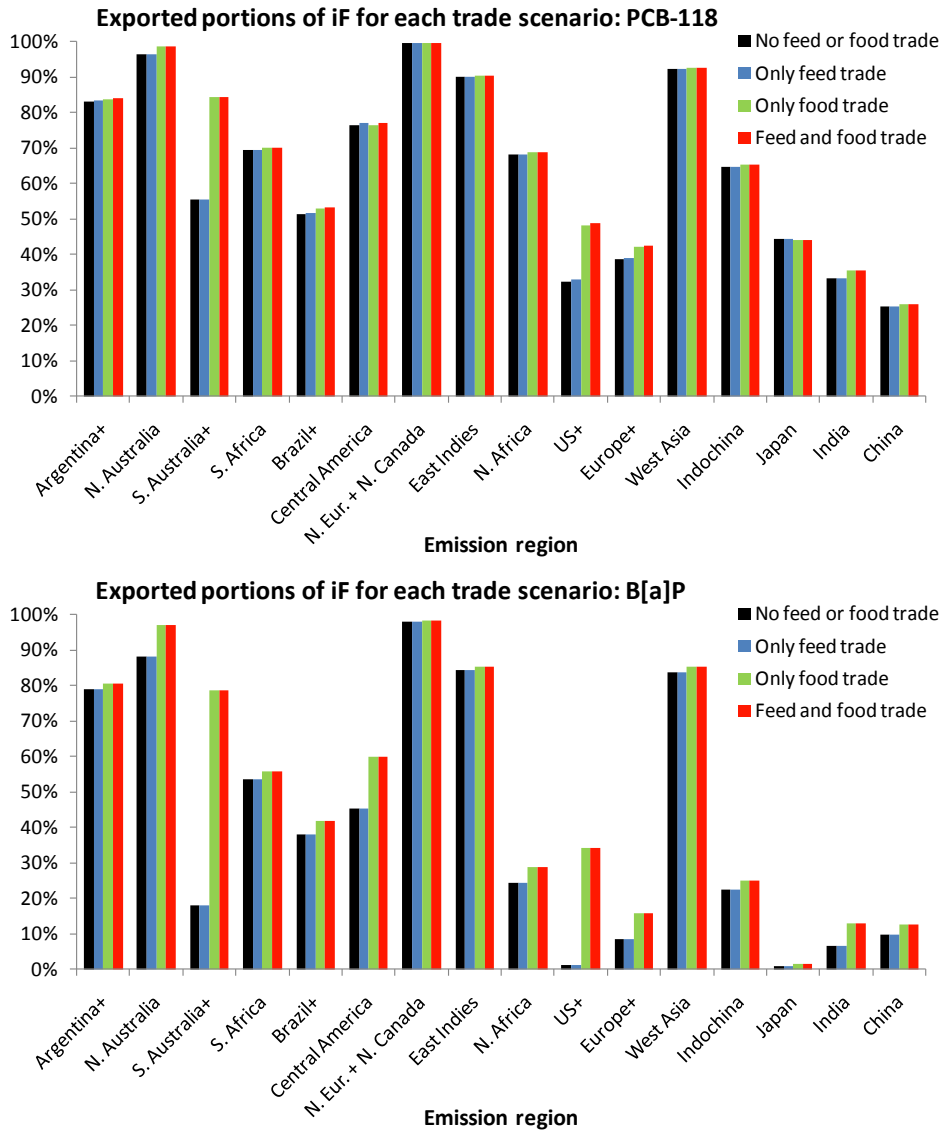

Fig. 3.5 Accounting for feed and food trade increases the amount of transboundary transport leading to intake. Exported portions of intake to the rest of the world are shown for each of the four scenarios with varying levels of feed and food trade.

In Fig. 3.5, we first consider the exported iF portions of PCB-118 and B[a]P by atmospheric advection that do not account for feed or food trade (black bars). Consistent with the results in section 2.3, PCB-118 has relatively high exported intake due to high

levels of intercontinental transport, with the exported iF portion ranging from 99% in the sparsely populated Northern Europe region to 25% in China, with a median of 66%. B[a]P, on the other hand, has lower intercontinental transport, with the exported share of the intake fraction ranging from 98% in Northern Europe to 1% in US+ and Japan, with a median of 31%.

When feed trade is accounted for (blue bars in Fig. 3.5), the exported iF portions increase only slightly, suggesting that feed trade on sub-continental scales has negligible contribution to inter-continental pollutant transport for the two pollutants considered here. This is consistent with the limited inter-region monetary exchange for feed (Fig. A3.10), and the finding that traded feed accounts for less than 1% of the animal intake rate.

In contrast, Fig. 3.5 shows that accounting for food exports increases the exported iF portion of many regions (green bars). For PCB-118, Southern Australia shows the largest increase in exported iF portion (29%), with increases also in the US and Europe. For B[a]P, accounting for food exports has a much greater effect on pollutant transboundary transport, increasing the exported iF portion in Australia and the U.S. by 61% and 33% respectively.

Fig. 3.6 delves into the more region-specific effects of accounting for food trade, showing the spatial intake fractions of PCB-118 and B[a]P, with the black outline indicating the portion of the intake fraction that has at some point travelled between regions through food. The portion of the iF not transported through food represents pollutant ingestion through either locally produced items or fish (since fish are not yet accounted for in the economic trade matrices). Note that pollutant can be transported out of the emitting region through the environment and then re-imported in the form of food (explaining, for example, the European intake of what was originally a European emission after food trade).

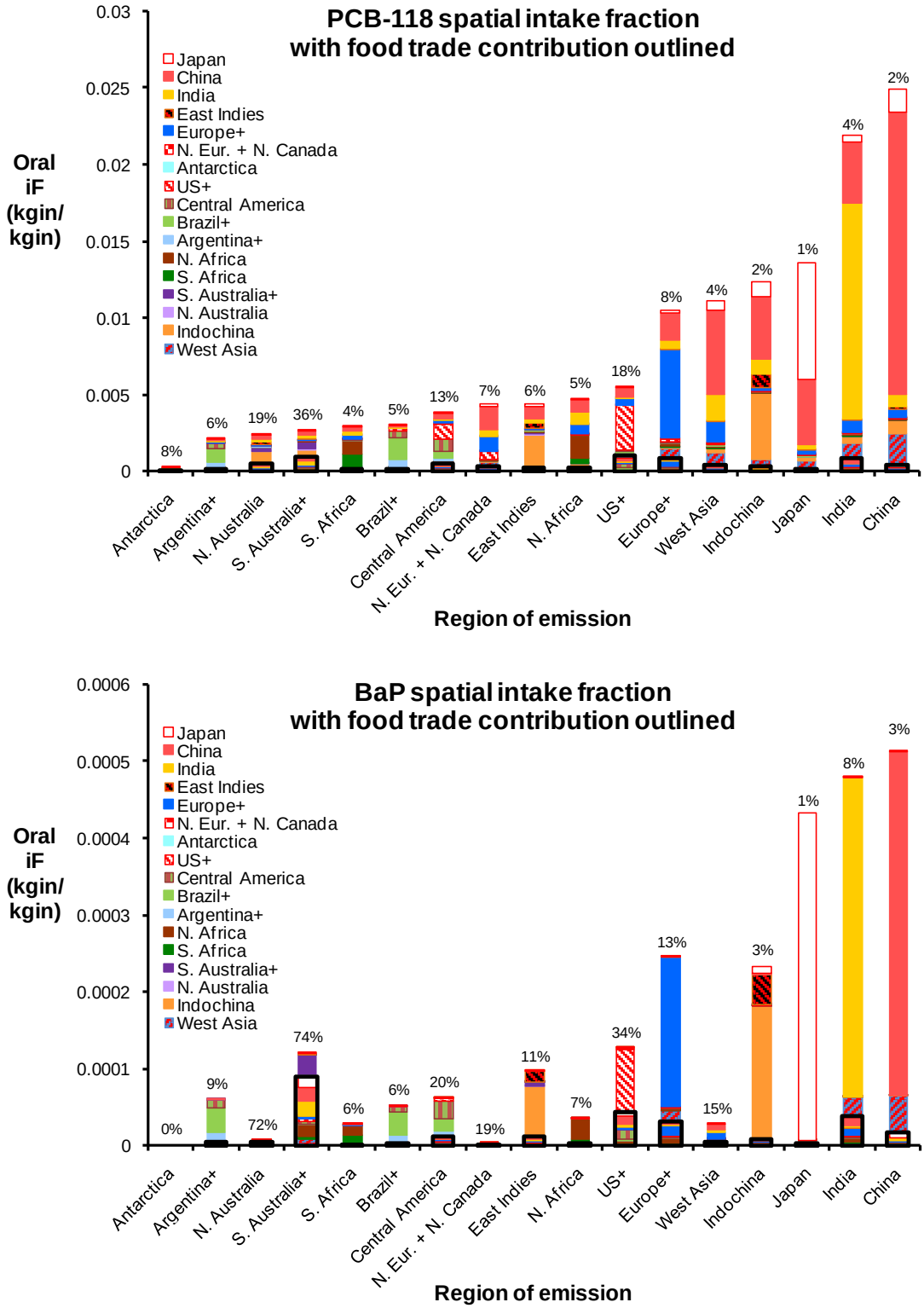

Fig. 3.6. Spatial intakefractions showing the oral ingestion in each region as a fraction of an emission in the region along the x-axis. The portion of each intake fraction that has been exchanged in food trade is outlined in black and expressed in percentages above each bar.

For PCB-118 intake fractions, Fig. 3.6 shows that the amount of pollutant transported between regions through food varies between 1% (Japan emissions) and 74% (South Australia), with a median of 6%. These percentages of pollutant export through food differ from the percentages of actual food exports (Fig. 3.4) due to two major reasons. First, pollutants bioconcentrate differently in different foods, therefore the total export of pollution is not a constant proportion of the total export of all food. More importantly in the case of PCB-118, the food distribution based on food trade shown in Fig. 3.4 does not account for fish trade, and PCB-118 has fish as a major intake pathway, as shown in Fig. 3.7. As a result, Fig. 3.6 exhibits a higher percentage of pollutant transported through food trade in regions where fish is not the dominant pathway (i.e., the U.S., Central America, and Southern Australia).

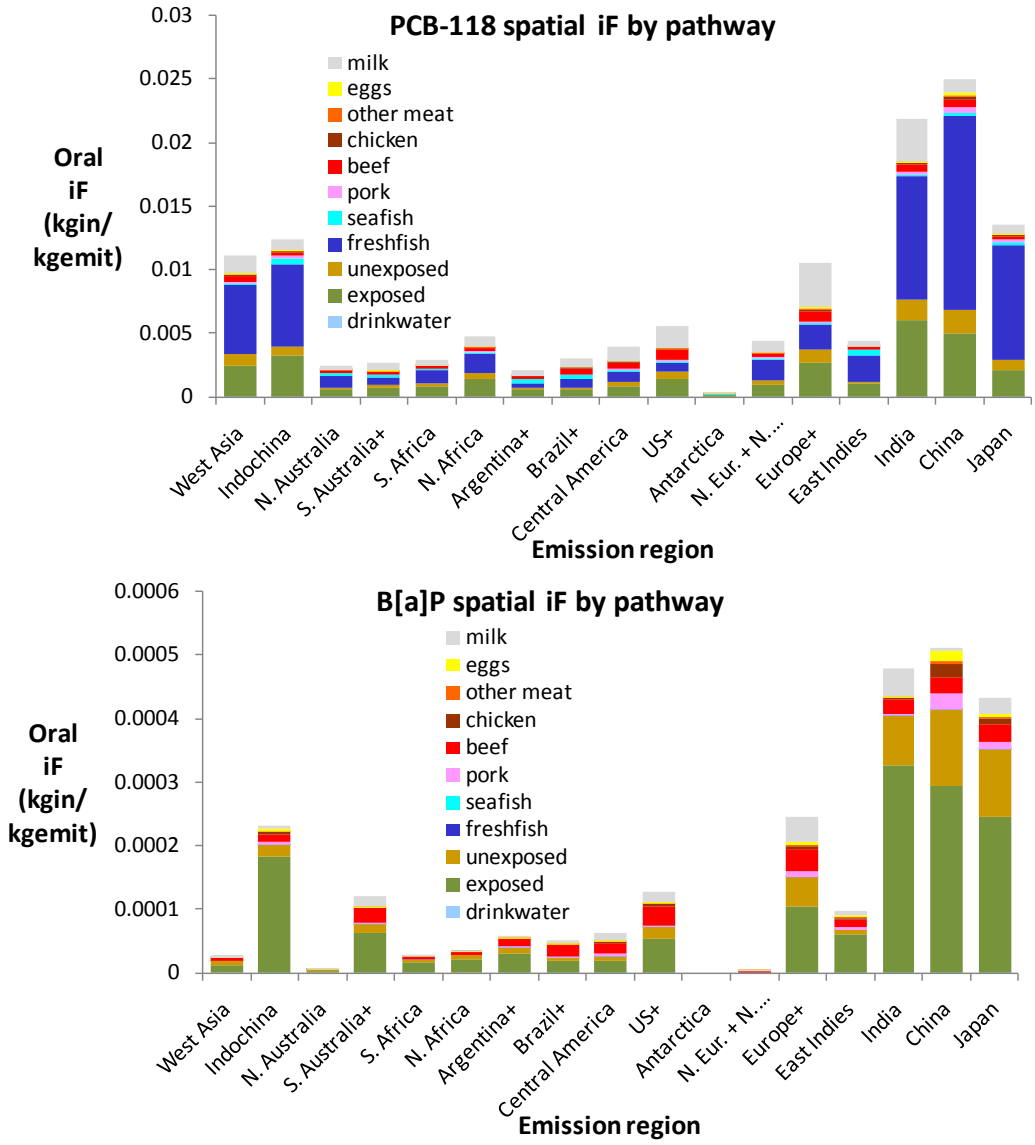

Fig. 3.7 Spatial intake fractions by exposure pathway[*] for PCB-118 and B[a]P[†]. (Note the different vertical scales.)

In contrast to PCB-118, Fig. 3.7 model results show that benzo[a]pyrene has most intake occurring through exposed and unexposed produce, with almost no intake through fish.[‡] So B[a]P intake is dominated by non-meat products, and the global food

[*] Note that inhalation is not included here as it accounts for less than 0.1% of intake, and it shouldn't be compared with ingestion intake since effects can differ.

[†] Since B[a]P has only been evaluated for specific regions of the IMPACT model, this figure is only a preliminary result of regional variation in the intake fractions.

[‡] In particular, we find that about 70% of the US intake fraction of B[a]P occurs through produce or dairy. This value falls within the wide range found in one U.S. study that 35-99%[‡] of B[a]P intake from food

distribution of non-meat products is very similar to that of all food (Fig. A3.18). It is therefore not surprising that for each region, the portion of the B[a]P intake fraction that travels through food exports (Fig. 3.6) is similar to the total portion of food exported (Fig. 3.4). In particular, Southern Australia and the U.S. both have similar percentages of food exports and the portion of B[a]P that experiences transboundary transport through food (close to 72% and 34%, respectively).

3.3.3 Changes in absolute intake by region due to food trade

Having determined the contribution of food transport to the spatial intake fractions of the two pollutants, we turn to absolute intake. We first multiply the spatial intake fraction by the global emissions inventories (Fig. 3.3) to yield the absolute pollutant intake in each region (Fig. 3.8). The total intake in each region is expressed as the sum over emission regions (the "receiving perspective" introduced in section 2.2.2). For PCB-118, the absolute annual intake by region accounting for food trade ranges from 0.1 kg in Northern Australia to 74 kg in Europe, the dominant emitter. Transboundary transport is evident, as shown by China's high intake due largely to emissions from Europe (discussed in Chapter 2). For B[a]P, China is the dominant emitter, thus it hast the largest intake of 651 kg (with a low of 0.2 kg in Northern Australia). B[a]P also has less overall transboundary transport than PCB-118.

---

occurs through non-meat products (Sinha et al., 2005). The median values of non-meat and meat intake in the single city studied yield a value of 94%.

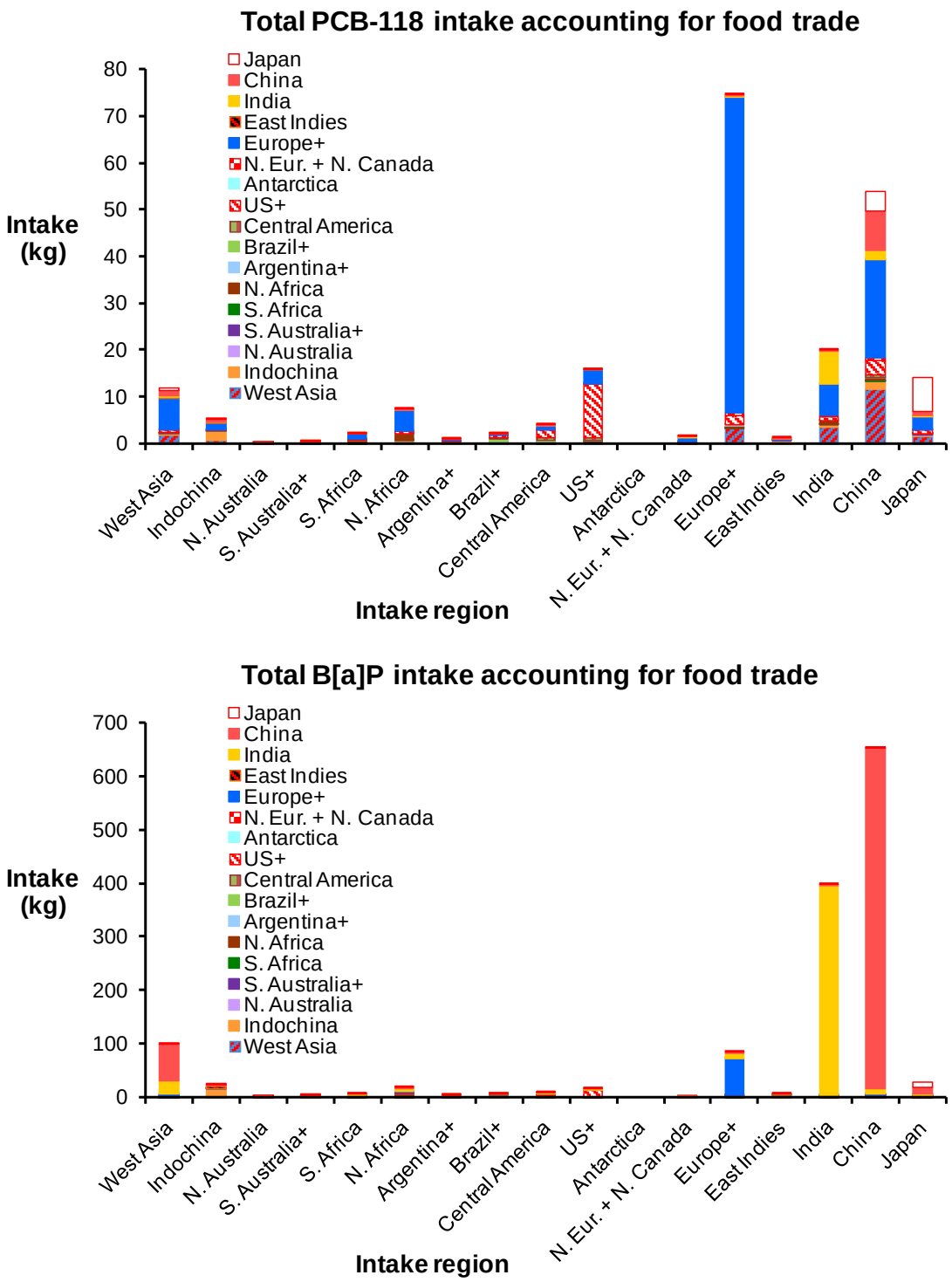

Fig. 3.8 Absolute intake is shown for both pollutants by intake region, with colors to indicate the original emitting region.

We now show how accounting for food exports in the consumption perspective yields results that differ from the traditional production perspective by calculating the difference in population intakes with and without (Fig. A3.20) accounting for food trade. Note that the consumption perspective may yield different regional intake from the production perspective, but it does not change absolute global intake. Fig. 3.9 shows that allocating food by consumption decreases pollutant intake allocated to Europe by 5 kg. We also find that the percentage change in intake by region can be substantial even if the absolute values are small, with food exports increasing pollutant intake allocated to Central America by up to 50%. Most PCB-118 emissions occur in the US and Europe (Fig. 3.3), which are also regions with relatively high food exports, resulting in the US and Europe exporting their contaminated food to Northern Africa, Central America, India, China and Japan.

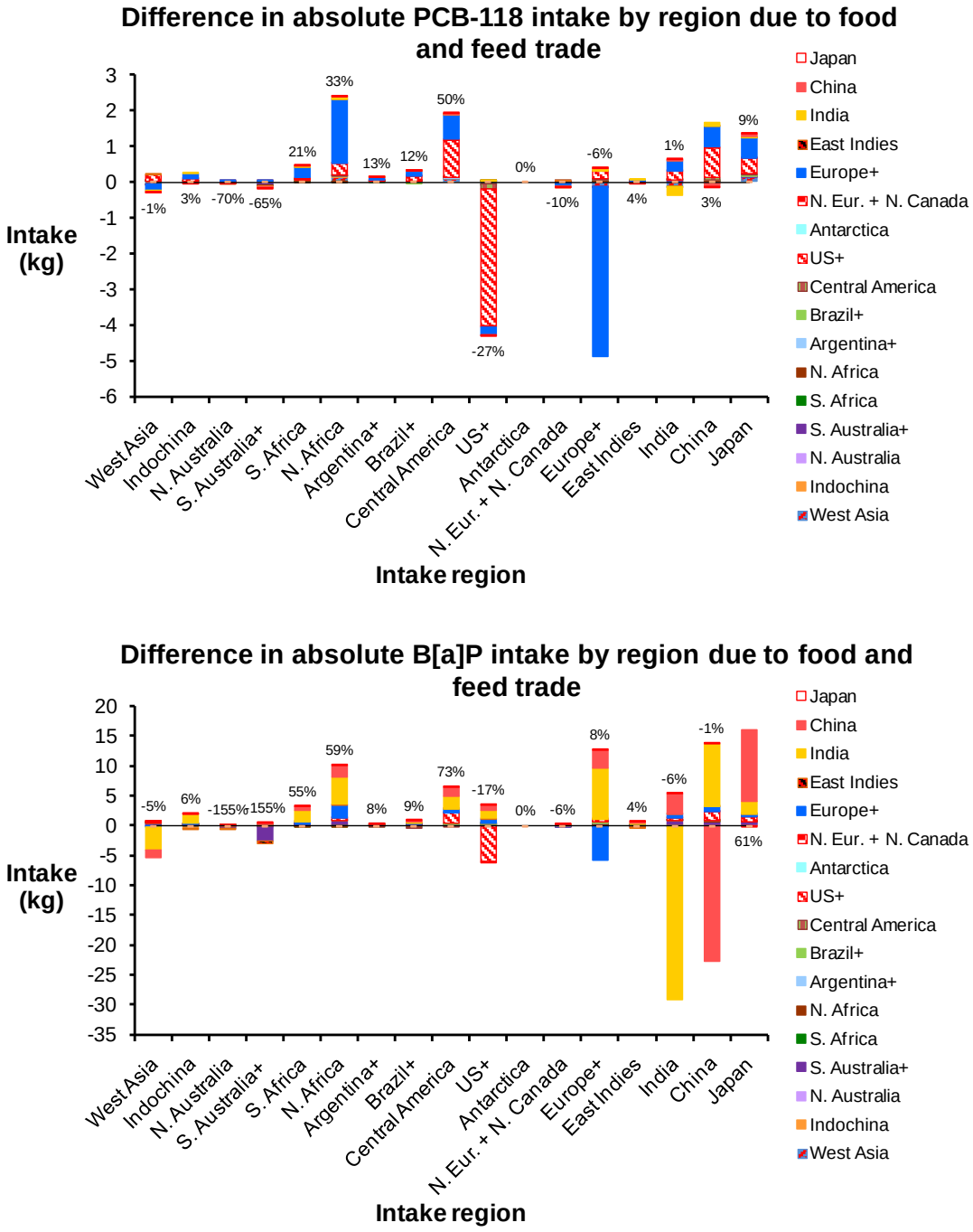

Fig. 3.9 Differences in absolute pollutant intake for each intake region due to accounting for food exports are shown here. The intake change in each region is expressed as a sum of the changes from each emitting region. Negative numbers indicate that accounting for food trade decreases the absolute intake in the considered region. Percentages indicate the total percentage change in absolute intake for each region.

In contrast to PCB-118, benzo[a]pyrene has most emissions in China and India (Fig. 3.3), both of which export relatively small fractions. However, since China and India produce large amounts of food, they still export substantial amounts of pollutant to Northern Africa (6.5 kg), Central America (3.7 kg), Europe (11.6 kg), and Japan (14 kg), which can represent a large share of the local intake.

3.4 Conclusions and discussion

The framework developed here achieves the objectives of enabling the modeling of fate in the economy in a similar way to the fate in the environment, and thus for the first time estimates global impacts by region of food producer and and region of ultimate food consumer. We address the emitter and receiver perspectives by introducing the historically risk assessment focus of region-specific consumption into a global impact assessment model. This allows the effects of food trade on pollutant intake to be assessed and compared to those of air transport. We discuss here the main conclusions of the model application to PCB-118 and B[a]P, and then outline future work on refining and applying the model.

We find that due to the limited food trade between the sub-continental regions considered here, pollutant transport through food exchange is generally smaller than that through air for PCB-118, benzo[a]pyrene (except in Southern Australia), and probably most other pollutants. Accounting for food exports, however, can still substantially alter pollutant intake patterns between the production and consumption perspectives. The inclusion of food trade decreases the allocated share of a region's PCB-118 iF by up to 29%, which is still smaller than but comparable to the intercontinental transport effect of up to 75%. For B[a]P, accounting for food exports increases the iF allocated to outside regions by up to 61% in Southern Australia, which is more than the 18% due to atmospheric transport. Similarly, regions that import a lot of food can greatly change the amount of allocated impacts between the production and consumption perspectives. For example, the U.S. and Europe have high PCB-118 emissions, so their food exports combine to increase Central American PCB-118 intake by 50%. Similarly, food exports

from China, India and Europe serve to increase the B[a]P intake in Northern Africa by 59%.

We also find that the global food trade distribution from producing to consuming regions, which represents the shifts in food intake by region, is not sufficient to allocate pollutant intake to the consumption region. Different pollutants bioconcentrate in, and subsequently have intake fractions through, different food pathways (Bennett et al., 2002a), so the dominant exposure pathways determine to what extent food exports can shift pollutant intake between production and consumption perspectives. Thus a model such as ours that implements food trade into an impact assessment framework is needed to fully understand the effects of food trade.

Multiple directions for future work are suggested by the model application presented here, including refinement and application of the current tool, as well as suggestions for future development of the economic model and the integrated model as a whole.

To begin with, the model framework can be applied to any pollutant with known environmental intermedia partitioning coefficients and degradation rates. This flexible capability of the model should be used to evaluate a set of test chemicals, which can then be used to determine for which chemicals and regions food trade is important (e.g., when the chemical bioconcentrates sufficiently more in vegetation and animal products rather than water). This work can begin by expanding upon the model evaluations of B[a]P in US and Europe to perform a global evaluation,, since the current study suggests that trade can substantially affect the intake patterns of B[a]P.

Furthermore, although the model framework can be applied to other well-specified pollutants, global emissions inventories are only available for a few pollutants. Since we find that food imports can greatly increase the pollutant intake allocated to a given region, a country may be missing a large portion of its population intake if it is only accounting for intake of domestic emissions. Governments should thus support investigation of globally distributed emissions (especially in regions from which much food is imported) to better quantify transboundary transport of pollutants through air, water and now food.

To further improve the economic model of food trade, the link between sector spending and actual food or feed should be better established. Another important improvement of the economic model would be the inclusion of fish trade, since many persistent pollutants bioconcentrate in fish, and fish account for a large portion of global food exports (Buzby, 2003). In addition, a future model version can also account for animal and fish farm feed in the economic model. Finally, the existing economic model is based on data from the year 2001, since which time global feed and food exports have increased by 50% (Fig. A3.1). Thus the values presented here are likely conservative estimates of the current impacts of food trade, and the data should be updated to examine the subsequent increase in the effect of food trade.

The final recommendations outline and address some of the uncertainties in the expanded model as a whole. Aside from the uncertainties in PCB-118 inventories and impact assessment discussed in Chapter 1 and 2, the necessary linkages of multiple models and datasets require many assumptions. These have been verified to yield sensible results at each step but should still be refined and improved where possible to obtain more accurate results. The largest contribution to uncertainty in the final results is likely due to the estimate of physical food trade based on economic flows between regions and sectors, which needed to be adjusted to ensure that the product of the FAO-provided food production data and the food trade matrix yielded the FAO-provided food consumption data. This required correction factors between 0.01 and 100, implying that the actual level of food trade could differ by this amount.

To address some of these uncertainties, an improvement for both aspects of the model is to refine it to the country level, which would decrease the uncertainties introduced by regional conversions and may also result in the effects of feed trade becoming detectable. At the country level, food trade will also increase, as will the inter-regional transport of pollutants through the environment, so the relative magnitude of the two would be interesting to compare. Another improvement to address the linkage between the two models is to better match the impact assessment food pathways with those from FAO or GTAP, which would also decrease uncertainties associated with the conversions between food sectors.

Acknowledgements related to this work:

We thank Jasper Kok for critical feedback on the manuscript. We thank the Graham Environmental Sustainability Institute and the University of Michigan Rackham graduate program for financial support.

CHAPTER 4

Quantification of environmental impacts on human health due to global production and consumption chains*

4.1 Introduction

Assessing environmental health impacts induced by consumer goods and services in a globalized economy requires a) accounting consistently for the impacts along global production-consumption chains, and b) considering not only long term global pollutants and impacts (like greenhouse gas emissions and climate change), but also short term local and regional pollutants and their impacts (like human health impacts of particulate matter).

When computing emissions of products (goods and services) over their entire life cycle, direct and indirect emissions must be considered. To avoid double counting, the classical territorial perspective (used in the Kyoto protocol) must be complemented with additional allocation schemes (Peters and Hertwich, 2008). Consumption-centered schemes, such as Environmentally Extended Input-Output (IO) models (Leontief, 1936), can be used to compute the so-called embodied emissions by re-allocating direct emissions from inventories to products within a given economy. IO models have rapidly developed in the last five years, evolving from simplified single-country models with multiple pollutants to multi-country models with partial or full trade linkages (Wiedmann et al., 2007), thereby substantially improving the robustness of the re-allocation of emissions among goods and countries (Lenzen et al., 2004). Existing multi-region models have so far generally been applied to global emissions such as greenhouse gases. Such

* This chapter is a manuscript currently in review at *Science*, co-authored with Damien Friot and myself as first and second main authors, Gabrielle Antille, Suren Erkman, Hy Dao, Sebastien Humbert, Stefan Schwarzer, Lucien Wald & Olivier Jolliet.

applications have demonstrated the inter-country variability of carbon intensities associated with production and have found that, on average, 22% of total CO2 emissions induced to meet the demand of a country for consumer goods take place outside its borders (Peters and Hertwich, 2007a).

The inter-country variability of health impacts from toxic emissions associated with global trade is expected to exceed that of carbon emissions due to large disparities in emission control technologies, as well as in the toxicity, mobility and population exposure of emitted pollutants (Rochat et al., 2006). Pollutant transport models for Europe have shown that trans-boundary transfers can be large; for example, as much as 60% of the concentration of primary particulate matter in Germany is due to transport from outside Germany (Klein et al., 2007).

To date, no model integrates production, consumption and trade, while quantifying pollutant fate, exposure and impacts at the global scale. To estimate and consistently allocate environmental health impacts, we developed the first spatially-explicit integrated model describing this full causal chain from consumption to environmental health impacts (Fig. 4.1).

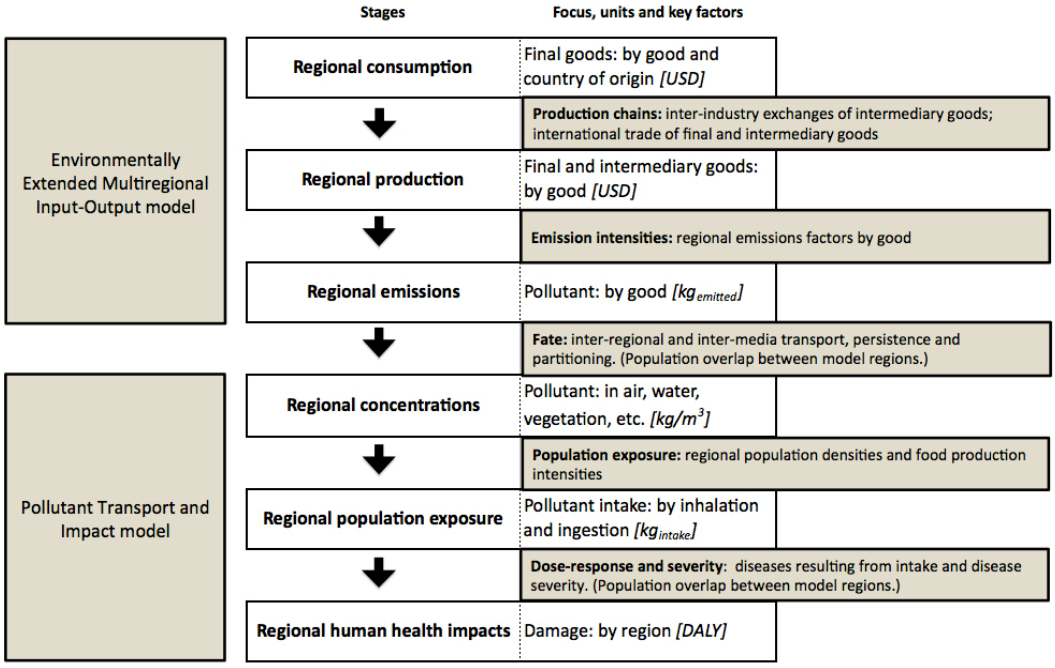

Fig. 4.1. Assessment stages and key factors of the integrated model, combining the Environmentally Extended Multiregional Input-Output model and the Pollutant Transport and Impact model.

4.2 Methods

Starting from the regional consumption of 24 types of goods in 19 regions for 2001 (Tables S1 and S3), the induced economic activities and emissions are computed and re-allocated from producing to consuming regions with a global inter-industry Environmentally Extended Multiregional Input-Output model (Friot and Antille, 2009). Using a Pollutant Transport and Impact model, IMPACTWorld, we then estimate regional pollutant concentrations and human exposure (through inhalation and ingestion), accounting for substance fate in 59 regions and three environmental media (air, water and soil) and for exposure based on urban and rural population distributions. Finally, epidemiology-based damage factors are used to estimate regional health impacts of this intake in disability-adjusted life years (DALYs) (WHO, 2008). Here, we applied this model to fine particulate matter (PM2.5), a major contributor to human health impacts from environmental emissions (Humbert et al., 2009; Schwartz et al., 2008).

4.3 Results

We first show that for a large open economy such as Germany, even though few products consumed by households are of foreign origin, 72% of the PM2.5 emissions induced by their production occur outside Europe due to the globally-distributed supply chains (Fig. 4.2). We then calculate exposure by accounting for urban and continental population densities, as well as cross-boundary transfers of PM2.5, and find that more than one third of these impacts occur in China, South Asia, and South-East Asia, where only 3% of the associated economic activity takes place.

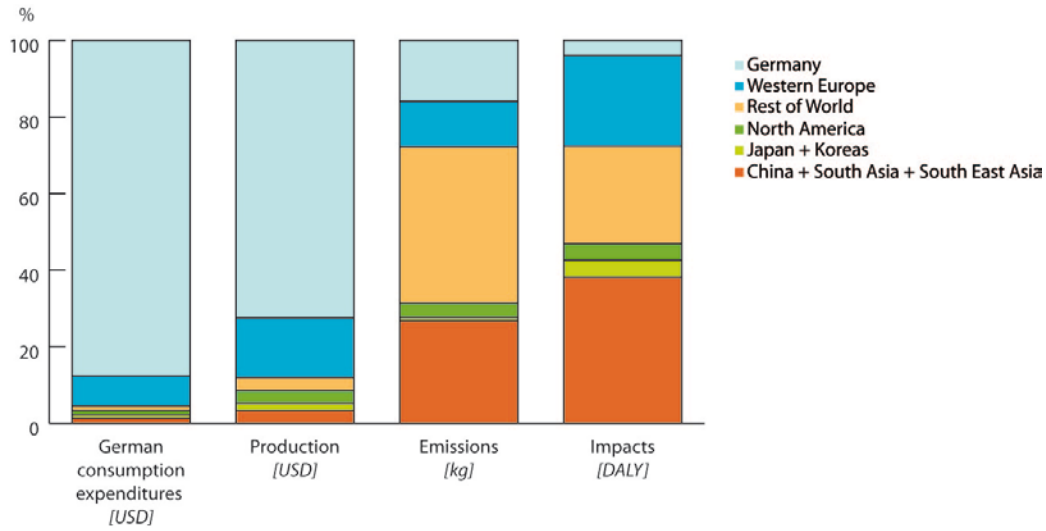

Fig. 4.2. Distributions by region of German consumer expenditures, induced production, fine particulate matter ($PM_{2.5}$) emissions, and associated human health impacts.

Expanding to the consumption of all countries around the globe, we find a similar pattern for Western Europe, as shown in Fig. 4.3, which contrasts the per capita disparity between (a) induced production, and (b) impacts. As expected, each consumer from North America, Japan & the Koreas, and Europe induces substantially more production than other consumers (Fig. 4.3a). Impacts from North America and Japan & the Koreas are mostly domestic, which is due to the US lower openness to trade (19%) and higher emissions intensities and high local exposures of mega-cities in Japan & the Koreas. Due to higher induced economic activity per capita in these regions, impacts are higher than those from Europe, both domestically and in the rest of the world.

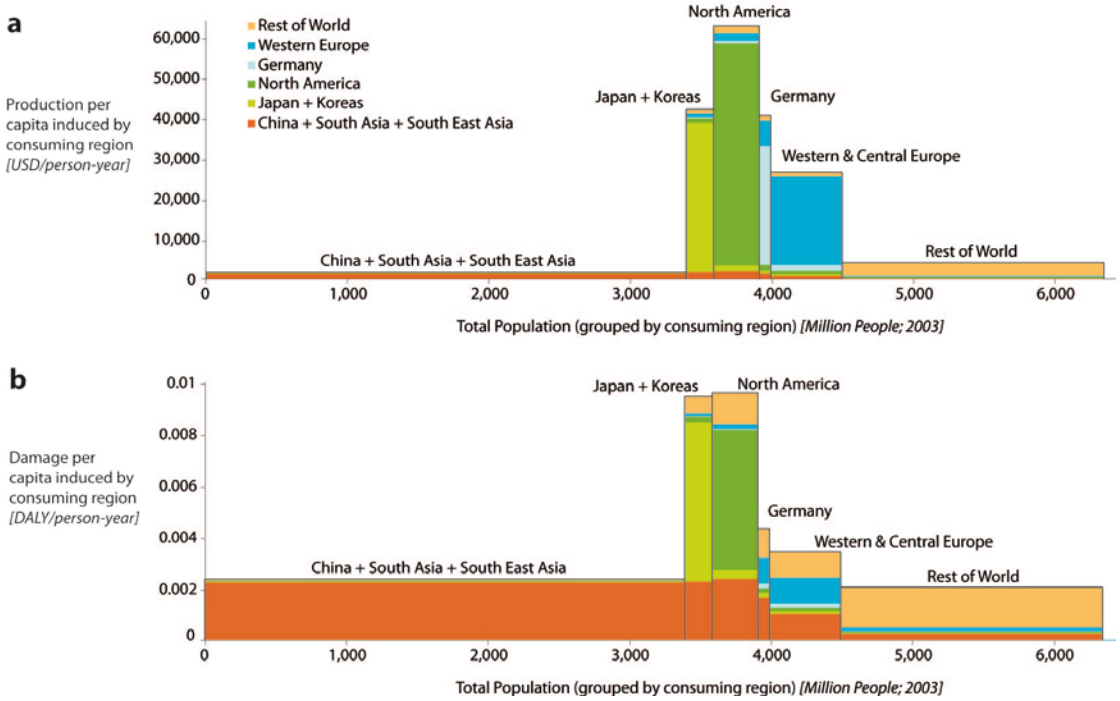

Fig. 4.3. Histogram of annual (a) production per capita (in USD 2001) and (b) impacts of fine particulate matter (PM2.5) (in disability adjusted life years - DALYs) per capita induced by each region's consumption. Column labels refer to the consuming region along the x-axis, which induces production and impacts in regions denoted by color. The area of each box represents total induced production or human health impacts. These six regions are groupings of the 19 regions used in the model (see Table A1).

Overall, the inhabitants in China and South and South-East Asia experience more than half (53%) of the worldwide health impacts due to PM2.5 emissions (total dark orange area in Fig. 4.3b) despite representing only 10% of the economic activity (Fig. 4.3a) induced to meet global consumption. Production for foreign consumers is responsible for 23% of these impacts, with the domestic consumption remaining the predominant source. On a per capita basis, each North American, Japanese and Korean consumer induces as much impact in China & South Asia & South-East Asia as each local consumer of this grouped region (Fig. 4.3b). Finally, the majority of impacts induced by Europe occur outside of its borders.

The world map in Fig. 4.4a shows the variation of impact intensities per dollar of production, which is mainly explained by differences in emissions intensities. Accounting for global supply chains, each dollar of production in China results, on average, in 37 times more PM2.5 emissions than it would in Germany and 6 times more emissions than

in the USA. This reflects the decades-long domestic abatement efforts for Germany, as well as differences in electricity mixes and industrial process efficiencies (IEA, 2006). In terms of exposure, we found that regional population density plays a limited role in the distribution of impacts, with inhalation dominated by urban exposure in large concentrated urban areas (responsible for 50-98% of regional intake; see supporting online text). As a result of regional variability in urban areas and, more importantly, emissions intensities, delocalizing production from Germany to China or India leads to, respectively, 40 or 100 times more impacts to human health per dollar of production (on average). The foreign share of these impacts is much larger than what would be predicted by the magnitude of trade and existing assessments of carbon emissions (Hertwich and Peters, 2009).

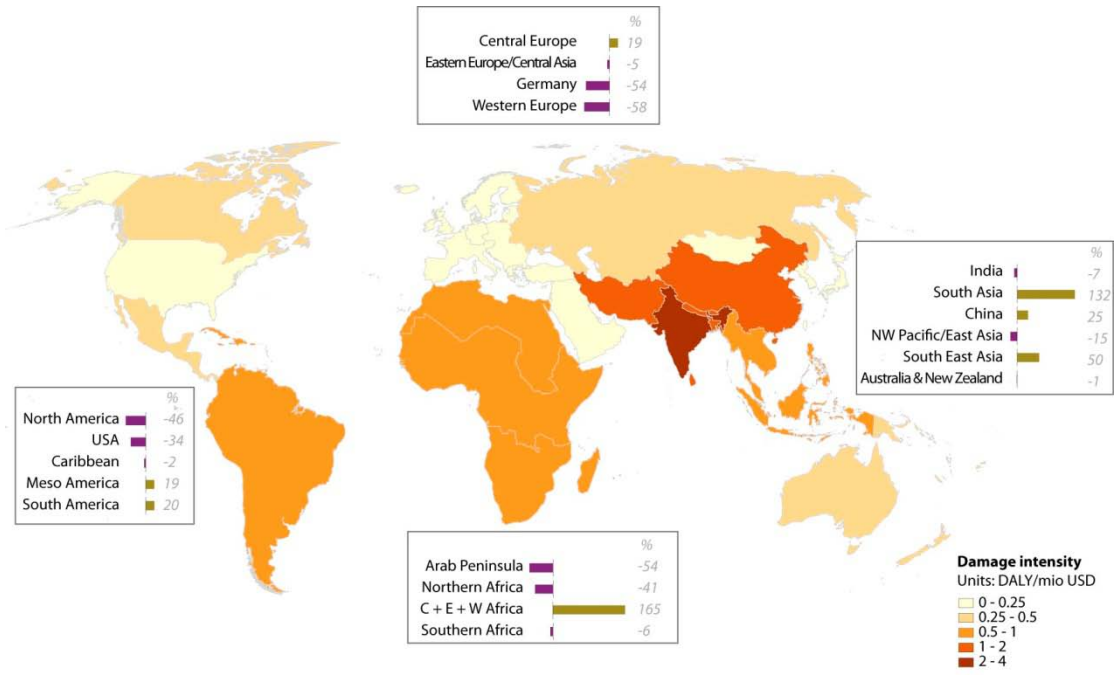

Fig. 4.4. Map of the damage intensity induced worldwide due to fine particulate emissions from regional production [DALY/mio USD] (where DALY is the disability-adjusted life years), with horizontal bars indicating direction and size of damage gap. The damage gap is the difference between experienced damage and induced damage globally through consumption as a fraction of induced damage [($DALY_{exposed}$ - $DALY_{induced\ globally}$) / $DALY_{induced\ globally}$].

In Fig. 4.4, we also observe apparent exports (intentional or not) of damaging activities, as indicated by a gap between impacts experienced by a given region and

impacts in the rest of the world induced by consumption in that region. OECD economies experience lower impacts than what they induce worldwide through their consumption. Central, Eastern and Western Africa (C+E+W Africa), South and South-East Asia, and China to a lesser extent assume some of the displaced impacts from the rest of the world's consumption (positive gap), especially from Western Europe, North America, the Arab Peninsula, and Northern Africa.

4.4 Conclusions

These results suggest that the current wave of delocalization of industrial activities to countries with largely fossil fuel-based electricity mixes and low pollution abatement technologies is leading to higher emissions and health impacts in absolute terms; although European countries increase filters on local emissions, it is essential to also track the induced emissions and impacts through delocalization. However, we do find that most impacts occurring in China and South Asia are also induced by consumption there.

A sensitivity study demonstrating the robustness of our model is shown in Appendix A4.2. Methodological improvements should first focus on the refinement of the sector resolution of PM2.5 emission factors and the reduction of their uncertainties. This finer resolution would reduce the potential aggregation bias within the model (Lenzen et al., 2004). In general, the data consistency, modelling of imports, and sector resolution need to be improved in global IO models (Peters and Hertwich, 2007b; Tukker et al., 2009; Wiedmann et al., 2007). To improve estimates of pollutant fate and exposure, jet streams should be included to account for long-range transport and the spatial resolution should be increased. We have already performed a first step in this direction by splitting rural and urban exposures. Further work should address impacts of additional pollutants when global inventories become available, as well as direct emissions by households during the use and disposal phases of products, which are not included here. Finally, indoor emissions throughout the value chain should also be considered due to their potentially large health impacts (Hellweg et al., 2009).

Environmental and health impacts will increase as global production/consumption and trade continue to grow faster than the diffusion of emission control technologies. Thus, interest is growing for quantification of environmental impacts along global value chains in a spatially explicit way, with such an approach already strongly needed for a number of important issues at all levels.

At the product level, there is a growing need for consumers, organizations (national, international, and non-governmental), and the distribution and retailing industry in general, to have sound scientific assessments of impacts in order to better inform schemes like eco-labelling or fair trade. Our study and model emphasize the need to account for the full global value chain in assessments of goods and services, and will help provide producers with the information needed to most cost-effectively decrease the main impacts.

At the country level, this approach can provide a sound scientific basis for indicators that can complement macroeconomic indicators in a globalizing world (e.g., environmental health indicators can be compared with the gross domestic product), the importance of which was re-emphazised by Stiglitz et al. (2006). Such an approach is needed to implement a sustainable development perspective (UN, 1987).

Domestic abatement policies in industrialized countries are increasingly counteracted, indirectly, by globalized production/consumption chains, as shown here with human health impacts of fine particles. Should OECD countries intend to have a net decrease in environmental impacts, our results for particulate matter suggest the following actions. First, they need to fully integrate the international dimensions of their direct and indirect impacts when developing pollutant inventories, models and policies. Second, they should promote systematic adoption of abatement technologies in Asia and other manufacturing countries. Third, foreign aid allocation schemes should start to integrate environmental aspects, thereby shifting priorities when fostering cooperation.

Ultimately, this paper provides essential information for current discussions on environmental equity and global environmental governance. In September 2009, the United Nations Environment Program released a sequence of steps to improve international environmental governance, stating as its first core objective: “Creating a

strong, credible and coherent science base." The approach presented in this paper precisely aims to contribute to this objective.

Acknowledgements related to this work:

The co-authors of this manuscript not mentioned in the chapter footnote contributed as follows. Gabrielle Antille helped create the Input-Output model and gave critical feedback in the writing of the paper; Sebastien Humbert helped create the global impact assessment model, designed the urban exposure calculations and collected urban data, and gave feedback in the writing of the paper; Hy Dao and Stefan Schwarzer used GIS to help create the regional divisions in the two models, analyze input data, and help transition between the two models; Suren Erkman and Lucien Wald gave feedback in the writing of the paper.

We thank Cédric Wannaz for the analysis of advection data; Michael Stanley-Jones from UNECE for fruitful discussions; and the GIAN (Geneva International Academic Network), Graham Environmental Sustainability Institute, and the University of Michigan Rackham graduate program for financial support.

CHAPTER 5

Conclusions

The objective of this thesis was to create a tool to quantify the globally-distributed health impacts of global emissions and products. In the Introduction (Chapter 1), I provided three specific aims to achieve this objective, namely the creation of a global impact assessment model (Chapter 2), the integration of food exports into the model to understand where the pollutants are eventually ingested (Chapter 3), and the combination of the model with Input-Output to estimate and allocate impacts induced by global consumption (Chapter 4). Below, I summarize the advances this thesis has produced for each of these distinct aims, relate these to the key criteria outlined in Chapter 1, review key limitations, and recommend future work specific to each aim. The specific limitations for each component of the model are discussed in the relevant chapter, so I highlight here the dominant limitations. Then I address the integrated tool as a whole (the combination of the environmental transport, food transport and global trade components) to discuss its general limitations and provide recommendations for future refinements and applications.

5.1 Review of the key criteria

Chapter 1 outlined five key criteria required for a model to quantify human health impacts of globally-distributed emissions (Table 1.2), so we will relate the conclusions in each chapter back to these criteria. The criteria for this life cycle impact assessment model, with elements of risk assessment to quantify globally-distributed impacts, are as follows: (i) multiple environmental media, (ii) multiple exposure pathways including food trade, (iii) inclusion of high exposure intensity areas (such as urban areas), (iv) multiple continents, and (v) low data and computational needs. I summarize below the results of each model component in the context of these criteria, and recommend future applications specific to each component.

5.2 Global impact assessment model developed and applied to case studies

5.2.1 Summary and conclusions

In Chapter 2, I developed the global human toxicity impact assessment model, IMPACTWorld. The application of IMPACTWorld provided, to our knowledge, the first calculation of the globally-distributed impacts of a global emissions inventory, integrating aspects of comparative risk assessment by calculating impacts by receiving population as well as emitting population. Application of the model to particulate matter (PM) and polychlorinated biphenyl-118 (PCB-118) demonstrated the importance of accounting for multiple environmental media; the dominant exposure pathway of PCB-118 is food ingestion, whereas for PM it is inhalation. Moreover, we found substantial regional variations in spatial intake fractions for PM and PCB-118, which reinforces the importance of accounting for multiple continents. Furthermore, we found that transboundary transport affects PCB-118 spatial intake fractions but has little effect on PM exposure. This is largely because of the urban exposure to PM, which amounts to 72-99% of the intake from a regional emission, and thus emphasizes the importance of the high exposure intensity criterion.

5.2.2 Limitations and recommendations for future work

One of the future applications of IMPACTWorld will be to provide human toxicity damage factors to a global life cycle impact assessment method in development, IMPACTWorld+. Specifically, IMPACTWorld+ will use the IMPACTWorld model results to provide tables of global human toxicity factors for regional emissions of a large set of pollutants. The method will then be implemented in life cycle assessment software programs for LCA practitioners to better estimate global impacts when the emission location is known. The availability of such a method will take advantage of increasingly location-specific emissions data, and is also intended to help stimulate the increased collection of globalized emissions inventories.

Regarding the key criterion of multimedia pollutant fate, the global model can be used to explore the contribution of atmospheric vertical exchange to pollutant long-range transport and ultimate intake. An upper air compartment has been added to

IMPACTWorld to allow for this possibility, but preliminary results indicate that accounting for vertical exchange merely provides a loss of pollutant from the region of emission (which is already included with only one vertical layer using a constant vertical loss rate constant). Thus the vertical exchange contribution to pollutant transboundary transport was preliminarily found to be negligible (smaller than that due to food export, for example), but a more systematic study across a range of pollutants should be conducted and should account for the periodic stratosphere-troposphere mixing (Stohl et al., 2003).

Further improvements can address the third key criterion of accounting for areas of higher exposure intensity. Since previous work has found that accounting for urban exposure in North America increases the average intake fraction by approximately an order of magnitude (Humbert et al., 2009), the issue of increased exposure intensity was addressed here by including areas of high population density. But to a lesser extent, previous work has also suggested the need to explicitly account for areas with higher agricultural intensity (Humbert et al., 2009; Rochat et al., 2006). Further study should examine the effects and optimal scale of accounting for agricultural intensity.

5.3 Comparison of pollutant exports through food trade and environmental transport

5.3.1 Summary and conclusions

Chapter 3 describes the inclusion of economic global food trade in the matrix framework of IMPACTWorld such that pollutant fate through the economy (through food exports) can be accounted for and modeled in a similar way to the fate through the environment. This is the first model to consistently account for pollutant impacts from the emitter, food producer, and food consumer perspectives, which increases the interpretation capabilities in life cycle impact assessment. The application to two persistent pollutants shows that although environmental pollutant transport is greater than transport through food, food trade can still export up to 61% of a region's pollutant intake (i.e. export the pollutant to be ingested elsewhere in the world). Moreover, when a pollutant is emitted in a region of high food exports (such as the U.S.) or a region of high

food production (such as China), the regions importing the food can increase their intake by up to 73%. Thus, these results suggest that the key criteria of accounting for food exports is not as crucial as atmospheric transport, but that it can still substantially affect the distribution of impacts.

5.3.2 Limitations and recommendations for future work

This food export portion of the model can be improved to address the second key criterion addressing multiple exposure pathways and accounting for food trade. Since many persistent pollutants bioaccumulate in fish, the most critical future work related to pollutant export through food is the inclusion of fish trade in the economic food trade model.

5.4 Integration of impact assessment model with global trade model

5.4.1 Summary and conclusions

Finally, Chapter 4 describes the integration of IMPACTWorld with a model of the global supply chain to estimate the origin and impacts of particulate matter emissions associated with global trade. The results of this application represent the first quantification of the shifts in global impacts associated with the shifts in global supply chains. These results suggest that the delocalization of industrial activities to countries with low pollution abatement technologies is not only shifting where impacts are occurring, but also leading to higher emissions and health impacts in absolute terms. Thus, any quantification of the impacts of a globally produced good needs to track the emissions and impacts induced through delocalization. Moreover, the multi-continental framework of IMPACTWorld allows direct comparison of the actual pollutant transport (through air) with the "virtual" pollutant transport due to exported factories and associated emissions. Such comparisons for PM show that "virtual" pollutant transport through delocalization of factories is the dominating factor determining global impacts in this case (atmospheric transport is less important in the case of PM due to its dominant

local urban exposure). However, more persistent pollutants, such as PCB-118, may have a higher contribution from long-range transport.

5.4.2 Limitations and recommendations for future work

In terms of future application, this integrated tool of impact assessment and global trade provides a framework to eventually inform decision-makers at the product level (quantifying impacts for schemes such as eco-labelling) and at the country level, where it can allow policy-makers to account for the impacts induced by delocalizing manufacturing.

Future development of the model should address emissions from other parts of the life cycle of globally traded goods. The tool has not yet been applied to emissions associated with consumer use (for example, the emissions due to laptop energy use while typing a thesis). Although OECD nations are generally decreasing their manufacturing emissions, they are still consuming substantial amounts of energy to use consumer products. Thus when consumer use is accounted for, OECD nations will likely be responsible for proportionally more of the global emissions than in the case considering only the globally supply chain.

5.5 General application, uncertainties, and future work

5.5.1 Application

This expanded IMPACTWorld model with food trade is recommended for use as a tool for comparative impact assessment across a broad array of scenarios, regions or pollutants, but it is not suitable for localized impact assessment due to the limitations inherent in the impact assessment and economic trade modeling. The integration of risk assessment concepts into an LCA tool represents a step in the recommended direction for general improvement and applicability of decision-making tools (Cowell et al., 2002), yet this model, like other LCIA models (Socolof and Geibig, 2006), still remains a tool that roughly estimates relative damage to identify key potential impacts and assumptions that should be further explored to calculate absolute impacts.

5.5.2 Uncertainties

Uncertainties exist at each step of the many linkages in the impact assessment, food trade, and global trade components of the model, and the relative uncertainties used for comparative assessment can be very different from the absolute uncertainties. The uncertainties in emissions depend greatly on the pollutant considered and the relevant processes or sectors, with pollutant discharges from US oil refineries varying by more than a factor of 10 (Matthews et al., 2002), PCB-118 global emissions varying by a few orders of magnitude between scenarios (and further variation over time and space), and PM emissions per production dollar varying by a factor of 76 depending on the region. In all three cases, comparative uncertainties are likely lower than absolute uncertainties, because many errors are likely systematic across regions and emissions processes.

The uncertainties in pollutant fate and exposure also depend on the pollutant considered due to the dominance of different processes (e.g., degradation, air and water advection, diffusion, etc.), and, as mentioned in Chapter 1, Pennington et al. (2006) estimate that a model predicting an average European characterization factor of a benzo[a]pyrene emission would have an uncertainty around a factor of 37. In the case of the pollutants considered here, the predicted concentrations of PM and PCB-118 (Chapter 2) were generally within an order of magnitude of somewhat analogous measured and modeled concentrations, but the transboundary transport of PCB-118 still may have relatively high uncertainties. As discussed in Chapter 3, the uncertainties in pollutant intake due to food transport are likely dominated by uncertainties in the food distribution matrix, which required correction factors that ranged over four orders of magnitude. Note that the actual uncertainty is likely much lower than this, particularly for comparative assessment, due to the similarity of each set of correction factors for a given food sector.

Finally, sensitivity studies in Appendix 4 indicate the level of uncertainty in the global trade application. The absolute impacts are most sensitive to whether or not urban areas are specifically accounted for, and the relative impacts on Asia versus the rest of the world appear to change by less than 30%, even with a factor of two change in various emissions and environmental parameters.

This summarizes the dominant uncertainties in each component of the model and application and highlights the need for a systematic uncertainty analysis or propagation, perhaps based on the work of Hong et al. (2010).

5.5.3 Future work

Since the model framework can be applied to a large number of pollutants, the first step in improving its applicability is a systematic model evaluation for a test set of pollutants. Thus, a set of pollutants with varying partitioning coefficients and degradation rates should be compared to globally distributed measurements at each measurable step in the model, including environmental concentrations, food concentrations, and population intake. In the case of a pollutant such as particulate matter, relating the measured intake to the original source can be difficult on a global scale, thus predicted intake fractions should be compared to results from region-specific or pollutant-specific models with higher resolution.

In addition, spatially refining some or all components of the impact assessment and global trade applications may further increase the magnitude of the results presented here. The country level originally was not included in IMPACTWorld because of the added complexity. However, since accounting for pollutant transport through food substantially alters intake on sub-continental scales, pollutant transport due to food trade at the country level could be substantial, and thus merit the added complexity. Moreover, country-scale divisions will help identify more specific shifts in impacts due to global trade, which have also been found to be substantial on a sub-continental scale.

An alternative spatial refinement, in line with the fifth key criterion of keeping computational needs low, can be addressed by using more sophisticated modeling techniques. An adaptive scale model that can have high resolution where needed (such as areas of high population densities or emissions) and low resolution in other regions will better optimize computational resources and is currently in development (by colleagues) based on the IMPACT model framework.

In summary, this thesis presents the development and application of a tool to quantify the impacts of globally-distributed emissions, revealing new insights into impacts associated with environmental pollutant transport, pollutant transport through

food, and “virtual” export of pollution through global trade. As such, this thesis thus identifies priorities in reducing global impacts and in further developing tools to quantify these impacts.

APPENDIX 1
Publications resulting from this work

Friot D*, **Shaked S***, Antille G, Erkman S, Dao H, Humbert H, Schwarzer S, Wald L, Jolliet O. Quantification of environmental impacts on human health due to global production and consumption chains. (under review in *Science*, submitted November 2010; * indicates two first co-authors)

Gronlund, CJ, Humbert, S, **Shaked, S**, O'Neill, MS, Jolliet, O, 2011. Dose-response, severity and characterization factors for life cycle assessment and the burden of disease of particulate matter. (to be submitted).

Hong, JL**, Shaked, S,** Rosenbaum, RK, Jolliet, O, 2010. Analytical uncertainty propagation in life cycle inventory and impact assessment: application to an automobile front panel. International Journal of Life Cycle Assessment 15, 499-510.

Humbert S, Marshall J, **Shaked S**, Spadaro J, Nishioka Y, Preiss P, McKone T, Horbath A, Jolliet O. Intake fractions and characterization factors for particulate matter: review and recommendations for life cycle assessment. *Environmental Science and Technology* (re-submitted after revisions).

Humbert S, Manneh R, **Shaked S,** Wannaz C, Horvath A, Deschenes L, Jolliet O, Margni M. Assessing regional intake fractions in North America. *Science of the Total Environment* **407**(17):4812-20. 2009.

Shaked S, Humbert S, Margni M, Schwarzer S, Wannaz C, Jolliet O. IMPACTWorld: Application of a multi-continental multimedia model to estimate global intake fractions and impacts of globally distributed emissions. (to be submitted to *Environmental Science and Technology*).

Shaked S, Friot D, Jolliet O. Food trade contribution to long-range transport of persistent organic pollutants. (in preparation).

Shaked, S, Jolliet, O. 2011. Global life cycle impacts of consumer products, in: Nriagu, J. (ed.), Encyclopedia of Environmental Health. Elsevier.

Two additional deliverables are a user-friendly global impact assessment model in Excel, as well as a handbook (in development) describing the underlying structure, algorithms and parameters, which I am coordinating and co-authoring with Rima Manneh, Manuele Margni, Ralph Rosenbaum, Peter Fantke, Sebastien Humbert, and Olivier Jolliet.

APPENDIX 2
IMPACTWorld: Development and application of a multi-continental multimedia model to estimate global intake fractions and impacts of globally distributed emissions

A2.1 Introduction

This section is included here to align other appendix sections with main text sections for easier cross-referencing.

A2.2 Further details on methods

A2.2.1 Overview of further details on methods

This section expands the intake fraction in the matrix framework, provides lists of countries by IMPACT region and FAO sectors by exposure pathway, and explains atmospheric transport and urban exposure in more detail. We also provide more detail on the properties of PCB-118 and fine particulate matter.

A2.2.2 IMPACTWorld description and parameterization

A2.2.2a Spatialized framework

The intake fraction matrix is a product of the fate **FF** and exposure **XP** matrices, so the $\underline{iF}$ in receiving region *r'* for an emission to compartment *m* in region *r* is expressed as follows:

$$iF^{m}_{r->r'} = \sum_{p}\left(\sum_{m'} FF^{m->m'}_{r->r'} XP^{m'->p}_{r'}\right) \qquad \text{A2-1}$$

where *m'* is the destination compartment that links to the exposure pathway *p*. The total *iF* represents the sum over different exposure pathways *p*, such as water and vegetables.

A2.2.2b Regionalization

The list of countries in each IMPACT region are detailed in Table A2.1. The main choices of regional divisions in the model include:

- Cut at the equator because of large differences in circulation between two hemispheres.
- Cut near the Arctic and Antarctic circles to account for important environmental differences between temperate zones and poles (temperatures, winds, ecosystems, population densities, etc.).
- Cut along country boundaries around 30^{o}N and 30^{o}S to account for differences between tropical and temperate climates (for impacts on ecosystems).
- Cuts generally following political boundaries for simplicity (when evaluating exposure data).
- China is divided in a way to avoid diluting its population in the less populated regions of Tibet and Xingjian.
- India is separated from the rest of Asia because of its high population density and application to the case study of a T-shirt manufactured in India.
- Indonesia has been separated from Northern Australia to avoid diluting its population in the Australian desert.
- Australia has been separated based on population density.
- The different coastal regions have been added as boxes between the terrestrial and ocean regions to better capture the impacts of marine ecosystems and the accumulation of pollutants within the fish

Table A2.1. List of countries within each IMPACT region

Region ID	Region Name	Countries in each region
W1	West Asia	Russian Federation, Afghanistan, Iran (Islamic Republic of), Kazakhstan, Kyrgyzstan, Mongolia, Tajikistan, Turkmenistan, Uzbekistan, Western China
W2	Indochina	Brunei Darussalam, Cambodia, Lao People's Democratic Republic, Malaysia, Maldives, Myanmar, Philippines, Singapore, Thailand, Viet Nam, Indonesia
W3	N Australia	Australia, Wallis and Futuna Islands
W4	S Australia+	Australia, New Zealand
W5	S Africa+	Angola, Botswana, Comoros, Lesotho, Madagascar, Malawi, Mauritius, Mozambique, Namibia, Rwanda, Réunion, South Africa, Swaziland, United Republic of Tanzania , Zambia, Zimbabwe, Democratic Republic of the Congo, Congo, Gabon, Kenya,

		Uganda, Saint Helena, Seychelles
W6	N Africa+	Democratic Republic of the Congo, Congo, Gabon, Kenya, Uganda, Algeria, Bahrain, Benin, Burkina Faso, Burundi, Cameroon, Cape Verde, Central African Republic, Chad, Côte d'Ivoire, Djibouti, Egypt, Eritrea, Ethiopia, Gambia, Ghana, Guinea, Guinea-Bissau, Iraq, Israel, Jordan, Kuwait, Lebanon, Liberia, Libyan Arab Jamahiriya, Mali, Mauritania, Morocco, Niger, Nigeria, Oman, Occupied Palestinian Territory, Qatar, Sao Tome and Principe, Saudi Arabia, Senegal, Sierra Leone, Sudan, Syrian Arab Republic, Togo, Tunisia, United Arab Emirates, Western Sahara, Yemen, Equatorial Guinea, Somalia
W7	Argentina+	Argentina, Chile, Falkland Islands (Malvinas), Paraguay, Uruguay
W8	Brazil+	Bolivia, Peru, most of Brazil, Colombia, southern Ecuador
W9	C America+	Anguilla, Antigua and Barbuda, Aruba, Bahamas, Barbados, Belize, Bermuda, British Virgin Islands, Cayman Islands, Costa Rica, Cuba, Dominica, Dominican Republic, El Salvador, French Guiana, Grenada, Guadeloupe, Guatemala, Guyana, Haiti, Honduras, Jamaica, Martinique, Mexico, Montserrat, Netherlands Antilles, Nicaragua, Panama, Puerto Rico, Saint Kitts and Nevis, Saint Lucia, Saint Pierre and Miquelon, Saint Vincent and the Grenadines, Suriname, Trinidad and Tobago, Turks and Caicos Islands, United States Virgin Islands, Venezuela (Bolivarian Republic of), part of Brazil, Colombia, northern Ecuador
W10	USA+	Southern Canada, USA (except Alaska)
W11	Antarctica	Antarctica
W12	N Europe + N Canada	Alaska, Greenland, Iceland, Finland, Northern parts of Canada, Norway, Sweden, Russian Federation
W13	Europe+	Gibraltar, Greece, Hungary, Ireland, Italy, Latvia, Liechtenstein, Lithuania, Luxembourg, TFYR Macedonia, Malta, Moldova, Monaco, Netherlands, Poland, Portugal, Romania, San Marino, Serbia, Slovakia, Slovenia, Spain, Switzerland, Turkey, Ukraine, United Kingdom ; Southern parts of Norway, Sweden, Russian Federation
W14	East Indies	Indonesia, American Samoa, Cook Islands, Fiji, French Polynesia, Guam, Kiribati, Marshall Islands, Micronesia (Fed. States of), Nauru, New Caledonia, Niue, Northern Mariana Islands, Palau, Papua New Guinea, Samoa, Solomon Islands, Timor-Leste, Tokelau, Tonga, Tuvalu, Vanuatu
IND	India+	India, Bangladesh, Bhutan, Nepal, Pakistan, Sri Lanka
CHI	E China	Eastern China, Hong Kong SAR
JAP	Japan+	Japan, North Korea, South Korea

A2.2.2c Pollutant fate

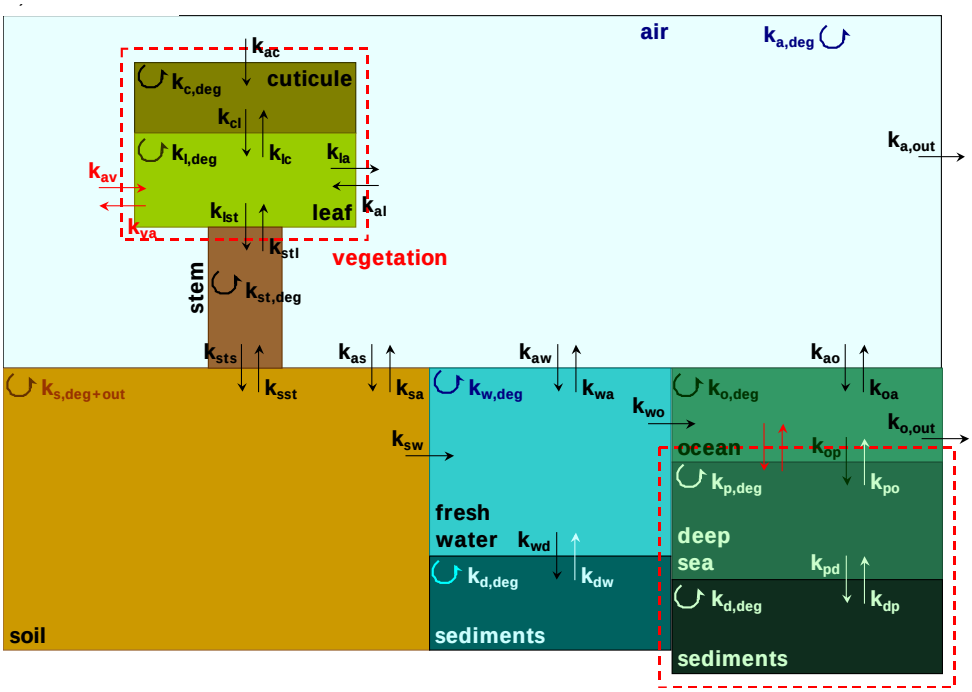

Fig. A2.1 Depiction of IMPACT environmental compartments, including rate constants for advection, intermedia transport, and degradation (copied from Margni (2003)).

Surface air concentrations are estimated by accounting for losses within each air compartment, and transfers to adjacent air compartments and other environmental media. Each air compartment includes rate constants to represent degradation, wet and dry deposition, diffusion, and dissolution to water, soil and vegetation (Pennington et al., 2005).

Based on temporally and spatially averaged horizontal wind speeds (from GEOS-Chem) at each region's boundary, each region has a non-zero advective inflow or outflow. Since many of the imbalances align with mountain ranges, they are likely due to vertical air exchange, as well as the averaging of wind speeds over large distances and many time-steps. Vertical wind speeds were not available and are generally much smaller than horizontal wind speeds, but they can accumulate over the large areas considered here to yield substantial flows (we performed a preliminary analysis of the effect of vertical flows on intake fraction and found a negligible contribution even when unrealistically high flows were considered). To balance the air flows, we devised an algorithm that begins with one region, adjusts adjacent flows such that the inflow and outflow meet at

half the difference, and then moves on to the next region without altering any region that has already been balanced.

Within each terrestrial zone, pollutant transport is included from surface waters (diffusion, deposition), from soils (infiltration, diffusion, and runoff), from sediments (re-suspension and burial), from generic agricultural vegetation (roots, stems and leaves), and for oceanic water (advective transport across the thermocline, diffusion, sedimentation) (Pennington et al., 2005).

A2.2.2d Pollutant exposure

We allocate the amount of feed for each region and the exposed and unexposed composition based on the FAO feed fractions for each region and crop (FAO, 2000) (described in more detail in Appendix 0 in the context of food trade). The predicted food concentrations have been compared to measurements in the Europe, North America, Canada, and Great Lakes version of the IMPACT model, and are generally within an order of magnitude (Humbert et al., 2009; Manneh et al., 2010; Pennington et al., 2005; Soucy, 2010).

Table A2.2. FAO food sectors grouped by IMPACT pathways

unexposed	**exposed**	**freshfish**	**poultry**
Starchy Roots + (Total)	Wheat	Freshwater Fish	Poultry Meat
Pulses + (Total)	Rice (Milled Equivalent)		
Treenuts + (Total)	Barley	**seafish**	**othermeat**
Sugarcrops + (Total)	Maize	Demersal Fish	Mutton & Goat Meat
Sugar & Sweeteners + (Total)	Rye	Pelagic Fish	Meat, Other
Spices + (Total)	Oats	Marine Fish, Other	Offals + (Total)
Oranges, Mandarines	Millet	Crustaceans	Fats, Animals, Raw
Lemons, Limes	Sorghum	Cephalopods	
Grapefruit	Cereals, Other	Molluscs, Other	**eggs**
Citrus, Other	Oilcrops + (Total)	Aquatic Products, Other + (Total)	Eggs + (Total)
Bananas	Vegetable Oils + (Total)	Fish, Body Oil	
Plantains	Apples	Fish, Liver Oil	**milk**
Pineapples	Dates		Milk - Excluding Butter + (Total)
	Grapes	**pork**	Butter, Ghee
	Fruits, Other	Pigmeat	Cream
	Vegetables + (Total)		
	Alcoholic Beverages + (Total)	**beef**	
	Stimulants + (Total)	Bovine Meat	

A2.2.2e Urban exposure details

Here, we provide some additional details and derivations related to eq 2-3. To restate some concepts in equation form, the intake fraction due to urban emissions is $iF_{\text{urb}} = iF_{\text{urb}}^{\text{urb}} + f_{\text{adv}} \cdot iF_{\text{rur}}$.

The fraction of urban emissions advected out, f_{adv}, is close to one for the many substances that live longer than the few hours it takes to be advected out of a city (Marshall et al., 2005). The effective regional advected fraction is as an emissions-weighted average of the ratio of the advective rate constant k_{adv} to the total loss rate constant $k_{\text{adv}} + k_{\text{loss}}$ (sum of advection and other losses):

$$\left\langle f_{\text{adv},i} \right\rangle = \frac{1}{\sum_i \dot{E}_i} \cdot \left(\sum_i \dot{E}_i \cdot \frac{k_{\text{adv}}}{k_{\text{adv}} + k_{\text{loss}}} \right) = \frac{1}{\sum_i \dot{E}_i} \cdot \left(\sum_i \dot{E}_i \frac{1}{1 + k_{\text{loss}} \frac{aL_i}{u_i}} \right) \qquad \text{A2-2}$$

where k_{adv} is the wind speed u divided by urban area length L; it is greater than 0.97 for all regions considered here.

To derive the right hand side of eq. A2-2, we first rewrite part of the left hand side as follows:

$$\begin{aligned} \frac{\sum_i N_i \cdot C_i}{\sum_i \dot{E}_i} &= \frac{1}{\sum_i \dot{E}_i} \cdot \sum_i \frac{N_i \cdot \dot{E}_i}{A_i \cdot H_i \cdot \left(k_{\text{adv}} + k_{\text{loss}}\right)} = \frac{1}{\sum_i \dot{E}_i} \cdot \sum_i \frac{N_i}{A_i} \cdot \frac{\dot{E}_i}{H_i \cdot \left(\frac{u_i}{aL_i} + k_{\text{loss}} \right)} \\ &= \frac{1}{\sum_i \dot{E}_i} \cdot \sum_i \frac{a}{u_i \cdot H_i} \frac{\dot{E}_i \cdot d_i \cdot L_i}{\left(1 + k_{\text{loss}} \frac{a \cdot L_i}{u_i} \right)} \end{aligned} \qquad \text{A2-3}$$

where the area $A_i = L_i^2$, and all other terms are defined in the main text. It is beyond the scope of this work to find the effective wind speed and mixing height of every urban area in the world and including diurnal and seasonal oscillations, so we assume a constant u and H, and express the effective dilution rate as the harmonic average of $u \cdot H$ in urban areas:

$$\frac{1}{(u\,H)_{\text{eff}}} \equiv \left\langle \frac{1}{u_i \cdot H_i} \right\rangle \qquad \text{A2-4}$$

The effective linear population density is the remaining weighted average in eq.A2-3, defined as:

$$(d\,L)_{\text{eff}} \equiv \frac{1}{\sum_i \dot{E}_i} \sum_i \frac{\dot{E}_i \cdot d_i \cdot L_i}{1 + k_{\text{loss}} \dfrac{a \cdot L_i}{u_i}} \qquad \text{A2-5}$$

where k_{loss} is the pollutant loss rate due to degradation and deposition and is generally negligible compared to the advective loss through wind (Marshall et al., 2005).

A2.2.3 Pollutants studied and description of model application

A2.2.3a PCB-118

Table A2.3 provides a summary of published ranges of PCB-118 physical-chemical properties, as well as the values chosen for the simulations described in the main paper. Note that the maximum iFs in Fig. 2.3 of the main text correspond to the minimum vegetation degradation rate, and the minimum iFs correspond to the maximum Henry's constant.

Table A2.3. Chemical properties and degradation rates used for PCB-118 (CAS: 31508-00-6)

Fig. A2.2 shows the change in global PCB-118 annual emissions over time, with the peak in 1970.

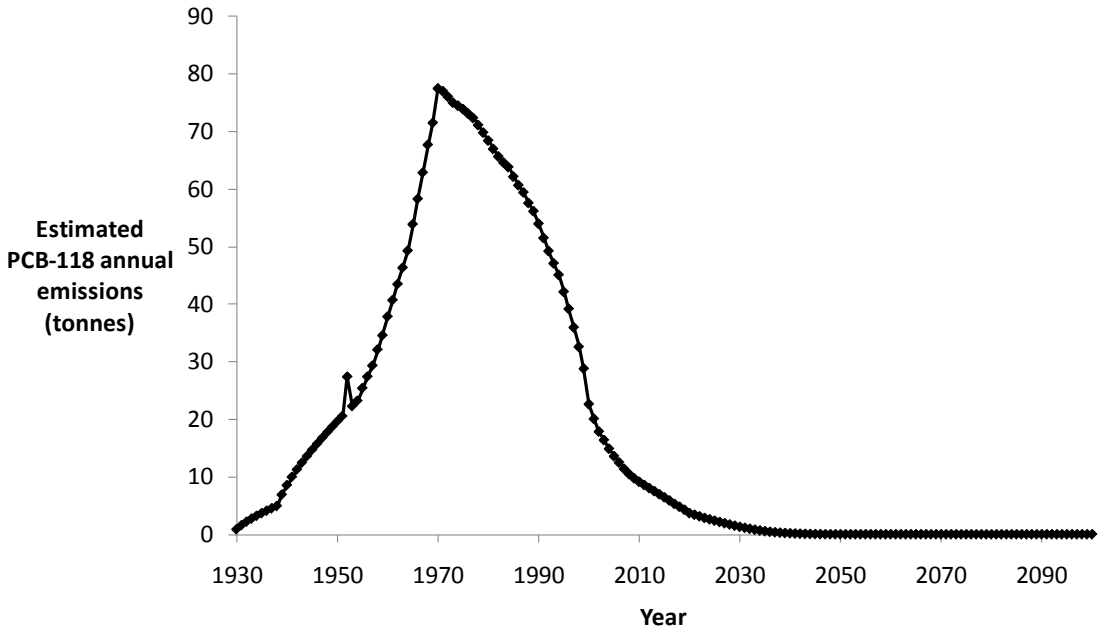

Fig. A2.2. Global annual PCB-118 emissions based on methodology presented in Breivik et al. (2010) and downloaded from http://www.nilu.no/projects/globalpcb/globalpcb2.htm.

To better understand how the intake fraction depends on the chemical properties, Fig. A2.3 shows a series of runs with the one-box European version of IMPACT, changing one property at a time between the minimum and maximum values. As expected, inhalation iFs are generally three orders of magnitude smaller than ingestion iFs. We also find that iFs are particularly sensitive to Henry's constant and vegetation degradation (factor 3 difference between minima and maxima of both), but we chose values in between these two extremes.

Fig. A2.3. Series of runs yielding global oral intake fraction for European emission, with chemical properties varying between minimum and maximum published values. Note that the 'used' values yield an oral iF in the middle, the minimum iF occurs when the max Henry's constant (K_{aw}) is used, and the maximum iF occurs when the maximum vegetation degradation rate is used.

Below we describe the rationale behind the key chemical property values used here.

- Henry's Constant: Paasivirta & Sinkkonen (2009) estimate a value of 149, but this is based on regression coefficients and is 5-15 times higher than values of Li et al. (2003), and other published values including EPI Suite (EPA, 2010).
- K_{ow}: no discussion necessary because values are close together and the iF is not sensitive to this variation.
- Tropospheric degradation half life: Most values are close to one another and the iF is not sensitive to this variation. The main outlier (Sweetman and Jones, 2000) is extremely different and measured only in one area (UK), so other values appear to be more representative.
- Water degradation half life: ranges from 4,000 to 60,000 hours, but these high values (Sinkkonen and Paasivirta, 2000) are at 7^{o} C, so we

use middle value from Paasivirta & Sinkkonen (2009) of 7800 hours.

- Sediment degradation half life: only variation is due to 7^{o} C values (Sinkkonen and Paasivirta, 2000).
- Vegetation degradation half life: There were no measured values in the literature, and estimates were usually expressed as a fraction of soil half life, so potential values range from largest soil half life to 1/16 of smallest soil half life. As recommended by Juraske (2008), we take 1/16 of the best soil estimate (Paasivirta and Sinkkonen, 2009), yielding 1,188 hours, which is between 540 hours and 19000 hours.
- Soil half life: use Paasivirta & Sinkkonen (2009) for consistency.
- BCF for fish: use EPI Suite value (EPA, 2010) from Gobas et al. and multiply by overall water concentration as recommended.

A2.2.3b Particulate matter

In modeling the fate and exposure of particulate matter, it is treated as a non-reactive air pollutant that is advected by wind and lost by wet and dry deposition.

To estimate the global residence time of particulate matter (for use in the intra-urban intake fraction calculation), we find the components of anthropogenic emissions of primary PM and take a weighted average of their residence times. Seinfeld & Pandis (2006) estimate anthropogenic PM emissions as 5% black carbon, 31% organic carbon, 38% industrial dust, and 26% secondary particulates. Using a global atmospheric model, Liu et al. (2009b) find that these components have respective residence times of 5.8, 5.3, and 5.3 days, so the fraction-weighted average residence time for primary PM is 5.3 days.

This lifetime corresponds to a $k_{loss} = 2.2 \cdot 10^{-6}\ s^{-1}$ in the intra-urban intake fraction (eq2-3). k_{loss} is highly variable depending on the type and size of particulate matter, but it is generally much smaller than loss from advection (Marshall et al., 2005), therefore a single representative value is chosen here.

A2.3 RESULTS OF MODEL AND CASE STUDY

A2.3.1 Application to PCB-118

A2.3.1a Evaluation of model application to PCB-118

Below is a table of modeled concentrations with globally distributed corresponding measurements and references.

Table A2.4. Table of modeled concentrations for each region and a variety of environmental compartments and exposure pathways, with measured concentrations and sources where available. *

IMPACT REGION	ENVIRONMENT																	
	air (fg/m3)						water (pg/m3)						soil (pg/g dry weight)					
	Model	Min	Median	Max	Num	Sources	Model	Min	Median	Max	Num	Sources	Model	Min	Median	Max	Num	Sources
W1	3.7						3.1						5.3					
W2	3.4						3.7						5.4	4.5	4.9	5.7	7	Meijer et al, 2003
W3	2.6						3.3						4.5	4.6	4.6	4.6	1	Meijer et al, 2003
W4	2.7						2.9						4.3	5.0	5.0	5.2	3	Meijer et al, 2003
W5	2.7						2.7						4.5	5.0	5.1	5.2	4	Meijer et al, 2003
W6	3.4						3.2						5.0	4.4	4.8	4.9	3	Meijer et al, 2003
W7	2.9						3.1						4.6	4.9	5.0	5.4	5	Meijer et al, 2003
W8	3.0						3.3						4.9	4.5	5.0	7.0	10	Meijer et al, 2003
W9	3.4						3.6						5.3	5.8	6.8	7.1	2	Meijer et al, 2003
W10	3.7						3.2						5.4	4.3	5.6	7.0	19	Meijer et al, 2003
W11	1.9						-0.1						3.5	5.0	5.0	5.0	1	Meijer et al, 2003
W12	3.6						3.9						5.3	3.9	4.0	4.1	2	Meijer et al, 2003
W13	4.2						3.1						5.9	4.2	5.7	7.5	125	Meijer et al, 2003
W14	3.0						2.9						4.9					
IND	3.5						3.6						5.3	5.0	5.1	5.3	4	Meijer et al, 2003
CHI	3.6						3.8						5.4					
JAP	3.8						4.1						5.8	4.5	5.7	6.0	2	Meijer et al, 2003
O1	3.0						0.8											
O2	3.2	3.1	3.3	3.7	4	Gioia et al., 2008b	1.1											
O3	3.0						0.7											
O4	3.8						1.5											
O5	2.4	2.3	2.9	3.1	8	Gioia et al., 2008b	0.1											
O6	2.4						0.0											
O7	3.2	2.0	2.6	3.3	33	Gioia et al., 2008b	1.3	1.3	1.8	2.2	4	Borga et al, 2005						
O8	2.4						0.2											
O9	2.2						0.0											
CCHI	3.6						2.3											
CEW1	3.6						2.0											
CEW10	3.6						2.1											
CEW14	2.8						1.6											
CEW2	3.1						2.0											
CEW3	2.4						1.1											
CEW4	2.6						1.1											
CEW5	2.5						1.2											
CEW6	3.3						1.8											
CEW7	2.8						1.4											
CEW8	2.6						1.7											
CEW9	3.2						2.1											
CIND	3.2						2.0											
CJAP	3.6						2.3											
CNW10	3.6						2.2											
CNW12	3.4						2.0											
CNW6	3.7						2.2											
CSW1	3.4						2.0											
CSW12	4.0						2.6											
CSW13	4.0						2.4											
CW11	2.1						0.6											
CWW10	3.4						1.9											
CWW12	3.4						1.8											
CWW13	3.9	2.7	3.2	3.8	8	Gioia et al., 2008b	2.2	4.7	4.9	5.1	2	Gioia et al, 2008a						
CWW14	2.9						1.3											
CWW2	3.3						1.8											
CWW3	2.5						0.9											
CWW4	2.5						0.9											
CWW5	2.6						1.1	3.3	4.5	4.8	5	Gioia et al, 2008a						
CWW6	3.3	2.8	3.2	4.0	10	Gioia et al., 2008b	2.7	3.7	4.4	4.6	3	Gioia et al, 2008a						
CWW7	2.6						2.1											
CWW8	2.9						2.5											
CWW9	3.3						1.9											

* The continental IMPACT regions 'W_' have full names provided in Table A3.1

IMP. REG.	FOOD							IMPACT REGION	fish (pg/g ww)						seafood (assumed fish)					
	butter (pg/g lipid)																			
	Model	Min	Median	Max	Num	Sources			Model	Min	Median	Max	Num	Sources	Model	Min	Median	Max	Num	Sources
W1	2.6							W1	2.8						2.8					
W2	2.3	1.8	1.8	2.2	3	Kalantzi et al, 2001		W2	3.4						3.4					
W3	1.5							W3	3.0						3.0					
W4	1.5	1.6	1.6	1.6	1	Kalantzi et al, 2001		W4	2.6						2.6					
W5	1.6	1.9	1.9	1.9	2	Kalantzi et al, 2001		W5	2.4						2.4					
W6	2.2	2.9	2.9	2.9	2	Kalantzi et al, 2001		W6	2.9						2.9					
W7	1.8							W7	2.8						2.8					
W8	1.8	1.6	2.5	2.6	8	Kalantzi et al, 2001		W8	2.9						2.9					
W9	2.2	2.0	2.6	2.9	9	Kalantzi et al, 2001		W9	3.2						3.2					
W10	2.5	2.3	2.6	2.8	18	Kalantzi et al, 2001		W10	2.9	2.5	4.1	4.8	5	Hayward et al, 2007	2.9					
W11	-1.0							W11	-0.4						-0.4					
W12	2.5							W12	3.6						3.6					
W13	3.0	2.0	2.6	3.0	20	Kalantzi et al, 2001		W13	2.7						2.7					
W14	1.9							W14	2.6						2.6					
IND	2.3	2.9	2.9	2.9	1	Kalantzi et al, 2001		IND	3.2						3.2					
CHI	2.4							CHI	3.4						3.4					
JAP	2.7	2.0	2.0	2.0	1	Kalantzi et al, 2001		JAP	3.8						3.8					
								O1	0.4						0.4					
								O2	0.8						0.8					
	beef (pg/g ww)							O3	0.3						0.3					
	Model	Min	Median	Max	Num	Sources		O4	1.2	1.3	2.8	3.8	16	Perugini et al, 2004	1.2					
W1	2.3							O5	-0.2						-0.2					
W2	2.0							O6	-0.3						-0.3					
W3	1.2							O7	0.9						0.9					
W4	1.2							O8	-0.1						-0.1					
W5	1.3							O9	-0.3						-0.3					
W6	1.9	1.3	1.4	1.5	2	Loutfy et al, 2007		CCHI	2.0						2.0	3.1	3.6	4.2	8	Zhao et al., 2005
W7	1.5							CEW1	1.7						1.7					
W8	1.5							CEW10	1.8						1.8					
W9	1.9							CEW14	1.3						1.3					
W10	2.2							CEW2	1.7						1.7					
W11	0.4							CEW3	0.8						0.8					
W12	2.2							CEW4	0.8						0.8					
W13	2.7							CEW5	0.8						0.8					
W14	1.6							CEW6	1.5						1.5	2.0	2.2	2.8	4	Loutfy et al, 2007
IND	2.0							CEW7	1.0						1.0					
CHI	2.2							CEW8	1.3						1.3					
JAP	2.4							CEW9	1.7						1.7					
								CIND	1.7						1.7					
								CJAP	2.0						2.0	2.4	2.6	3.2	6	Sasamoto et al., 2006
	chicken (pg/g ww)							CNW10	1.9						1.9					
	Model	Min	Median	Max	Num	Sources		CNW12	1.7						1.7					
W1	0.4							CNW6	1.9						1.9					
W2	0.1							CSW1	1.7						1.7					
W3	-0.7							CSW12	2.2						2.2					
W4	-0.7							CSW13	2.1						2.1					
W5	-0.6							CW11	0.3						0.3					
W6	0.0	1.9	2.0	2.0	2	Loutfy et al, 2007		CWW10	1.6						1.6					
W7	-0.4							CWW12	1.5						1.5					
W8	-0.3							CWW13	1.9						1.9					
W9	0.1							CWW14	1.0						1.0					
W10	0.4							CWW2	1.4						1.4					
W11	-1.5							CWW3	0.5						0.5					
W12	0.3							CWW4	0.6						0.6					
W13	0.9							CWW5	0.7						0.7					
W14	-0.3							CWW6	2.4						2.4					
IND	0.2							CWW7	1.8						1.8					
CHI	0.3							CWW8	2.2						2.2					
JAP	0.5							CWW9	1.6						1.6					

To estimate butter lipid concentrations, we adjust the modeled milk concentrations, assuming 4% fat (Travis and Arms, 1988) and that its lipid concentration is the same as that for butter. For fish, a generic factor has been used to correct measurements for wet weight.

A2.3.1b PCB spatial intake fraction

Fig. A2.4 shows the connection between regional food production intensity and total global oral intake fraction.

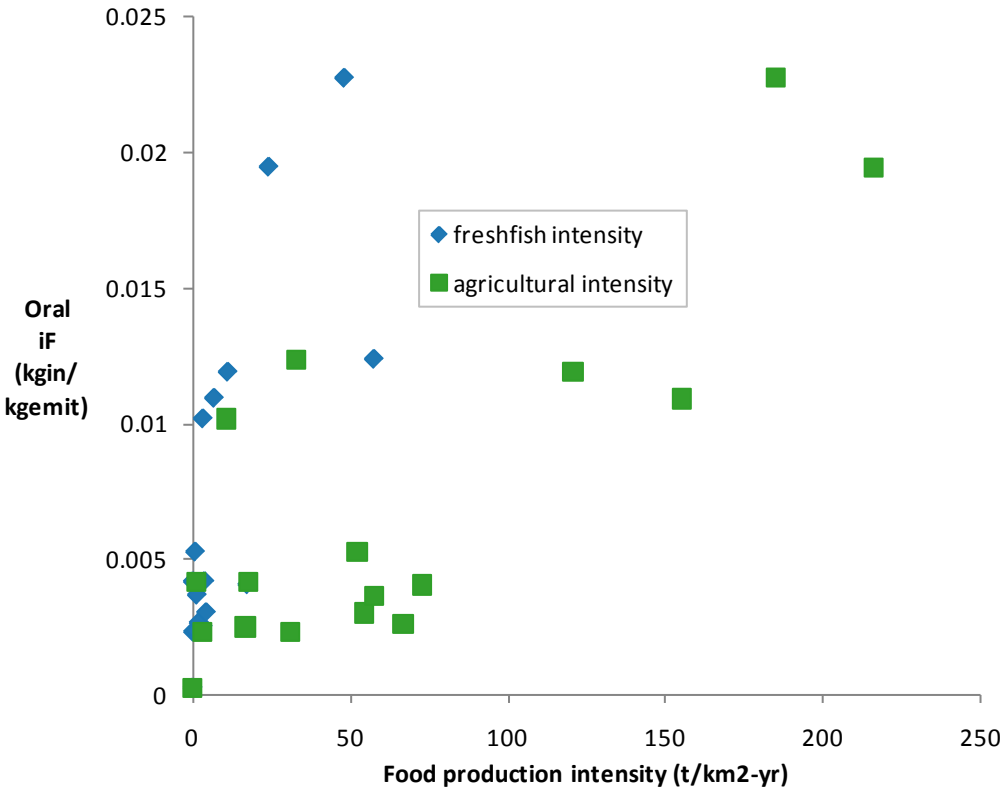

Fig. A2.4. Comparison between total global oral intake fraction (iF) and food production and freshfish intensities in the region of emission (bottom). The scatter is mostly due to trans-boundary transport to regions with higher fish or agricultural intensities.

A2.3.2 Application to PM

A2.3.2a Comparison of PM concentrations:

Here, we provide more details on the comparison between IMPACTWorld predicted concentrations and the Liu et al study (2009b). Because the world is divided into different sets of sub-continental regions in the two studies, it was difficult to exactly compare inter-continental transport matrices in the two models. But by creating matrices of overlapping areas among the different regions, we were able to roughly estimate concentrations and transport in IMPACT regions given the concentrations in the Liu et al

regions. Fig. A2.5 compares the total concentrations (a) and share of concentration due to local emissions (b) for black carbon, organic carbon and dust in the two models considered. Fig. A2.6 compares the region-specific trans-boundary transport for black carbon, showing that IMPACTWorld captures the right magnitude of transport, but misses some of the long-range transport. Other implications of these two Fig.s are discusses in the main text.

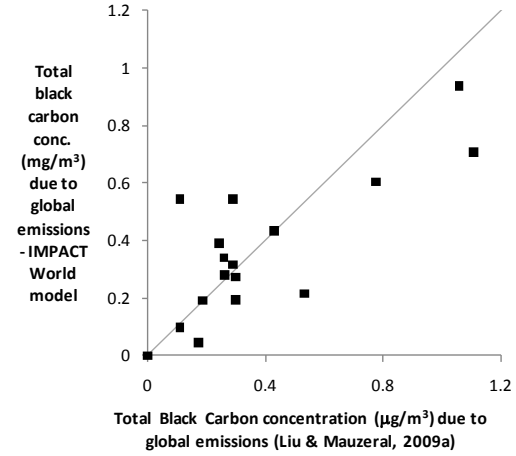

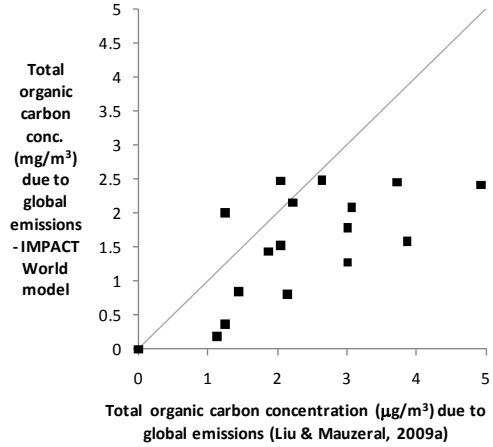

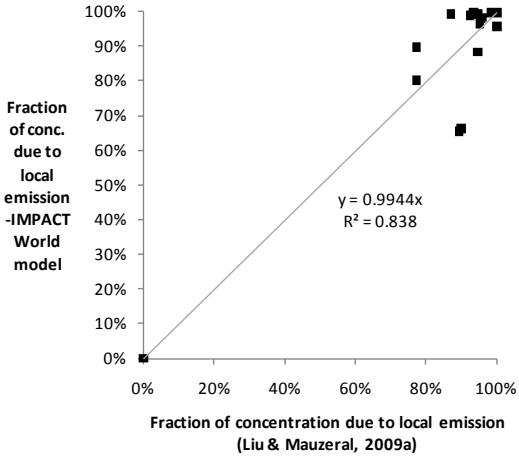

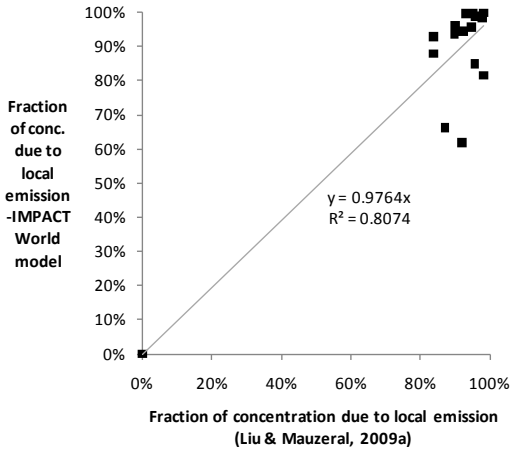

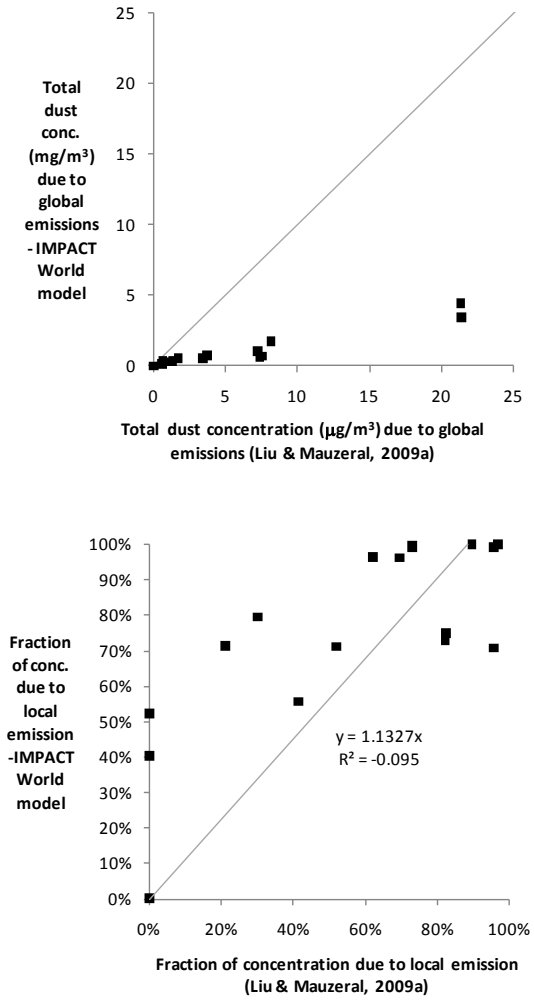

Fig. A2.5. Comparison of IMPACTWorld with model predicting black carbon, organic carbon, and dust $PM_{2.5}$ regional concentrations due to global emissions. Liu & Mauzeral et al. (2009a) use a high-resolution atmospheric model to simulate black carbon emissions and transport between 10 different regions, and then provide the local and global contributions to the resulting increase in concentration in each region. We convert between regions and enter emissions in IMPACTWorld to also calculate total regional concentrations and the share due to local emissions.

Fig. A2.6. Breakdown of regional concentrations due to trans-boundary transport; comparison between IMPACTWorld and Liu et al. (2009b).

A2.3.2b PM spatial intake fraction predicted by IMPACTWorld:

Below is a table of the population, area, urban characteristics and intake fractions for each IMPACT region.

Table A2.5. Key parameters and intake fractions for pollutant transport model.

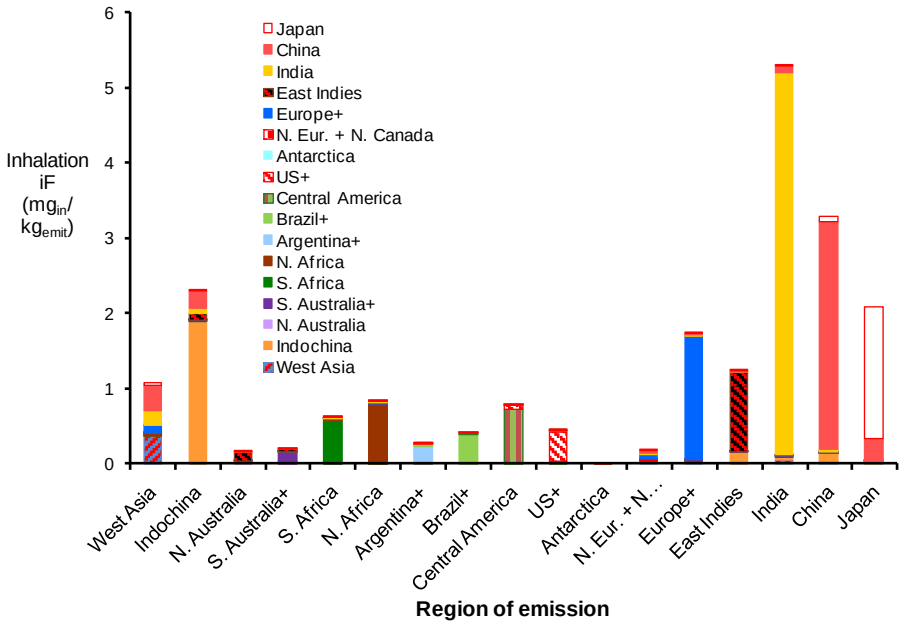

Fig. A2.7. Spatial intake fraction of particulate matter, without accounting for urban emissions and intake.

Fig. A2.8. Correlations between inhalation intake fraction of particulate matter and continental and linear population densities. Note that the total inhalation iF is much better correlated with the linear population density, but the iF that doesn't account for urban areas is better correlated with the continental population density (not shown here).

A2.4 DISCUSSION

The stack height of emissions can also play a key role in exposure, but detailed information at the level of this model is not available.

In addition to the model uncertainties discussed above, there are uncertainties associated with the emissions estimated by input-output and conversions between impact and economic regions.

Impacts due to PM intake vary widely based on type of particulate matter, population distribution, background levels, etc. (Humbert et al, 2010). The uncertainty in effect factors can have a large effect on total impacts, but will not greatly change the distribution of impacts (except perhaps in cases where there are large differences in age distributions and impact differ greatly with age).

APPENDIX 3
Food trade contribution to long-range transport of persistent organic pollutants

A3.1 Further details for the introduction

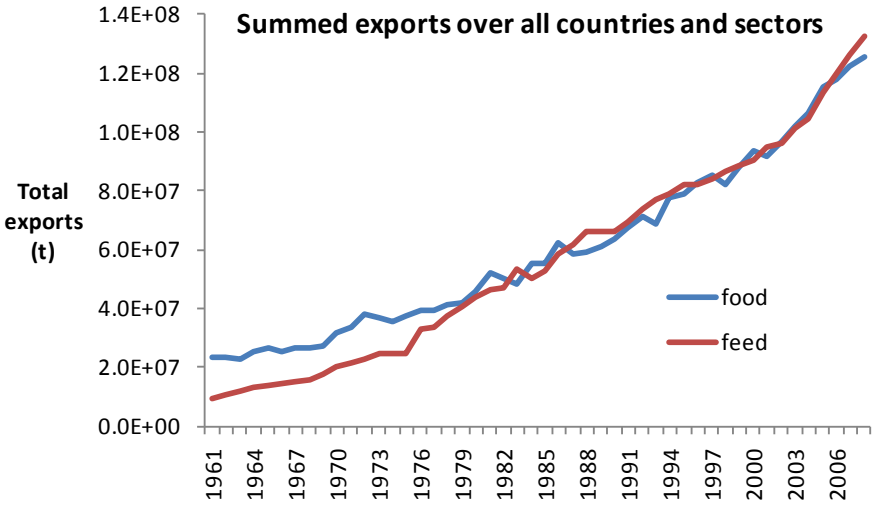

Fig. A3.1 Historical increase in non-fish food and feed exports summed over all countries and sectors (data obtained from FAO (2000)).

A3.2 Further details on methods

A3.2.1 Lists of IMPACT regions, IO regions and GTAP sectors

Table A3.1 List of abbreviations used in appendix for the IMPACT regions, IO regions and GTAP sectors.

W1	West Asia (W1)	**IO1**	Aus_SouthPac	**pdr**	Rice
W2	Indochina (W2)	**IO2**	China_large	**wht**	Wheat
W3	N. Australia (W3)	**IO3**	NWPac_EastAs	**gro**	Other cereals
W4	S. Australia+ (W4)	**IO4**	SE_Asia	**v_f**	Vegetables, fruits & nuts
W5	S. Africa (W5)	**IO5**	South_Asia	**osd**	Oil seeds, oleagineous
W6	N. Africa (W6)	**IO6**	North_Americ	**c_b**	Sugar plants
W7	Argentina+ (W7)	**IO7**	Usa	**pfb**	Textile plants
W8	Brazil+ (W8)	**IO8**	Meso_Americ	**ocr**	Seeds, cereal straw, live plants & forage,
W9	Central America (W	**IO9**	South_Americ	**ctl**	Bovine, Sheep
W10	US+ (W10)	**IO10**	Caribbean	**oap**	Swine, poultry, eggs, skins
W11	Antarctica (W11)	**IO11**	Western_Euro	**rmk**	Milk
W12	N. Eur. + N. Canada	**IO12**	Germany	**wol**	Textile animal parts
W13	Europe+ (W13)	**IO13**	Central_Euro	**fsh**	Fishing, hunting and related service activi
W14	East Indies (W14)	**IO14**	EEuro_CAsia	**cmt**	Bovine meat, most animal offals and fats
IND	India	**IO15**	ArabP_Mas_Ir	**omt**	Swine meat, all meat preparations and pr
CHI	China	**IO16**	North_Africa	**vol**	Oil vegetable
JAP	Japan	**IO17**	South_Africa	**mil**	Dairy products
		IO18	W_E_CAfr_WIn	**pcr**	Rice prepared
		IO19	India	**sgr**	Sugar
		IO20	Antartic AND Arctic	**ofd**	Prepared food & nec
				b_t	Beverages & tobacco products

A3.2.2 Details and assumptions of Input-Output application

We use a modified version of the TREI-C multi-region input-outptut model (see full description in Chapter 4) depicting the monetary flows between economic sectors and regions to re-allocate feed and food from producing to consuming regions. To be consistent with the physical information from FAO data, we use the structural information from the input-output model (i.e., the distribution of monetary flows), and calibrate it with the absolute values of food and feed production and consumption from FAO. This is the best possible approximation to benefit from the strengths of both models. MRIO models, while allowing for the modeling of global production chains, have one serious weakness: due to their aggregated nature, they consider only one "average" product per sector thus inducing potential inconsistencies between these models in value and exchages in physical units. Future work could improve this

approximation by developing models that better reflect physical units. This issue is a long lasting one in the input-output community and no easy solution has been identified yet.

Several assumptions were required to adapt the matrix of flows from the TREI-C model. The first assumption is that any money spent by a livestock sector on a crop sector is assumed to be used for feed. This includes feed for non-edible livestock and livestock used for breeding, which will not be ingested by humans. The distinction between these uses and the edible livestock is performed by accounting for the ultimate product of the livestock sector – we only consider the value of production which is sold to for ultimate use as food.

In addition, the model currently does not include feed made from animal products due to the difficulty of determining the associated economic flows, but the matrix framework can in principle be adjusted to allow for this. Processed feed is also not included for the same reason.

For food trade, we assume that any inter-regional sale between food sectors represents food transfer. Although the fraction of this transfer due to seed transfer should be removed from the total food transfer, seed use accounts for less than 2% of food production worldwide (FAO, 2000), so that neglecting seed transfer should have a minor impact on our results. We assume that the full pollutant content of crops is transferred to beverages and processed food derived from these crops.

Note that the Input-Output data does account for non-market crops and livestock, and thus considers both food entering the economic system and subsistence farming. We however do not account for the partitioning of consumed food between humans and pets, and thus slightly overestimate intake.

The next section describes further details on the actual implementation of the trade matrices.

A3.2.3 Matrix framework spanning impact and trade models

Each element in eq. 3-1 is actually a product of matrices, many of which are needed to bridge the different sets of regions and sectors between the IMPACT and IO models. Each element is fully expanded in the sections below.

A3.2.4 Sequence of matrices from environmental concentrations to intake

A3.2.4a Fate concentration matrix

The fate concentration matrix consists of a traditional fate matrix **FF**, with each element divided by the mass of its compartment (indicated here by the diagonal matrix of the inverse environmental compartment mass vector $\overrightarrow{Minv}^{IMP}$):

$$\mathbf{FF}^{CONC} = \mathbf{diag}(\overrightarrow{Minv}^{IMP}) \cdot \mathbf{FF}^{IMP} \qquad \text{A 0-1}$$

The diagonalized inverse mass matrix is a diagonal matrix with an inverse mass entry for each environmental compartment in each zone.

A3.2.4b Feed trade matrix

The physical feed trade matrix is expressed as a product of matrices that first converts pollutant concentrations from the IMPACTWorld regional compartments to IO regional economic sectors, and then distributes the feed from each region based on economic feed trade data, and computes the resulting pollutant concentrations in consumed feed per region.

$$\mathbf{FEED}^{TR} = \mathbf{FEED}^{TR-IO} \cdot \mathbf{diag}(\overrightarrow{prodinv}^{GTAP-IO}) \cdot \mathbf{FAOtoGTAP}^{IMPtoIO} \cdot \mathbf{diag}(\overrightarrow{prod}^{FAO-IMP}) \cdot \mathbf{EtoFAO}^{IMP} \qquad \text{A 0-2}$$

where each matrix is defined below, starting at the right side of the equation.

EtoFAO^{IMP} converts environmental concentrations to FAO crop concentrations by allocating each FAO crop to an IMPACT environmental compartment (e.g., carrots have the concentration of the vegetation stem compartment because they are produce unexposed to airborne pollutants, whereas lettuce has the concentration of the vegetation leaf and surface compartment because it is exposed to airborne pollutants). **EtoFAO^{IMP}** has a column for each environmental compartment and a row for each FAO crop, with an entry of 1 wherever the crop matches the compartment (Table A3.2) (the rows add to 1 to keep concentration consistent). In contrast to previous versions of IMPACT, cereals and grains are included as produce 'exposed' to air based on previous comparisons with measurements (Margni et al., 2004). Note that although this section is intended to only

calculate feed concentrations, we also calculate fish concentrations in IMPACT regions. Doing so takes advantage of the coastal regions in IMPACT with more accurate coastal concentrations (as explained in section 2.2.2). The bioaccumulation from water to fish concentrations is described in Section A3.2.4c on bioaccumulation for all animal products.

Table A3.2. FAO crops to environmental compartments. ‘exposed’ corresponds to vegetation surface and leaf, and ‘unexposed’ corresponds to vegetation stem.

After calculating pollutant concentrations in FAO crops, these are then converted to pollutant masses based on FAO production by IMPACT region; we mathematically describe this operation as the diagonal matrix consisting of the FAO crop production values $\mathbf{diag}(\overrightarrow{prod}^{FAO-IMP})$ (Fig. A3.2). Future work can base this conversion solely on crop production intended for feed, but concentrations associated with total crop production should be similar to those just for feed crop production.

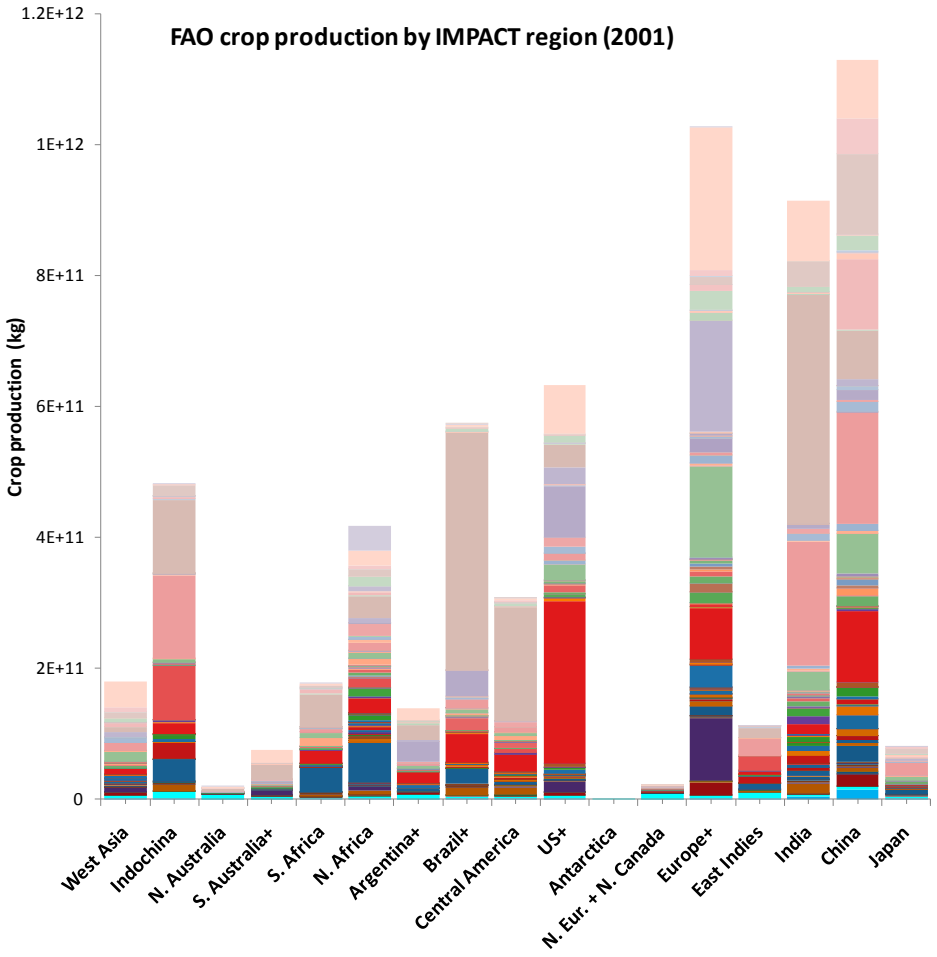

Fig. A3.2 FAO crop production by IMPACT region for the year 2001 (legend is on following page).

For **FAOtoGTAP**, each FAO crop is assigned to a GTAP sector to obtain GTAP production by IMPACT region (it has a column for each FAO crop and a row for each GTAP sector, with columns adding to one to conserve mass). **IMPtoIO**$^{\mathbf{GTAP}}$ then converts GTAP sector production from IMPACT regions to IO regions based on overlapping production in the countries of each region, (allocation for air, water, fish and roughage estimated by overlapping population) (Fig. A3.3). The combination of the two conversions yields the **FAOtoGTAP**$^{\mathbf{IMPtoIO}}$ matrix.

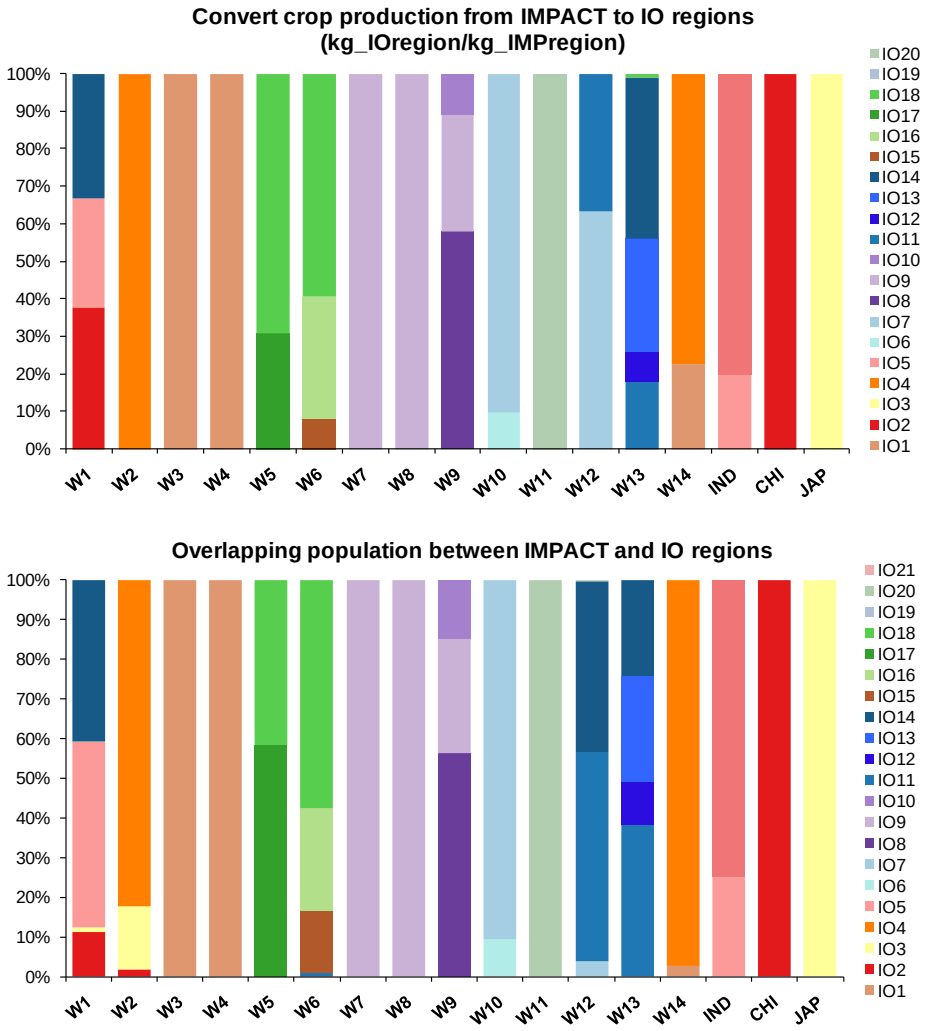

Fig. A3.3 Conversion matrices to transform GTAP crop production by IMPACT region to GTAP crop production by IO region.

To convert back to pollutant concentrations, we divide each matrix element by its crop production mass (with air, water, and fish based on IMPACT intake rates adapted to IO regions), which is achieved by multiplying by the diagonal matrix of the inverse GTAP crop production by IO region, $\mathbf{diag}(\overrightarrow{prodinv}^{GTAP-IO})$. The globally aggregated matrix for PCB-118 linking environmental concentrations to crop concentrations is shown in Fig. A3.11.

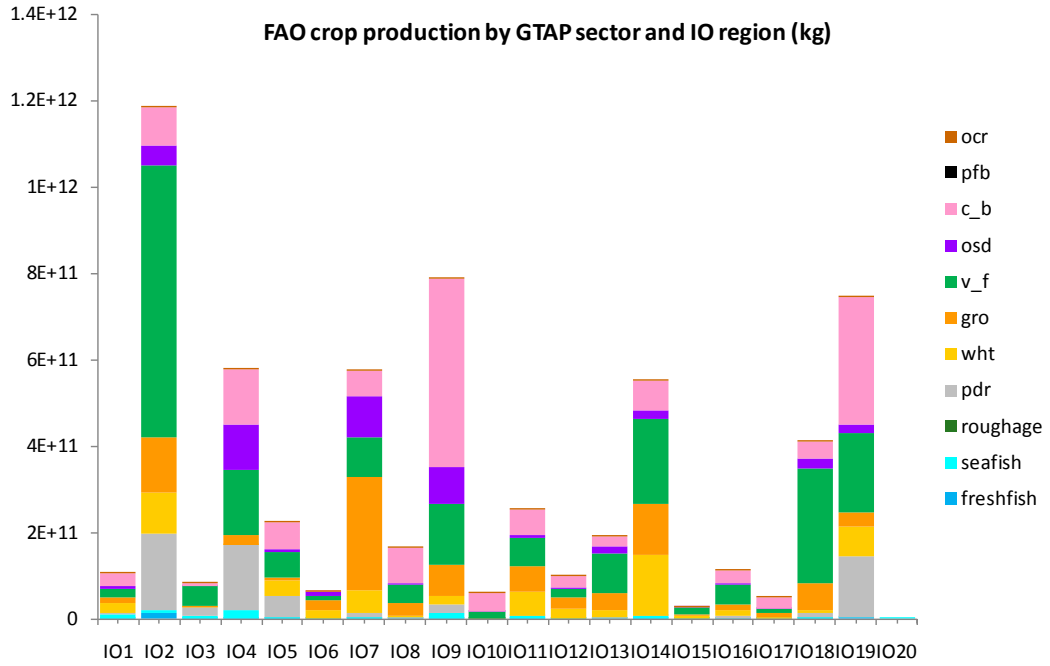

Fig. A3.4 FAO crop production by GTAP sector and IO region to convert pollutant masses back to feed concentrations.

The result of the above matrix multiplications is pollutant concentration in feed by IO region and sector, which we multiply by the economic feed trade matrix, $\mathbf{FEED}^{\mathbf{TR\text{-}IO}}$, to attain traded feed concentrations. We calculate the traded feed concentrations in each sector and region as money-weighted averages over the concentrations in each contributing region. As is commen in IO analysis, the GTAP database assumes that the price per feed is similar for the feed producing region regardless of which region or animal sector is purchasing. For example, a dollar spent by the IO1 cattle industry on IO3 grain is assumed to buy the same amount of grain as a dollar spent by the IO2 poultry industry on IO3 grain. This can be justified by the fact that international prices are usually equal regarless of the purchasing industry. To attain $\mathbf{FEED}^{\mathbf{TR\text{-}IO}}$, we aggregate each sector's feed in a given region, regardless of the specific purchasing meat industry; each sector's feed is then re-distributed to each meat industry based on animal production intake rates as described in section A3.2.4c. Future work on the model can add further complexity by tracking feed by each meat industry rather than grouping it within each region.

As shown in the graphs below depicting money spent between regions for each vegetation sector, most money is spent on feed from within the region, although there is substantial trade between certain regions, particularly in the ‘gro’(other cereals) and ‘osd’(oil crops) sectors.

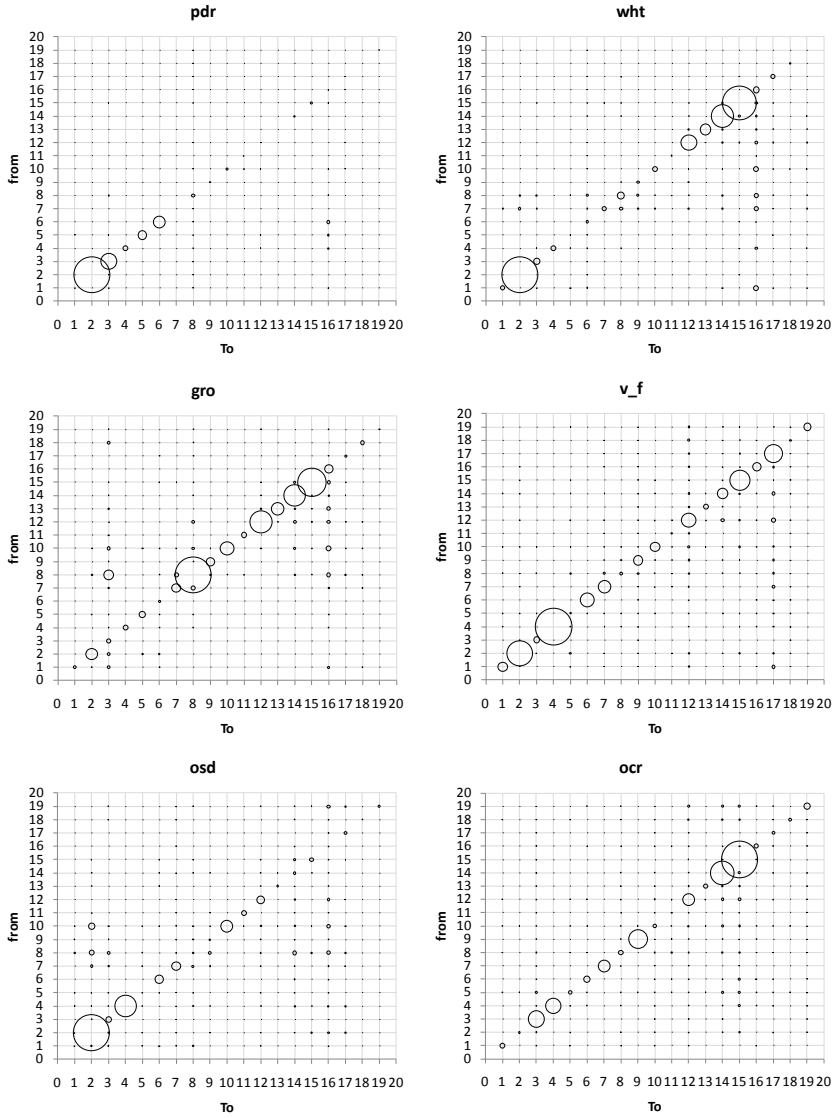

Fig. A3.5 Distribution of dollars spent in the ‘from’ region to provide feed for the ‘to’ region. The sizes of circles are a relative indicator of the money spent, with the total amount of money spent differing between graphs. Abbreviated GTAP sectors are defined In Table A3.1.

We normalize the rows (destination regions) of the matrix of absolute monetary flows between feed sectors in each region, which provides the matrix $\mathbf{FEED}^{\mathbf{TR\text{-}IO}}$. This matrix will thereby express the feed concentration in each destination sector as a dollar-weighted aggregation of the feed from contributing regions. As explained in the section

on the bioaccumulation factor, animal intake rates of feed are based on IMPACT model data, but the concentration of this feed is based on feed trade between regions as described above. Note that we also track the concentration of roughage eaten by animals, which is assumed not traded here. We assume no pollutant degradation associated with feed trade.

A3.2.4c Bioaccumulation from feed to food

The full BAF matrix has columns for every IO region, each with an air, water, and fish entry, as well as entries for GTAP raw vegetable sectors and soil and roughage ingested by animals. It has a row to match each column, with additional rows in each region for the three GTAP meat sectors. The factor linking air, water and vegetation concentrations to concentrations in substances taken in by humans is not actually a bioaccumulation factor, but we call it an effective BAF here for to keep the matrix applied consistently.

The effective BAF linking air concentrations to inhaled concentrations is simply 1. The effective BAF linking surface water to drinking water is not as simple, because of the need to account for water treatment and different water sources. It is a product of the fraction of drinking water that comes from surface water (the rest comes from groundwater), the pure to bulk water concentration ratio, and the pollutant fraction remaining after treatment (all standard parameters in the IMPACT model) (Pennington et al., 2005). For PCB-118, the pure to bulk water concentration ratio is 0.21 and we assume that none is removed through treatment. The BAF for fruits and vegetables is effectively equal to 1.

Animals breathe air, drink water, and eat soil and produce, all of which can cause pollutant accumulation in the animal. The types of meat considered here are pork, beef, poultry and other meat (mostly goat and sheep). The estimated BAF is a product of the pollutant biotransfer factor (*BTF*) from feed or environment to food and the animal intake rate (IR^{feed}). The pollutant-specific *BTF* for each animal is input for each substance or calculated based on other properties (Rosenbaum et al., 2009).

The animal intake rates for each animal and feed are calculated here by adjusting average animal intake rates used in previous IMPACT models (Margni, 2003) by the region-specific feed and animal production.

The intake rates above correspond to average vegetation intake for European animals, but animals in other regions will have different amounts of roughage and vegetable feed, with different distributions of exposed and unexposed. The European data from Margni (2003) correspond to Table A3.3 linking total vegetative intake rates, industrial feed production, and animal production. Using European data, we derive the total vegetation intake rates of each animal (roughage and industrial), and the ratios of meat production to total vegetation for feed for each animal product. For example, we find that each kg of beef requires about 120 kg of vegetation intake, 3.6 kg of which is industrial feed in Europe. This is consistent with global estimates of 3 kg of industrial feed per kg of beef (UNEP, 2003). Then we apply this ratio globally, based on FAO data for each region's industrial feed production and meat production. Assuming a globally constant ratio of meat to total vegetation feed, we can calculate the necessary amount of roughage and thus allocate intake rates to industrial feed for each region and animal.

Table A3.3 Use of European intake rates to estimate global ratio of meat production to total feed. The top half is data from European IMPACT, and the bottom half presents a series of calculations resulting in the ratio applied to calculate vegetation feed intake for all regions.

Animal	IR_feed-industrial	IR_roughage	Industrial feed	Meat production
	(kg/d/head)	(kg/d/head)	(kg)	(kg)
pork	1.15	7.70	60067	13843
beef	0.83	25.80	20595	5658
poultry	0.02	0.35	37757	6445
other meat	0.17	4.60	12013	1085
eggs	0.14	0.12	13730	4969
milk	3.21	56.00	27459	116069

frac_ industrial-feed	IR_veg-total	I_veg-total	I_roughage	Ratio of meat to total feed
(-)	(kg/d/head)	(kg)	(kg)	**(-)**
0.13	8.85	4.63.E+05	4.03.E+05	**0.030**
0.03	26.63	6.64.E+05	6.44.E+05	**0.009**
0.05	0.37	7.23.E+05	6.85.E+05	**0.009**
0.03	4.77	3.46.E+05	3.34.E+05	**0.003**
0.54	0.26	2.55.E+04	1.18.E+04	**0.195**
0.05	59.21	5.06.E+05	4.79.E+05	**0.229**

The intake rates by IMPACT sectors are allocated to GTAP sectors based on overlapping FAO crop production. Note that we don't separate raw and processed feed, since data is only available on how much of the crop eventually becomes some type of feed; due to feed trade calculations, this implicitly assumes that processed feed is exchanged proportional to its raw counterpart for lack of more detailed feed trade data.

A3.2.4d Food trade matrix

The complete food trade matrix first converts raw food pollutant concentrations to pollutant masses, then follows these masses through trade and processing, and finally converts masses back to concentrations by IMPACT region and pathway. All elements in the equation below are defined in the subsections that follow:

$$\mathbf{FOOD}^{\mathbf{TRPR}} = \mathbf{diag}(\overrightarrow{procinv}^{\mathbf{PATH-IMP}}) \cdot \mathbf{GTAPtoPATH}^{\mathbf{IOtoIMP}} \cdot \mathbf{FOOD}^{\mathbf{TR-IO}} \cdot \mathbf{diag}(\overrightarrow{prod}^{\mathbf{GTAP-IO}}) \quad \text{A3-3}$$

$\overrightarrow{prod}^{\mathbf{GTAP-IO}}$ is the vector of FAO crop and livestock production grouped by GTAP sector and IO region (Fig. A3.6). For air, water, soil and fish, the diagonal is set to the population intake rates (based on population and fish production from IMPACT regions converted to IO regions based on overlapping population).

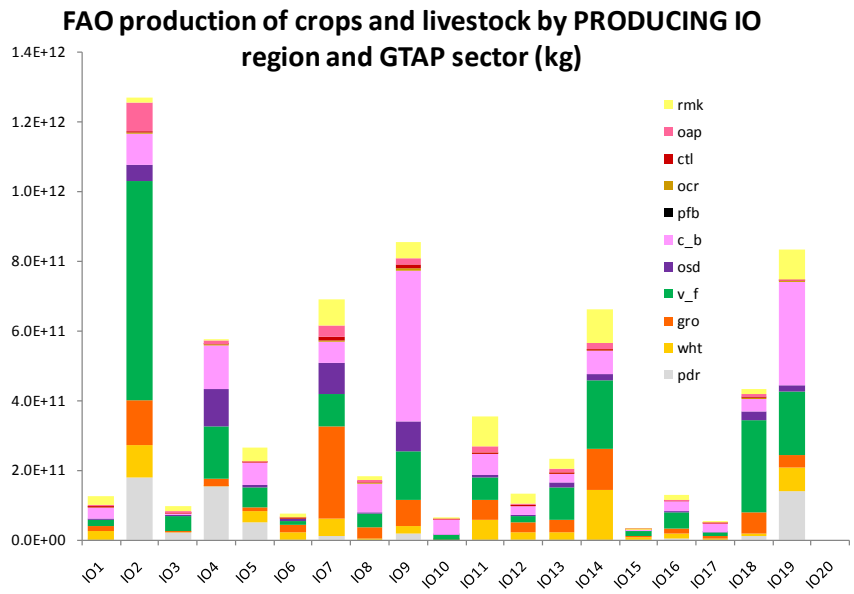

Fig. A3.6 FAO production of crops and livestock by IO region and GTAP sector. IO and GTAP abbreviations explained in Table A3.1.

FOOD$^{\text{TRPR-IO}}$ matrix is actually created by running the adapted TREI-C model for each of the consuming regions, thus generating a matrix of global food production needed to satisfy food consumption, and then aggregating this matrix per consuming sector. By applying basic input-output analysis techniques developed by Leontief (Leontief), the magnitude and structure are computed of the total production needed for delivering one unit of a good to final consumers. This provides the link between a consumed good in a region and all the sectors involved in its production from a global perspective.

However, the food supply predicted by applying the conomic food trade matrix to the FAO food production does not exactly match the FAO food supply (they are similar, but the economic food trade matrix consistently over or underestimates certain sector production). As discussed in Section 3.2.2, the food trade matrix is adjusted to match the FAO food supply. Thus, the economic food trade matrix contains an additional constant conversion factor for each purchasing region and sector (Fig. A3.7) to ensure that the FAO food supply is attained. Since this matrix expresses the portion of raw food that ends up traded, processed and purchased, it accounts for food losses during trade and processing.

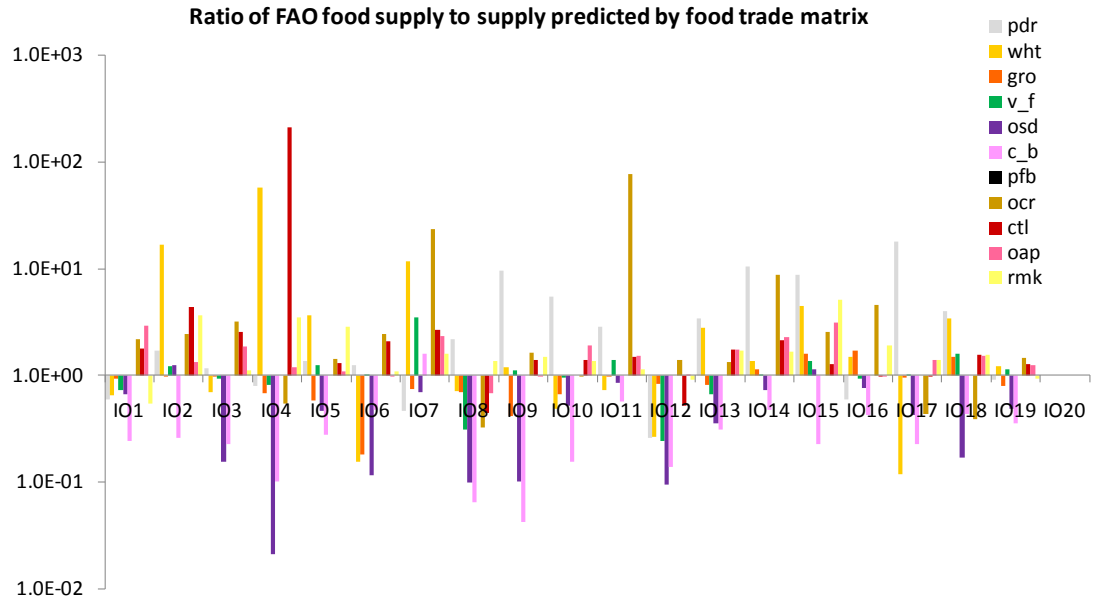

Fig. A3.7 Ratio of FAO food supply to supply predicted by food trade matrix. These factors by region and purchasing sector are used to adjust the economic food trade matrix such that it is consistent with the FAO food supply.

The result of multiplying FAO production by the economic food trade matrix shows the amount of food traded between regions and is displayed in the results section (Fig. A3.17). In the scenario assuming no food trade, we still use the $\mathbf{FOOD}^{\mathbf{TR\text{-}IO}}$ matrix to calculate how raw food is converted to processed sectors (as shown in results Fig. A3.19), but we assume all processed food remains in the region containing the raw food.

To convert food masses by IO region and GTAP sector to IMPACT regions and pathways, we create the $\mathbf{GTAPtoPATH}^{\mathbf{IOtoIMP}}$ matrix, as a product of a matrix converting GTAP sectors to IMPACT pathways and a matrix converting pathways by IO region to pathways by IMPACT region: $\mathbf{GTAPtoPATH}^{\mathbf{IOtoIMP}} = \mathbf{IOtoIMP}^{\mathbf{PATH}} \cdot \mathbf{GTAPtoPATH}$.

The (region-independent) sector conversion $\mathbf{GTAPtoPATH} = \mathbf{FAOtoPATH} \cdot \mathbf{GTAPtoFAO}$ is the product of a matrix converting GTAP to FAO sectors and another converting FAO sectors to IMPACT pathways. **GTAPtoFAO** is calculated by normalizing the columns of $\mathbf{GTAPtoFAO}^{\mathbf{PROD}}$, which allocates each FAO crop to GTAP raw and processed sectors by first using the allocation to raw sectors and then using

$\mathbf{TR}^{\mathbf{FOOD}}$ to also distribute allocation to processed sectors (for example, it distributes apple production to raw fruits, as well as prepared food and beverages). **FAOtoPATH** simply assigns each FAO crop to an IMPACT exposure pathway.

The inter-region conversion $\mathbf{IOtoIMP}^{\mathbf{PATH}}$ is performed across all exposure pathways based simply on overlapping population. Ideally, this would be allocated based on consumption patterns, but data is not currently available on consumption of processed foods (all processed food is expressed as the raw crop equivalent).

To get back to traded food concentrations, we multiply all of this by the diagonal matrix of inverse processed (and raw) traded food masses by IMPACT region and pathway, $\mathbf{diag}(\overrightarrow{procinv}^{\mathbf{PATH-IMP}})$. This is based on the FAO food supply data used to normalize the economic food trade matrix, distributed between raw and processed sectors based on that matrix, but expressed by IMPACT region and pathway.

A3.2.4e Population intake rate details

$\mathbf{IR}^{\mathbf{POP}}$ is a square matrix with its dimension equal to the product of the number of IMPACT regions and pathways. For non-fish food, the intake rates are the same values as those used above, $\overrightarrow{procinv}^{\mathbf{PATH-IMP}}$, the amount of processed and raw food consumed by region and pathway (after trade and losses). In the scenario assuming no trade, the intake rate is adjusted to reflect that all processed food is assumed ingested in the region of production.

For air and water, intake rates are taken from existing IMPACT models based on regional populations and average daily breathing and drinking rates. In the case of water, we still use IMPACT model parameters for the fraction of drinking water taken from surface water, with the remainder from groundwater. Freshwater fish and coastal fish intakes are currently allocated to the region of production, since no trade data is available. Ocean fish are currently distributed equally to all regions in a very rough approximation that doesn't currently affect final results due to the very small contribution of ocean fish to intake fraction.

A3.3 More detailed results

A3.3.1 Intermediary matrices from environment to raw untraded food concentrations

A3.3.1a TRANSFER - Fate matrix:

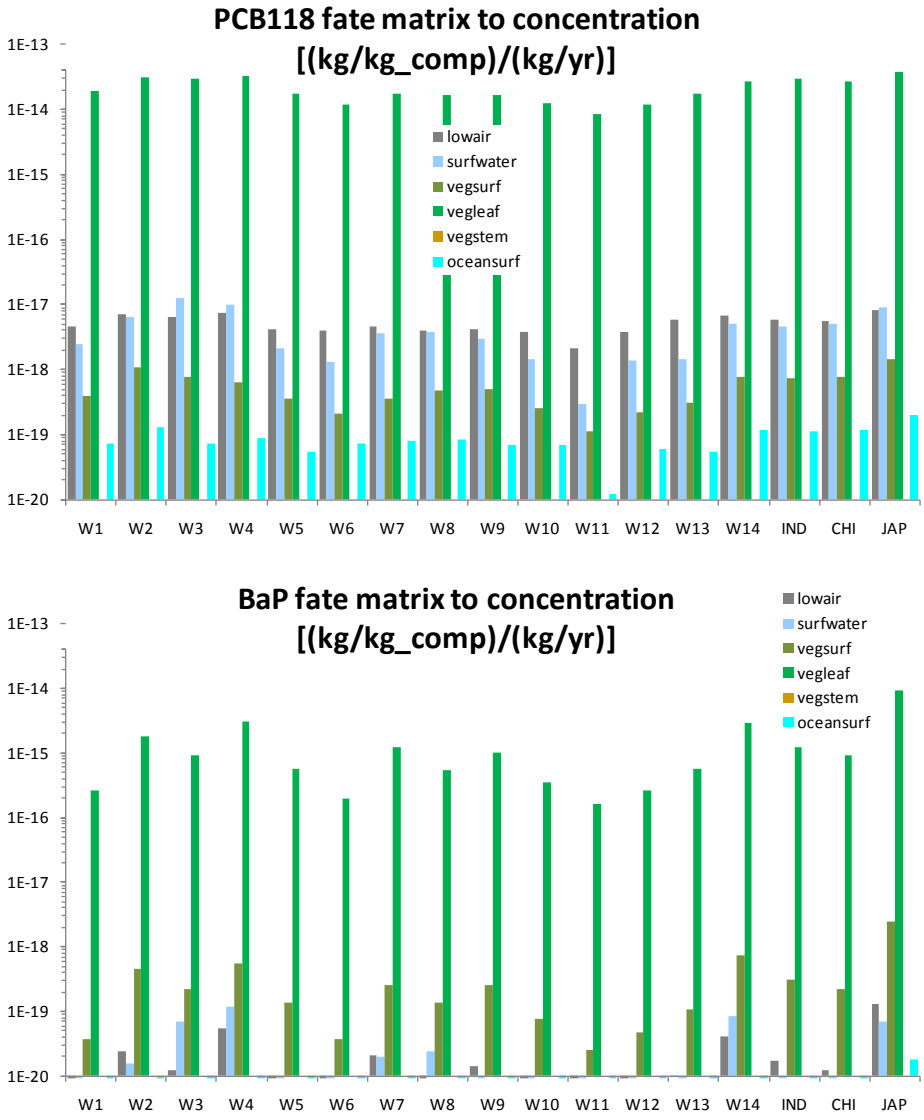

Fig. A3.8 IMPACTWorld matrices expressing environmental concentrations for each annual unit emission. PCB-118 concentrates most in surface vegetation, but also in air and water, whereas benzo[a]pyrene concentrates more in vegetation.

A3.3.1b MEASURABLE – Environmental concentrations

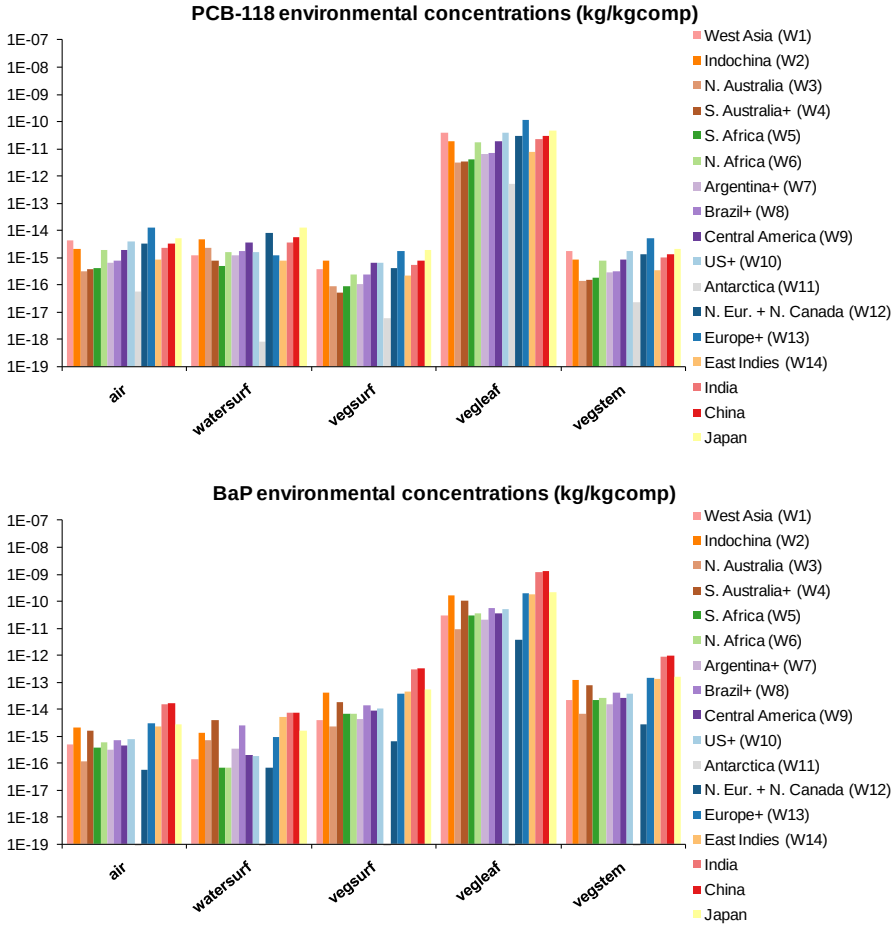

Fig. A3.9. IMPACTWorld predicted environmental concentrations for PCB-118 and B[a]P. Note that consistent with the fate matrix above, B[a]P vegetation concentrations ('vegsurf' and 'vegleaf') are higher than those in other compartments. Also note that the ratio of PCB-118 surface water ('watersurf') to vegetation concentrations is higher than the ratio for B[a]P (which is also consistent with the fate matrix).

A3.3.1c TRANSFER - Feed trade matrix:

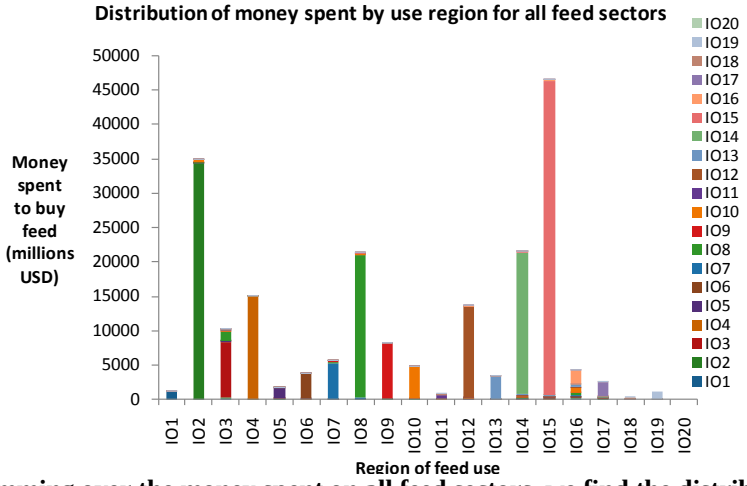

Fig. A3.10. By summing over the money spent on all feed sectors, we find the distribution of money spent on feed by each region consuming feed. Region IO16 has the most distributed spending, but very small absolute feed consumption.

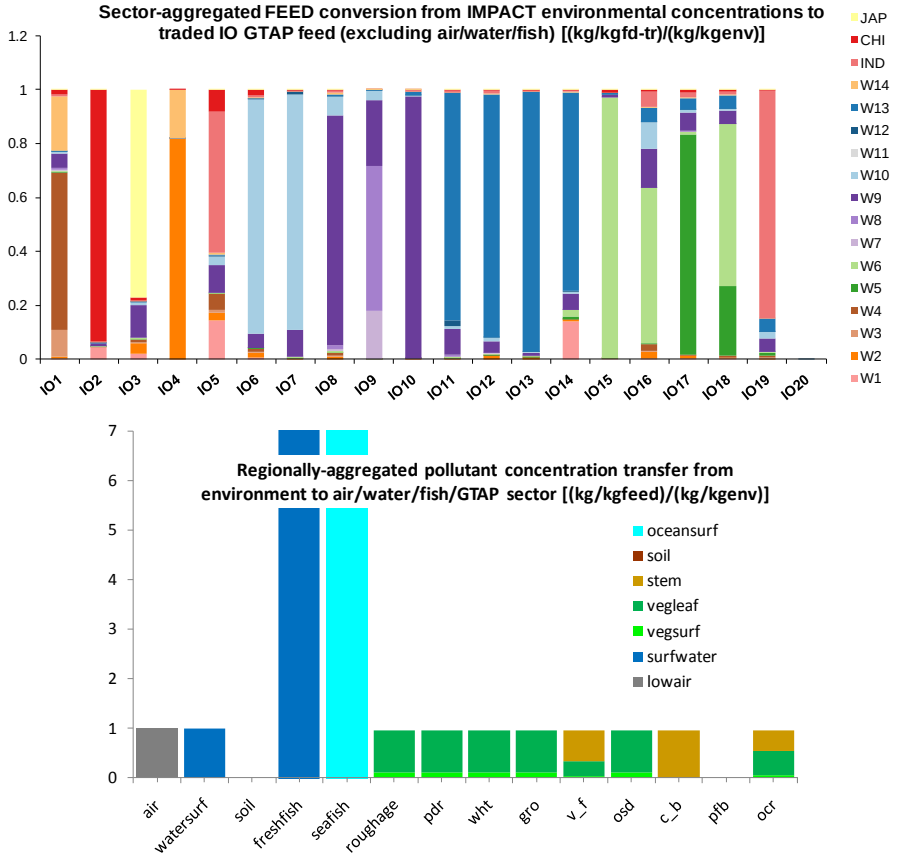

Fig. A3.11. Aggregated the FEED^{TR} matrix first by sector and then by region to show the conversion from IMPACT to IO regions, the level of trade between regions, and the link between environmental concentrations and GTAP sector concentrations. These matrices link environmental compartments and sectors and are therefor independent of pollutant (except that the fish entry, extending past the height of this graph, is the BAF of the considered pollutant).

A3.3.1d MEASURABLE – Concentrations after feed trade:

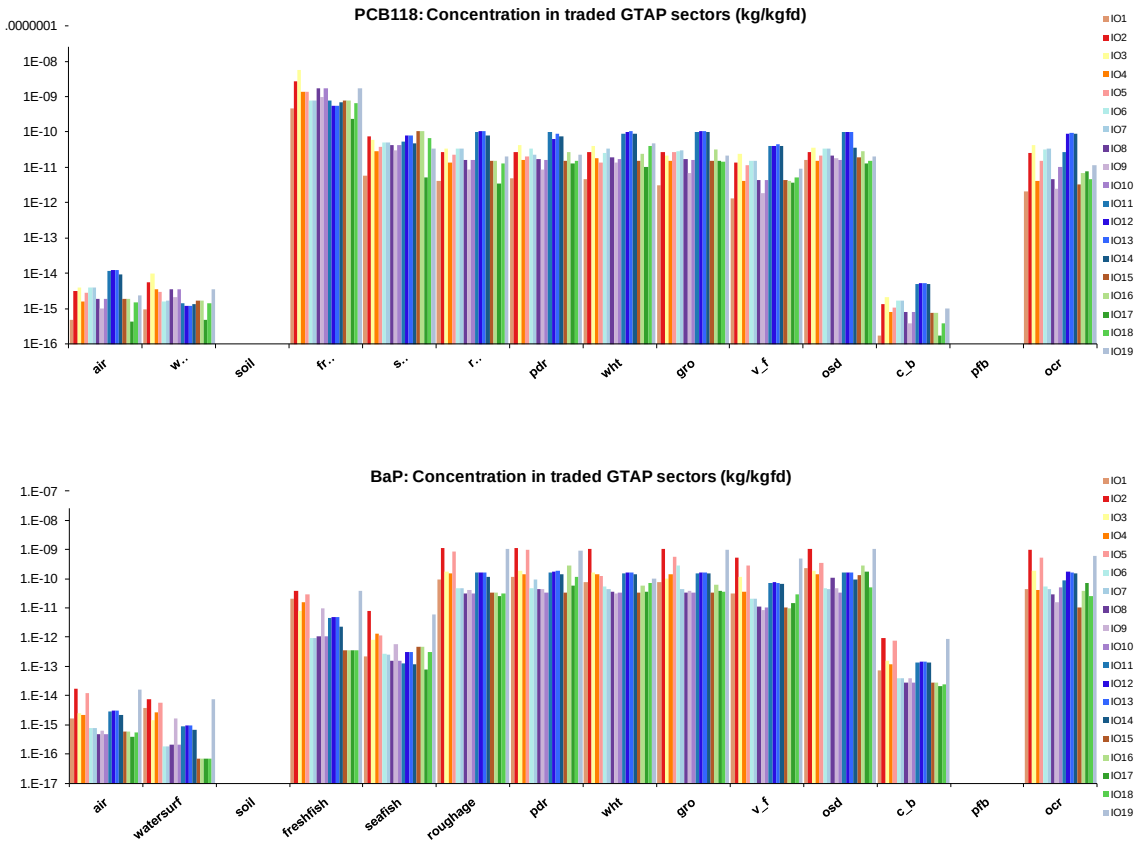

Fig. A3.12. The product of the FEED^{TR} matrix and environmental concentrations above yields the concentrations in traded feed GTAP sectors. The similar colors allow the regional patterns in environmental concentrations to be seen in the feed concentrations. Note that for PCB-118, fish concentrations about one order of magnitude higher than other foods, with the reverse pattern in B[a]P.

A3.3.1e TRANSFER - Bioaccumulation factor matrix

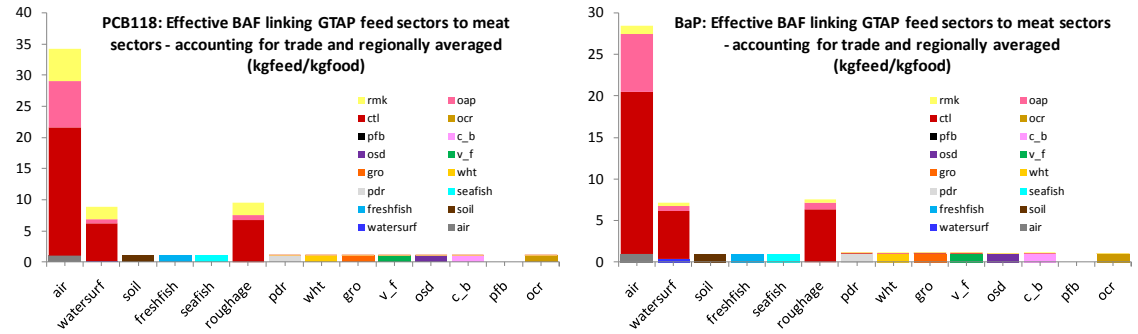

Fig. A3.13. The effective BAFs averaged over all regions, where the x-axis represents the feed compartment and the y-axis represents the factor by which the original concentration is multiplied in the food compartment (thus a factor of one for any vegetation compartment, where feed and and untraded food have the essentially the same concentration).

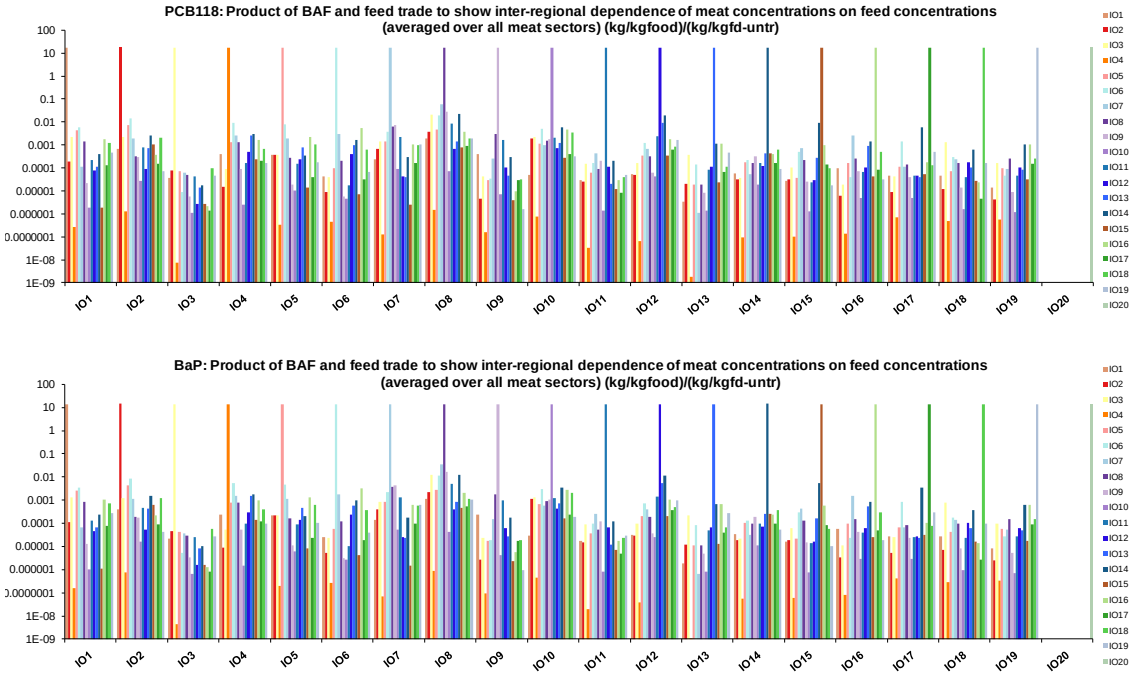

Fig. A3.14. The product of the FEED^{TR} matrix and the BAF matrix above shows how the concentrations in raw untraded food depend on each region's untraded feed concentrations. The two pollutants look very similar here, because the FEED^{TR} matrix is the same for both, and the BAF matrices are similar. Note that traded feed contributes less than 1% of pollutant to food compared with local feed (the traded feed contributions are more than two orders of magnitude lower than the local feed contributions).

A3.3.1f MEASURABLE – Raw food concentrations

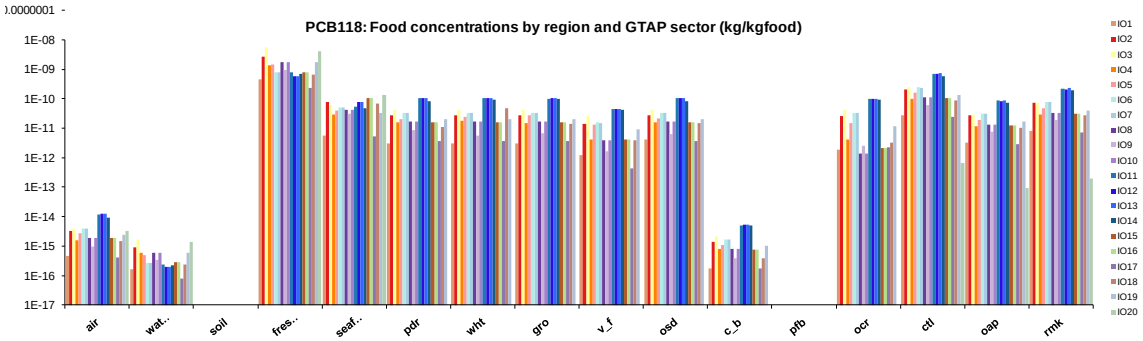

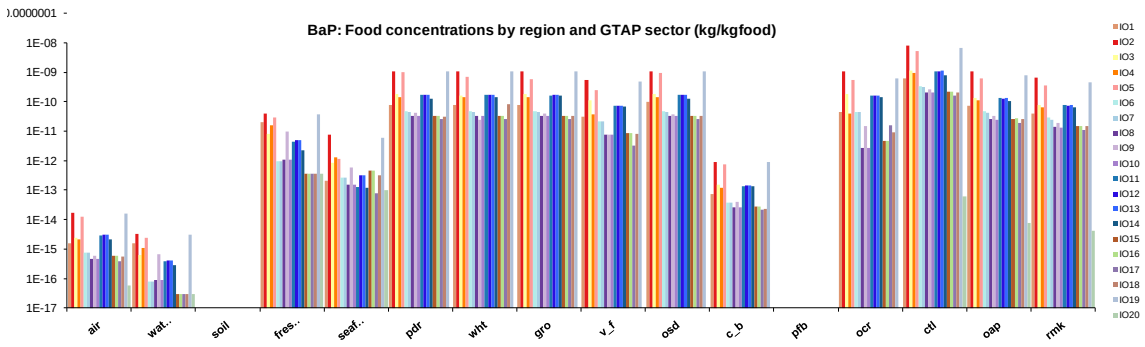

Fig. A3.2.4e.15. The product of the BAF matrix and traded feed concentrations yields the concentrations in raw untraded food GTAP sectors. Note that in contrast to PCB-118, B[a]P has higher concentrations in the fruit and vegetable sectors (pdr, wht, gro, v_f, osd, ocr) than the fresh fish and sea fish sectors.

A3.3.2 More details on food trade matrix, intake rate and absolute intake

A3.3.2a TRANSFER - Intake rate matrix

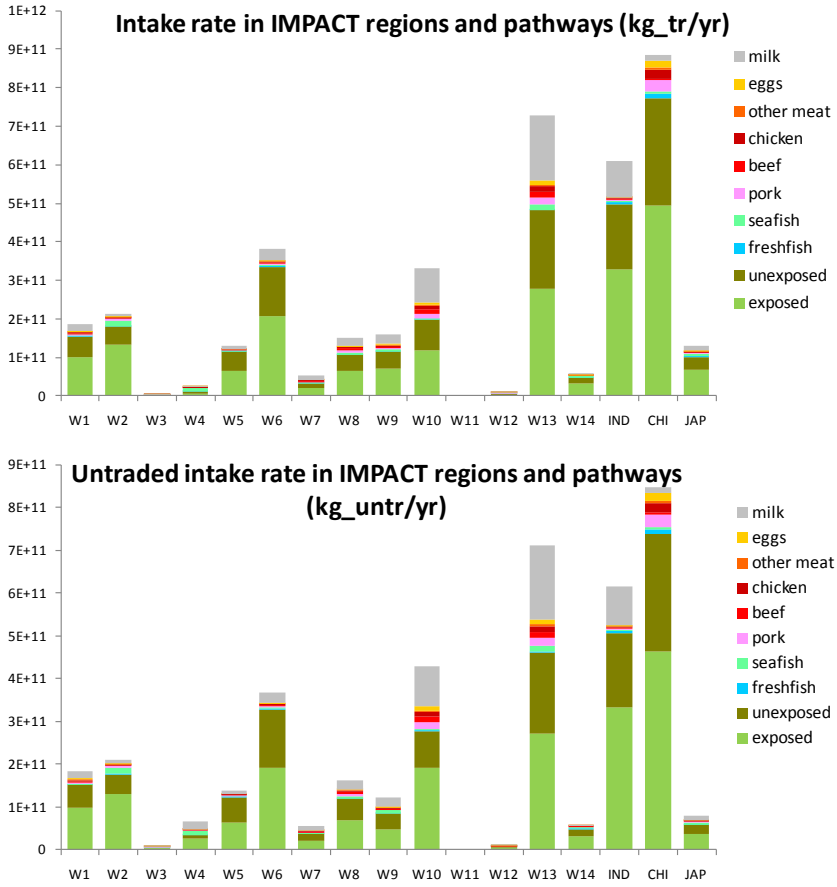

Fig. A3.16 Food intake rates (kg/yr) accounting for food trade (top) and without accounting for food trade (bottom) by IMPACT region and sector, based on FAO food supply data.

Table A3.4 Globally averaged fraction of produced food that is eventually sold to households. Some sectors have the same fraction due to overlap in GTAP versions of sectors.

	exposed produce	unexposed produce	pork	beef	chicken	other meat	eggs	milk	fresh fish	sea fish
Food fraction	51%	51%	97%	98%	97%	97%	97%	87%	91%	79%

A3.3.2b Global food distribution matrix

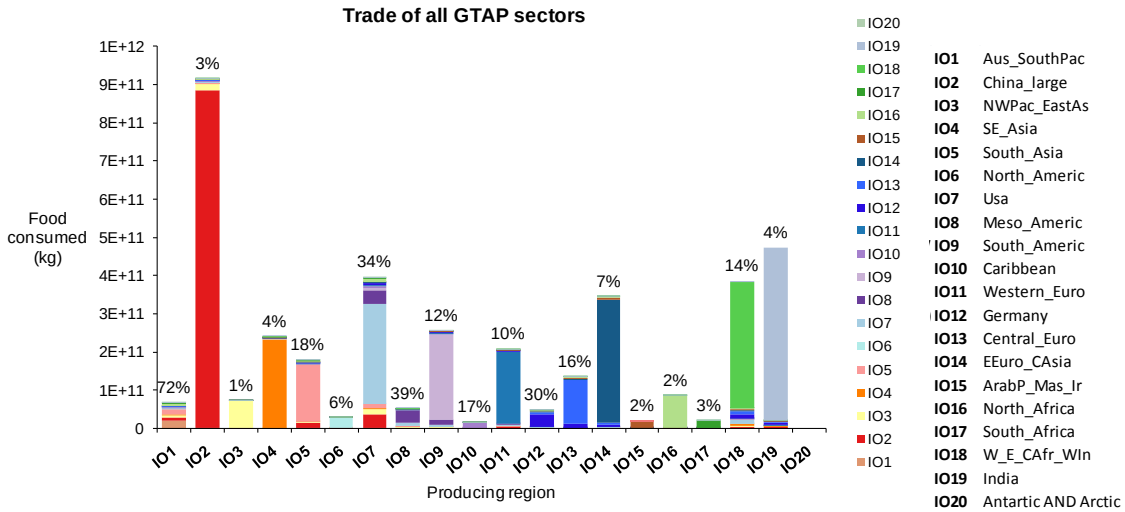

Fig. A3.17. Global food distribution from producing to consuming IO regions (total food over all GTAP sectors).

The masses and percentages of trade found by integrating our global economic model with FAO data are within a factor two of country specific studies of food exports for the US and UK (Buzby, 2003). Our model finds that 21% of US non-meat food consumption is imported, which is consistent with USDA reports that US imports 19.5% of its fresh fruit consumption and 13.6% of fresh vegetable consumption (these percentages exclude bananas and potatoes that are mostly domestically produced, but account for less than 20% of fruit and vegetable consumption).

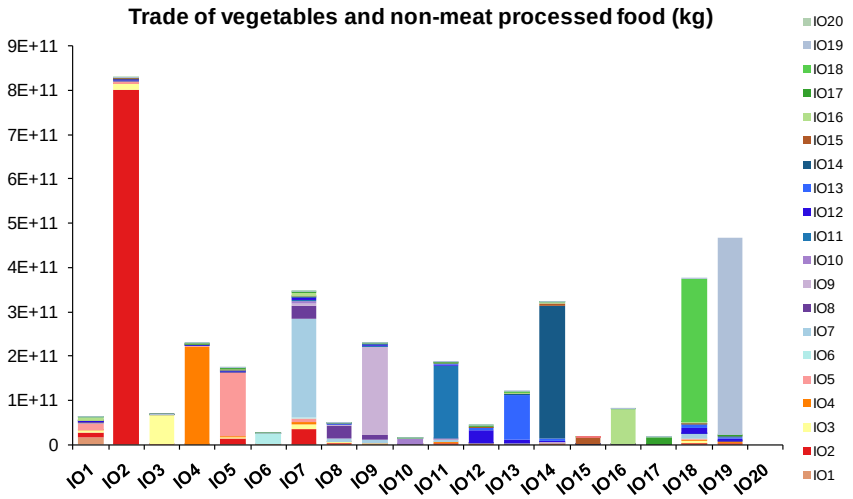

Fig. A3.18 Global food distribution from producing to consuming IO regions, including only only non-meat sectors.

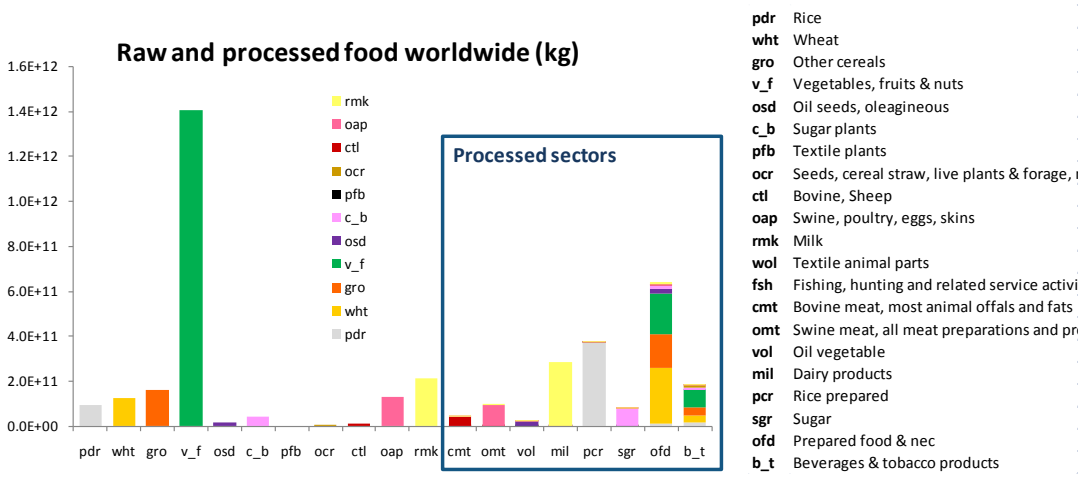

Fig. A3.19 Transformation from raw crops to processed food, summed over all regions.

A3.3.2c MEASURABLE – Intake

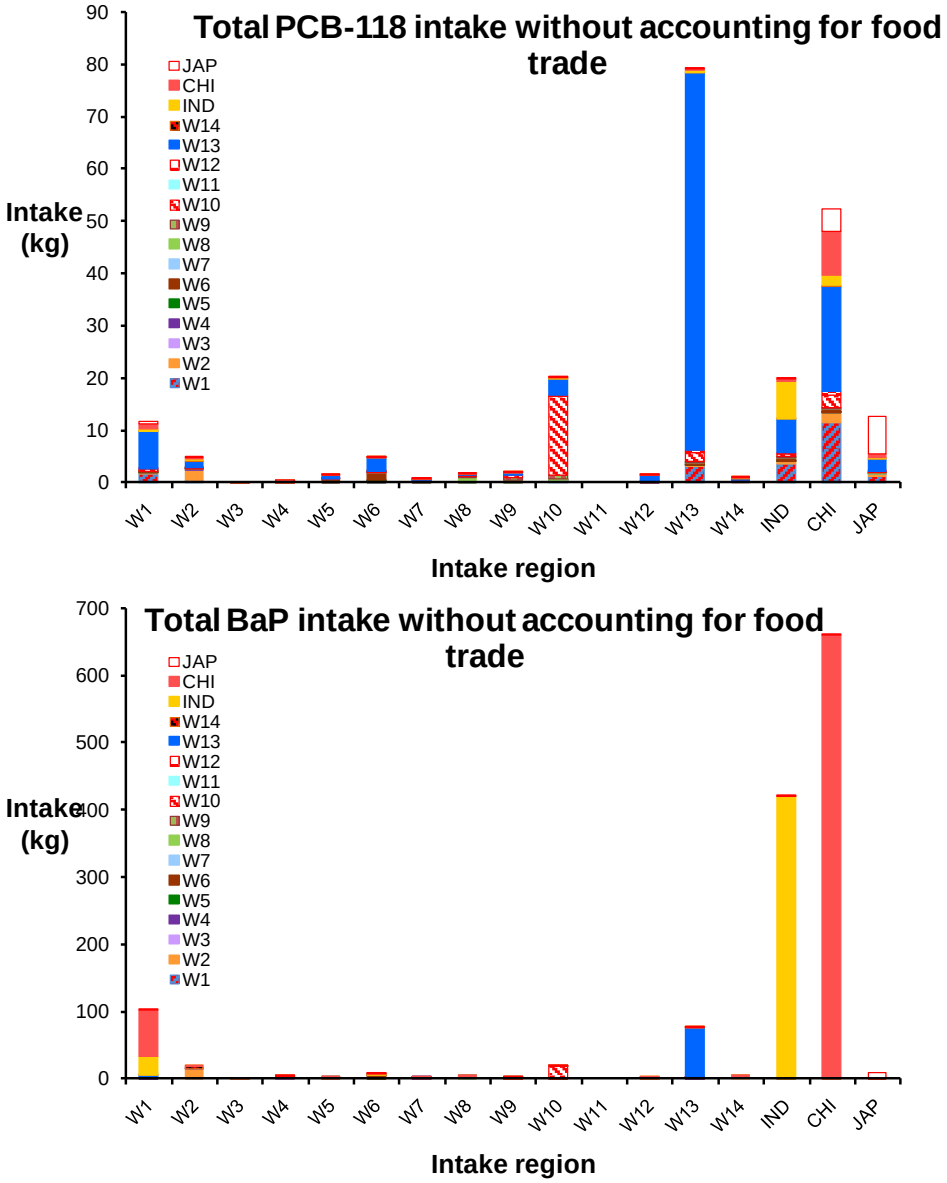

Fig. A3.20 Total pollutant intake based on applying spatial intake fractions (without accounting for food) to global emissions inventories.

Because B[a]P has not yet been evaluated in the IMPACTWorld application, we compare the US intake after accounting for food trade with the average intake from a study in a single location of the US. Our results for the US amount toa B[a]P intake rate of approximately 15 ng/person/day. This intake is lower but of similar order of magnitude as a localized US study finding intake rates ranging from 35 to 200 ng/person/day (Sinha et al., 2005).

APPENDIX 4
Quantification of environmental impacts on human health due to global production and consumption chains

A4.1 Methods – further details

A4.1.1 Overview

The Input-Output model (Friot and Antille, 2009; Miller and Blair, 1985; Peters and Hertwich, 2007b) (19 regions, 24 goods) describes inter-industrial relationships and inter-regional trade at basic prices for 2001. It is based on the widely used global economic database GTAP v. 6 (Dimaranan, 2006). Import matrices are based on trade shares. International transport is specifically considered with three supra-national sectors. The number of sectors reflects the availability of environmental data. We extended the economic model by developing a global inventory of PM2.5 by sector, and estimating PM2.5 with existing national and global inventories and modelled data sets (see below). The consumption scenarios include the three components of final demand: household consumption, government consumption and investment demand.

The global impact assessment model (IMPACTWorld) extends to a global scale the spatial version of the IMPACT 2002 multimedia model, initially evaluated for Europe (Margni et al., 2004; Pennington et al., 2005). It estimates steady state pollutant concentrations and human exposure and intake for continental, oceanic and coastal regions. Within each region, the urban intake fraction (Humbert et al., 2009) is estimated using urban population (and some area) data for 3,670 urban areas (covering 2.2 billion people) provided by the United Nations and the World Bank (Angel et al., 2005; UN, 2008), and allocating PM2.5 emissions between urban and rural areas by population. Trans-boundary transport is simulated by air flows based on annually averaged winds from a global tropospheric chemistry model (Bey and et al., 2001). Damages to human health (in DALYs) from PM2.5 are calculated based on pollutant-specific incidences of resulting diseases from epidemiological studies (Schwartz et al., 2008).

A4.1.2 Regional divisions

Table A4.1 presents the regions and region groupings for the environmentally-extended multiregional Input-Output model. Groupings and names are based on the UN classification (United Nations), with the exception of Israel, which is grouped according to its geographical position (with the Rest of Middle East) and Turkey which is grouped into Central Europe.

Table A4.1 List of regions in Input-Output model.

6 aggregated regions	19 regions	87 countries and regions from the GTAP database (Dimaranan, 2006)
China + South Asia + South-East Asia	China	China, Hong Kong, Taiwan
	India	India
	South-East Asia	Indonesia, Malaysia, Philippines, Singapore, Thailand, Vietnam, Rest of Southeast Asia
	Rest of South Asia	Bangladesh, Sri Lanka, Rest of South Asia
Japan + Koreas	Rest of North West Pacific and East Asia	Japan, Korea, Rest of East Asia
North America	Rest of North America	Canada, Rest of North America
	USA	USA
Germany	Germany	Germany
Western and Central Europe	Central Europe	Rest of Europe, Albania, Bulgaria, Croatia, Cyprus, Czech Republic, Hungary, Malta, Poland, Romania, Slovakia, Slovenia, Estonia, Latvia, Lithuania, Turkey
	Rest of Western Europe	Austria, Belgium, Denmark, Finland, France, United Kingdom, Greece, Ireland, Italy, Luxembourg, Netherlands, Portugal, Spain, Sweden, Switzerland, Rest of European Free Trade Association
Rest of World	Arabian Peninsula/Mashriq/Israel	Rest of Middle East
	Northern Africa	Morocco, Tunisia, Rest of North Africa
	Southern Africa	Botswana, South Africa, Rest of South African CU, Malawi, Mozambique, Tanzania, Zambia, Zimbabwe
	Western/Eastern/Central Africa/ Western Indian Ocean	Rest of Southern African Development Community, Madagascar, Uganda, Rest of Sub-Saharan Africa
	Caribbean	Rest of Free Trade Area of the Americas, Rest of the Caribbean
	South America	Colombia, Peru, Venezuela, Rest of Andean Pact, Argentina, Brazil, Chile, Uruguay, Rest of South America
	Meso-America	Central America
	Australia and New Zealand/South Pacific	Australia, New Zealand, Rest of Oceania
	Eastern Europe/ Central Asia	Russian Federation, Rest of Former Soviet Union

The 17 regions in the pollutant transport and impact model (Table S2) are similar to those chosen for the Input-Output model, but with some key differences due to less emphasis on geographical boundaries and more on population densities and meteorological conditions. Because of such considerations, some countries have been

split between two regions. 42 additional regions, not presented here, are designed to cover pollutant fate and transport in oceans and coastal areas.

Table A4.2 List of regions in global transport and impact model.

Region ID	Region Name	Countries in each region
W1	**West Asia**	Russian Federation, Afghanistan, Iran (Islamic Republic of), Kazakhstan, Kyrgyzstan, Mongolia, Tajikistan, Turkmenistan, Uzbekistan, Western China
W2	**Indochina**	Brunei Darussalam, Cambodia, Lao People's Democratic Republic, Malaysia, Maldives, Myanmar, Philippines, Singapore, Thailand, Viet Nam, Indonesia
W3	**N Australia**	Australia, Wallis and Futuna Islands
W4	**S Australia+**	Australia, New Zealand
W5	**S Africa+**	Angola, Botswana, Comoros, Lesotho, Madagascar, Malawi, Mauritius, Mozambique, Namibia, Rwanda, Réunion, South Africa, Swaziland, United Republic of Tanzania , Zambia, Zimbabwe, Democratic Republic of the Congo, Congo, Gabon, Kenya, Uganda, Saint Helena, Seychelles
W6	**N Africa+**	Democratic Republic of the Congo, Congo, Gabon, Kenya, Uganda, Algeria, Bahrain, Benin, Burkina Faso, Burundi, Cameroon, Cape Verde, Central African Republic, Chad, Côte d'Ivoire, Djibouti, Egypt, Eritrea, Ethiopia, Gambia, Ghana, Guinea, Guinea-Bissau, Iraq, Israel, Jordan, Kuwait, Lebanon, Liberia, Libyan Arab Jamahiriya, Mali, Mauritania, Morocco, Niger, Nigeria, Oman, Occupied Palestinian Territory, Qatar, Sao Tome and Principe, Saudi Arabia, Senegal, Sierra Leone, Sudan, Syrian Arab Republic, Togo, Tunisia, United Arab Emirates, Western Sahara, Yemen, Equatorial Guinea, Somalia
W7	**Argentina+**	Argentina, Chile, Falkland Islands (Malvinas), Paraguay, Uruguay
W8	**Brazil+**	Bolivia, Peru, most of Brazil, Colombia, southern Ecuador
W9	**C America+**	Anguilla, Antigua and Barbuda, Aruba, Bahamas, Barbados, Belize, Bermuda, British Virgin Islands, Cayman Islands, Costa Rica, Cuba, Dominica, Dominican Republic, El Salvador, French Guiana, Grenada, Guadeloupe, Guatemala, Guyana, Haiti, Honduras, Jamaica, Martinique, Mexico, Montserrat, Netherlands Antilles, Nicaragua, Panama, Puerto Rico, Saint Kitts and Nevis, Saint Lucia, Saint Pierre and Miquelon, Saint Vincent and the Grenadines, Suriname, Trinidad and Tobago, Turks and Caicos Islands, United States Virgin Islands, Venezuela (Bolivarian Republic of), part of Brazil, Colombia, northern Ecuador
W10	**USA+**	Southern Canada, USA (except Alaska)
W11	**Antarctica**	Antarctica
W12	**N Europe + N Canada**	Alaska, Greenland, Iceland, Finland, Northern parts of Canada, Norway, Sweden, Russian Federation
W13	**Europe+**	Gibraltar, Greece, Hungary, Ireland, Italy, Latvia, Liechtenstein, Lithuania, Luxembourg, TFYR Macedonia, Malta, Moldova, Monaco, Netherlands, Poland, Portugal, Romania, San Marino, Serbia, Slovakia, Slovenia, Spain, Switzerland, Turkey, Ukraine, United Kingdom ; Southern parts of Norway, Sweden, Russian Federation
W14	**East Indies**	Indonesia, American Samoa, Cook Islands, Fiji, French Polynesia, Guam, Kiribati, Marshall Islands, Micronesia (Fed. States of), Nauru, New Caledonia, Niue, Northern Mariana Islands, Palau, Papua New Guinea, Samoa, Solomon Islands, Timor-Leste, Tokelau, Tonga, Tuvalu, Vanuatu
IND	**India+**	India, Bangladesh, Bhutan, Nepal, Pakistan, Sri Lanka
CHI	**E China**	Eastern China, Hong Kong SAR
JAP	**Japan+**	Japan, North Korea, South Korea

A4.1.3 Commodities in the Input-Output model

The 24 commodities are an aggregation of the commodities from the GTAP database v.6 (Dimaranan, 2006) (Table A4.3).

Table A4.3 List of commodities in the multi-regional Input-Output model.

Commodities of the IO model	GTAP sector names
Rest of crops	Cereal grains nec / Vegetables, fruit, nuts / Oil seeds / Sugar cane, sugar beet / Crops nec
Rice	Paddy rice
Plant-based fibers	Plant-based fibers
Cattle and other animals products	Bovine cattle, sheep and goats, horses / Animal products nec / Raw milk / Wool, silk-worm cocoons
Forestry	Forestry
Fishing products	Fishing
Land transport	Transport nec
Water transport	Water transport
Air transport	Air tranport
Coal	Coal
Crude petroleum	Oil
Gas	Gas
Minerals	Minerals nec / Mineral products nec
Processed food	Bovine meat products / Meat products nec / Vegetable oils and fats / Dairy products / Processed rice / Sugar / Food products nec / Beverages and tobacco products
Textiles and leather	Textiles / Wearing apparel / Leather products
Wood and papers products	Wood products
Petroleum products	Petroleum, coal products
Chemicals	Chemical, rubber, plastic products
Ferrous metals	Ferrous metals
Non-ferrous metals	Metals nec
Other manufactured goods	Metal products / Motor vehicles and parts / Transport equipment nec / Electronic equipment / Machinery and equipment nec / Manufactures nec
Electricity	Electricity
Sales	Trade
Services	Gas manufacture and distribution / Construction / Communication / Financial services nec / Insurance / Business services nec / Recreational and other services / Public Administration, Defense, Education, Health / Dwellings

A4.1.4 Sources and methods for $PM_{2.5}$ emissions inventory

The $PM_{2.5}$ global emissions inventory is based on official emissions inventories from the Convention on Long-range Ttransboundary Air Pollution (EEA, 2009), NAMEA satellites of the national accounts (Eurostat, 2001), modelled data from the RAINS model (Klimont et al.) for European regions, national emissions inventories for Canada, USA and Mexico (Instituto Nacional de Ecología et al., 2006), modelled data from the GAINS database for China and India (Dentener et al., 2008), and a modelled inventory for Asia (CGRER, 2006). Emissions for other regions are modeled based on the Mexican inventory, assuming similar emissions factors per dollar of production in Purchasing Power Parity. Industrial emissions are separated from direct household emissions based on data from the literature.

Emissions are then re-classified from source categories to sectors in two steps. First, a straightforward allocation is done for all emissions except those from transport. Then transport emissions are re-allocated to all sectors, to include own-transport, replicating the EU NAMEA approach (Eurostat, 2003), and average European ratios.

A4.1.5 Exchange rates

Multi-regional Input-Output models require the use of a single currency, in our case the 2001 US dollar (USD). As is typically done in this type of model, the conversion to USD is based on the market exchange rate (Peters and Hertwich, 2007b). We are aware that a conversion based on Purchasing Power Parity would account for the differences in cost of living between different countries, and thus better represent volumes.

A4.2 Supporting results

A4.2.1 Distribution of fine PM emissions from the inventory among commodities

The distribution of fine particulate ($PM_{2.5}$) emissions associated with the different commodities in Germany, USA and China is shown in Fig. A4.1. Commodities are

grouped into five categories: primary goods, transport, manufactured goods, electricity, and services including sales.

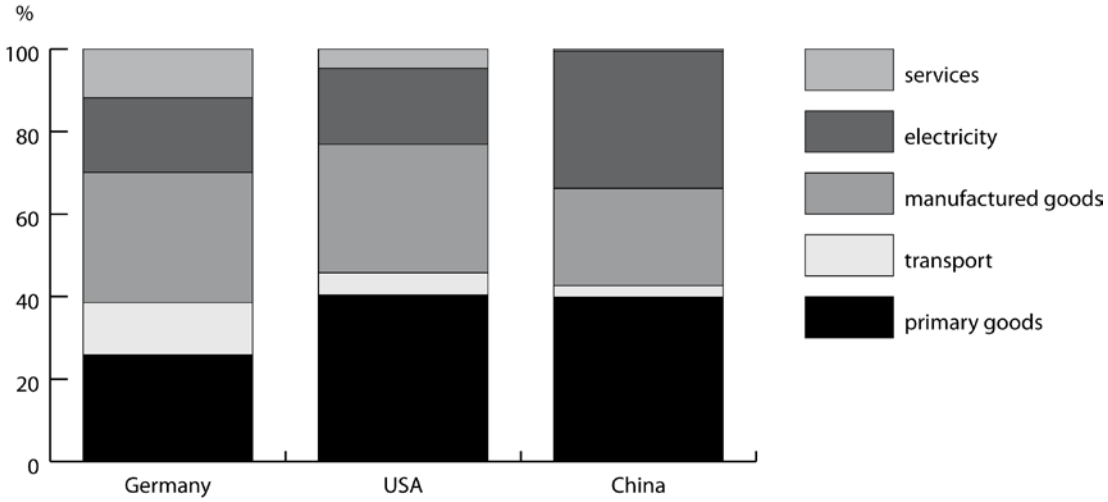

Fig. A4.1 Distribution of fine particulate emissions associated with different commodities for Germany, USA and China.

A4.2.2 Intake fractions

The intake fraction (iF) is defined as the fraction of pollutant emitted that is eventually taken in by a population (Bennett et al., 2002b). In a simple box model, it is estimated by assuming that any emissions immediately diffuse evenly in the box, using the subsequent concentration and population densities to estimate intake fraction. A recent spatialized study of North America (Humbert et al., 2009) showed that this method can severely underestimate iFs by falsely diluting urban emissions and exposure in the surrounding regional or continental box. The authors find that a key factor determining iFs of urban emissions is the average linear population density of the urban area. Using equation S2 of the study and urban population data from the United Nations and World Bank (Angel et al., 2005; UN, 2008), we estimate the average intra-urban iF of each region in our global impact assessment model. The emissions-weighted average (here estimated as a population-weighted average) of the intra-urban iF and continental iF yields an estimated iF for urban emissions (‘urban intake fraction’). Key model parameters and these intake fractions are provided in Table S4. The stack height of

emissions can also play a key role in exposure, but detailed information at the level of this model is not available.

Table A4.4 Key parameters and intake fractions for pollutant transport model.

Impact region	Population	Area	Urban fraction	Urban linear pop. density	Intake fraction - continental emission	Intake fraction - urban emission
	(millions)	(km^2)	(-)	(persons/ km)	(mg_{intake}/ $kg_{emitted\_rural}$)	(mg_{intake}/ $kg_{emitted\_urban}$)
W1	220	1.69E+13	52%	53,000	1.04	5.97
W2	375	3.26E+12	43%	109,000	1.92	10.12
W3	3	6.58E+12	88%	23,000	0.15	3.71
W4	22	1.54E+12	88%	42,000	0.2	6.51
W5	297	1.01E+13	35%	69,000	0.56	4.77
W6	796	2.42E+13	45%	72,000	0.84	6.52
W7	66	4.19E+12	88%	88,000	0.25	13.54
W8	241	1.08E+13	82%	92,000	0.41	13.42
W9	265	5.93E+12	73%	86,000	0.68	11.57
W10	339	1.45E+13	81%	53,000	0.45	7.46
W11	0	2.79E+13	0%	-	0	0
W12	18	1.83E+13	71%	19,000	0.17	2.56
W13	759	8.57E+12	71%	49,000	1.73	7.84
W14	207	1.96E+12	49%	105,000	1.21	9.98
IND	1,540	4.63E+12	29%	114,000	5.18	11.08
CHI	1,323	6.43E+12	43%	66,000	3.26	8.23
JAP	200	5.98E+11	69%	239,000	2.64	30.01
World[a]	6,671	1.66E+14	49%	82,000	2.49	11.13

[a] first two columns are sums; remaining columns are population-weighted averages based on urban fractions.

The model framework has been evaluated for a spatial version of Europe (Humbert et al., 2009), but few studies are available to compare with the continental

intake fractions presented here. Fig. A4.2 shows a comparison of the model's predicted intake fractions with published intake fractions for Europe, North America and China. The North American and China intake fractions match well, but the European intake fractions calculated here are substantially higher, which may be because the published data are taken from a study that did not explicitly account for urban intake.

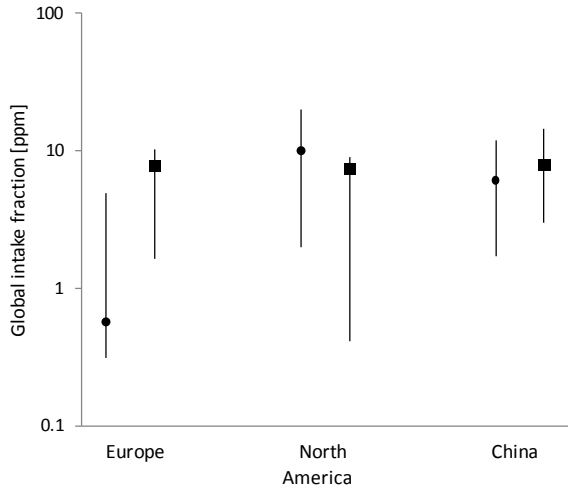

Fig. A4.2. Global intake fractions (in parts per million; mg inhaled for every kg emitted) for emissions in the regions along the x-axis. Circles represent published values for Europe (Tainio and et al., 2009; van Zelm and et al., 2008), North America (Humbert et al., 2009) and China (Zhou et al., 2006), and squares represent intake fractions estimated by the model presented here. Lines span the minimum and maximum published values and the continental and urban intake fractions for the model presented here.

A4.2.3 Regional values at several stages in the model, emissions factors and openess to trade

For each stage of the model described in Fig. 4.1, the regional quantities are shown in

Table A4.5. Two ratios, emissions intensities and openess to trade, are also included.

Table A4.5 Annual (2001) regional values at several stages in the model and emissions factors.

Regions	Regional consumption of final goods	Regional production	Average emissions intensities	Openness to trade: (Imports + Exports) / GDP	Regional emissions of $PM_{2.5}$	Regional population exposure by inhalation	Regional health damage experienced
	(mioUSD)	(mioUSD)	($kg_{emitted}$/ USD)	(-)	(kg_{emit})	(kg_{in})	(DALY)
Australia and New Zealand/ South Pacific	397,814	784,554	4.57E-04	38.1%	3.59E+08	1894	265,141
China	1,467,212	4,117,185	1.06E-03	45.1%	4.35E+09	34967	4,895,425
Rest of North West Pacific and East Asia	4,400,897	8,332,033	4.36E-05	19.9%	3.63E+08	11126	1,557,639
India	465,101	865,165	2.19E-03	21.4%	1.89E+09	17652	2,471,345
South-East Asia	550,014	1,338,820	7.53E-04	84.7%	1.01E+09	11161	1,562,564
Rest of South Asia	145,675	257,293	1.17E-03	32.0%	3.01E+08	7008	981,139
Rest of North America	647,953	1,244,080	3.55E-04	60.1%	4.42E+08	2372	332,010
USA	10,431,507	17,933,325	8.23E-05	18.6%	2.95E+09	22841	3,197,776
Meso-America	675,246	1,176,338	2.57E-04	41.2%	3.03E+08	3845	538,261
South America	1,066,864	1,903,826	4.82E-04	23.3%	9.17E+08	11776	1,648,658
Caribbean	152,506	253,860	3.62E-04	48.1%	9.18E+07	1019	142,648
Rest of Western Europe	6,196,628	11,732,302	4.82E-05	31.4%	5.66E+08	4199	587,876
Germany	1,642,581	3,498,763	2.88E-05	54.6%	1.01E+08	1152	161,323
Central Europe	601,536	1,397,372	1.81E-04	67.5%	2.52E+08	2794	391,217
Eastern Europe/Central Asia	364,122	1,414,981	4.86E-04	49.8%	6.88E+08	3548	496,675
Arabian Peninsula/ Mashriq/Israel	611,968	1,013,740	2.01E-04	58.7%	2.04E+08	884	123,700
Northern Africa	230,100	459,703	9.29E-04	46.7%	4.27E+08	1475	206,499
Southern Africa	131,898	303,023	1.51E-03	48.2%	4.57E+08	1437	201,203
Western/ Eastern/ Central Africa/ Western Indian Ocean	173,749	313,032	8.81E-04	64.3%	2.76E+08	4298	601,724

A4.2.4 Impact intensities

Fig. A4.3 displays several impact intensities by emissions, production dollars and consumption dollars. The impacts induced worldwide per kilogram emitted [DALY/$kg_{emitted}$] in each region (Fig. A4.3a) mostly depend on the urban population densities in the region of emission. The impacts induced worldwide per dollar of regional production [DALY/$USD_{production}$] in each region (Fig. A4.3b) represent global impacts due to local emissions from local production; this is in contrast to the values in the map in Fig. 4.4 which represent global impacts due to emissions from local production as well as from the supply chain needed for that local production (making it is a more comprehensive measure of the impacts of production within a given region). Fig. A4.3c shows the impacts induced worldwide per dollar of consumption [DALY/USD of consumption]. Multiplying these figures with the total consumption of each region provides the sum of impacts induced by the consumption of each region as provided in Fig. A4.3b.

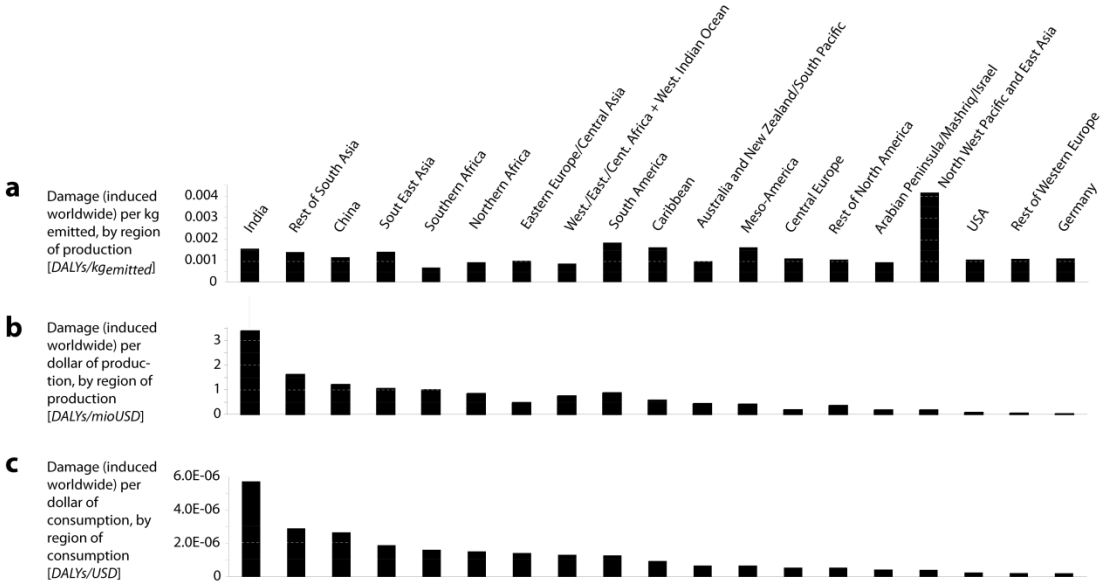

Fig. A4.3 Damage factors per kilogram emitted, per dollar of production and per dollar of consumption in each region.

A4.2.5 Evaluating the environmentally extended multi-regional Input-Output model.

We calculated how sensitive key results are to uncertain input parameters. Taking the input emissions intensities (kg $PM_{2.5}$ emitted per dollar of production) for China,

USA and Germany, we multiplied and divided each by two to examine subsequent changes in impacts (Fig. A4.4). We focused on changes in the total global impacts, the share of impacts in Asia (China, South Asia and South-East Asia) induced by global consumption, and the share of impacts in Asia induced by German consumption. As expected, we found that these indicators are most sensitive to changes in Chinese emissions intensities, followed by changes in US emissions intensities. However, our model results are still relatively robust, since doubling or halving Chinese emissions intensities, leads to less than 30% change in the results presented here.

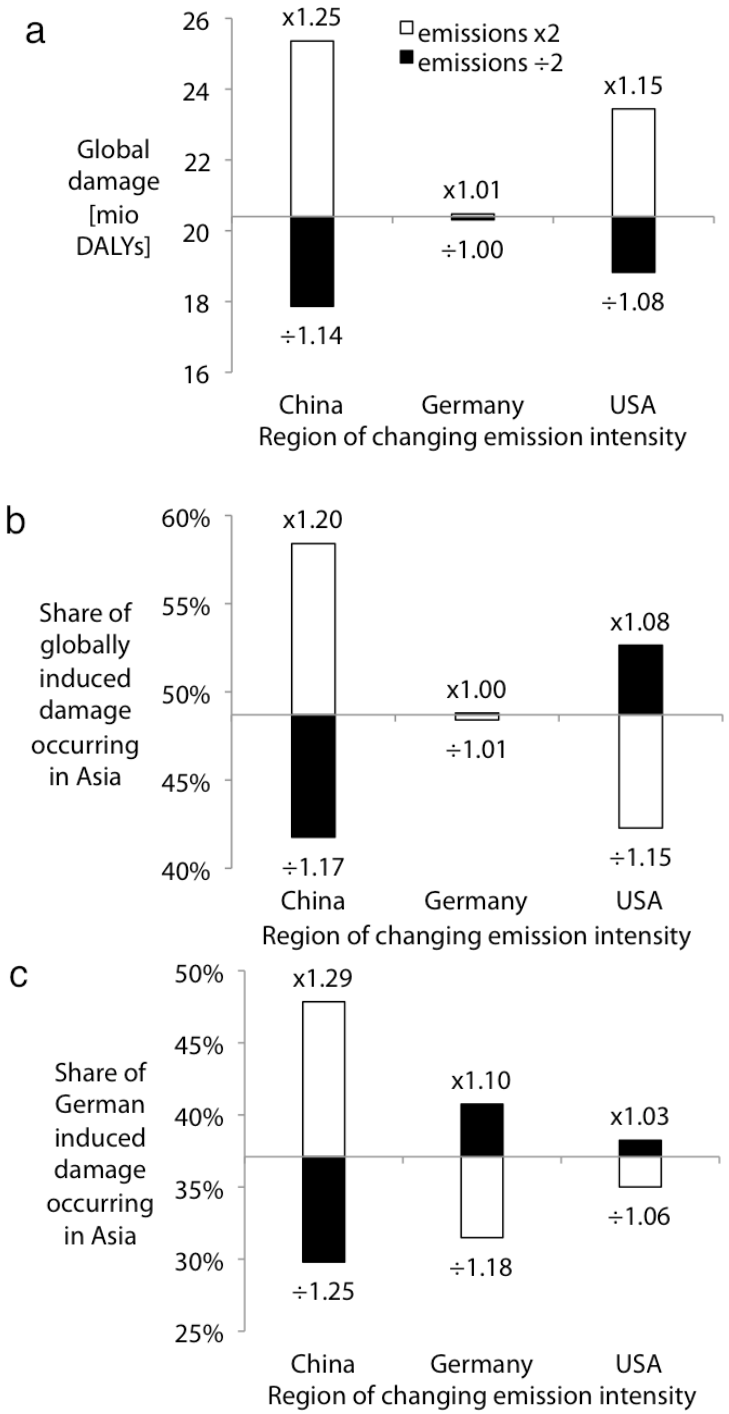

Fig. A4.4. Sensitivity studies of various output parameters in the impact model to key input parameters in the multi-regional Input-Output model. Output parameters examined are (a) change in global human health impacts (due to change in $PM_{2.5}$ emissions to meet global final demand), (b) change in share of global induced impacts occurring in Asia (China, South Asia, and South-East Asia), and (c) change in share of German-induced impacts occurring in Asia. Bars represent changes due to multiplying by two (white bars) or dividing by two (black bars) the emissions per dollar for the region on the x-axis. Factors above positive bars and below negative bars represent, respectively, the factors increase and decrease of the default model value.

A4.2.6 Evaluating pollutant transport and impact assessment

A sensitivity study was conducted on the dependencies of the pollutant transport and intake model by examining the effects of changing key input parameters (Fig. A4.5). As would be expected from the dominance of urban intake on total global intake, we find that the total global health impact strongly depends on urban parameters, but has little dependence on trans-boundary winds and particulate deposition rates. If we assume an average intake fraction in each region based on the average regional population density (as is typically done in global models), rather than separately calculate and then combine the urban and rural intake fractions (as done here), the total global impacts are underestimated by a factor 4 and the Asian shares of impacts are overestimated (bar marked 'urban correction'). The total global health impacts also depend on the assumed urban dilution rate, which is a product of the wind speed and mixing height in urban areas. Here, we use the average urban dilution rate from 75 U.S. urban areas[16], and apply this to all regions due to lack of urban dilution rate data in the rest of the world. Our sensitivity study shows that increasing and decreasing the 'urban dilution rate' by a factor 2 causes an increase and decrease in total impacts of 1.67 and 1.58, respectively, but does not substantially change the Asian share of impacts. Finally we double and halve the 'transboundary dilution' and 'deposition' rates by changing the inter-regional wind speeds and particulate deposition rates, finding that neither has a large effect.

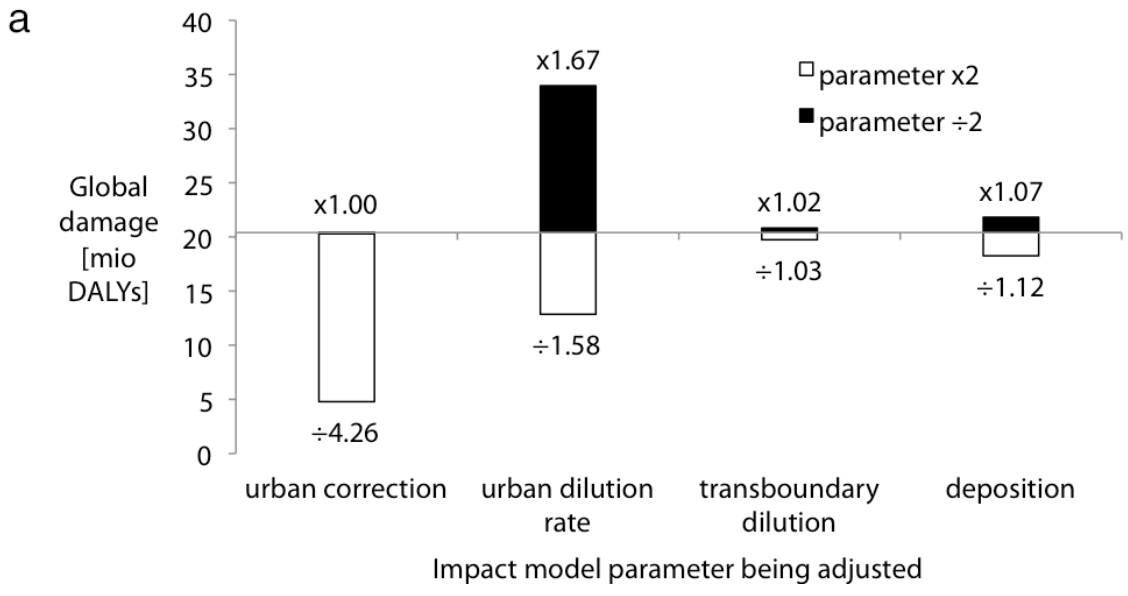

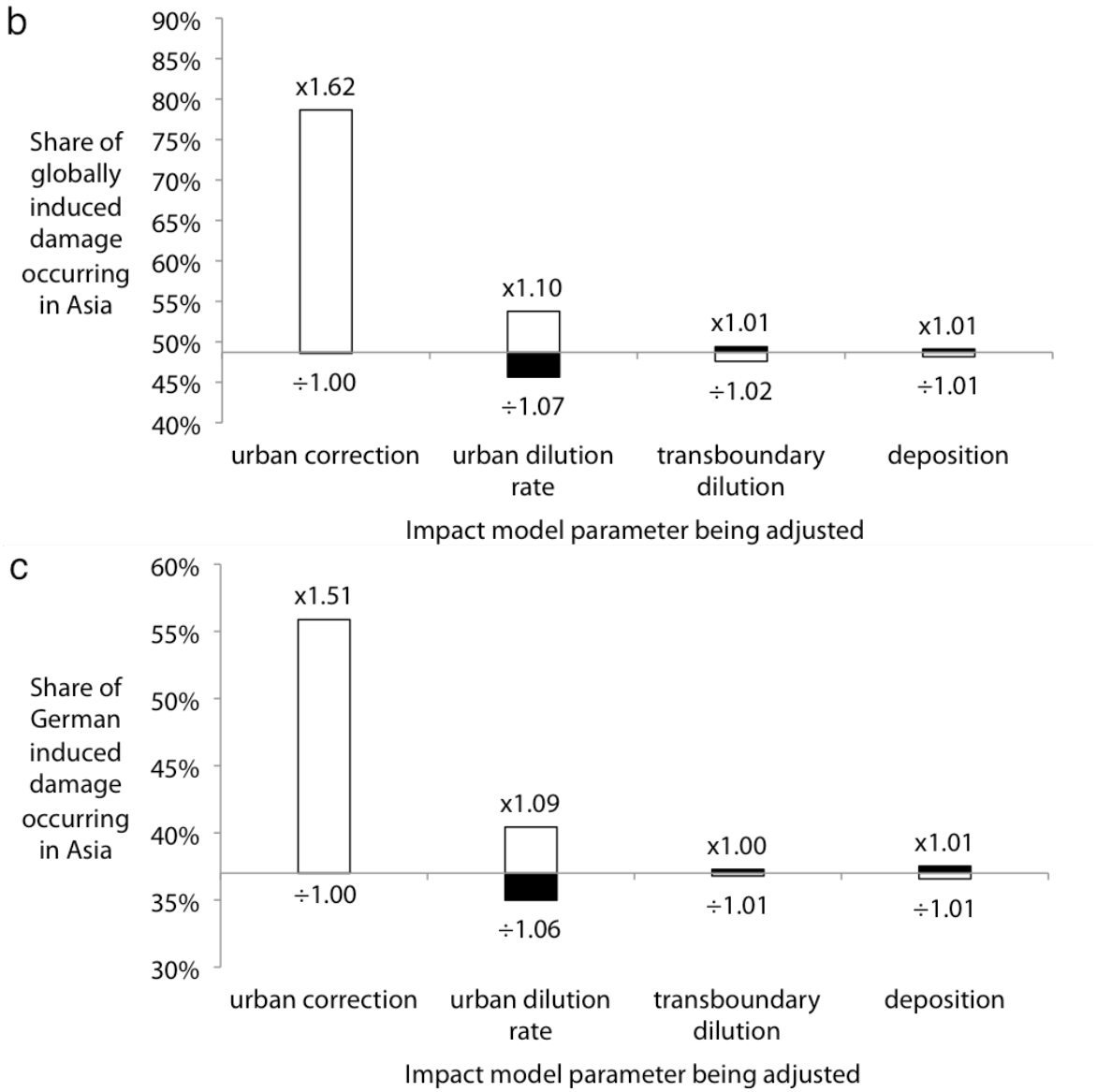

Fig. A4.5. Sensitivity studies of various output parameters in the pollutant transport model to key input parameters. Output parameters examined are (a) change in global human health impacts (due to $PM_{2.5}$ emissions to meet global final demand), (b) change in share of global impacts in Asia (China, South Asia, and South-East Asia), and (c) change in share of German-induced impacts in Asia. Input parameters listed along the x-axis have been adjusted as follows: 'Urban correction' bars show the change in the output parameter if no urban correction is included in the model, and the other bars represent changes due to halving (black bars) or doubling (white bars) the input parameter on the x-axis. Factors above and below bars represent, respectively, the factors increase and decrease in the original global human health impact.

The sensitivity study confirms what has been suggested by a previous study (Humbert et al., 2009) that the explicit inclusion of urban areas is important when the gridsize is larger than around 100 km. In such a case, it is likely that accounting for the

urban archetype is more important than increasing resolution. The sensitivity study also shows that transboundary transport does not greatly influence the final global impacts or share of impacts.

REFERENCES

Anex, R.P., Focht, W., 2002. Public participation in life cycle assessment and risk assessment: A shared need. Risk Analysis 22, 861-877.

Angel, S., Sheppard, S., Civco, D., 2005. The dynamics of global urban expansion. Transport and Urban Development Department, The World Bank, Washington, D.C.

Bare, J.C., 2006. Risk assessment and Life-Cycle Impact Assessment (LCIA) for human health cancerous and noncancerous emissions: Integrated and complementary with consistency within the USEPA. Human and Ecological Risk Assessment 12, 493-509.

Bare, J.C., Norris, G.A., Pennington, D.W., McKone, T., TRACI, The tool for the Reduction and Assessment of Chemical and other Environmental Impacts. Journal of Industrial Ecology 6, 49-78.

Bascom, R., Bromberg, P.A., Hill, C., Costa, D.L., Devlin, R., Dockery, D.W., Frampton, M.W., Lambert, W., Samet, J.M., Speizer, F.E., Utell, M., 1996. Health effects of outdoor air pollution. American Journal of Respiratory and Critical Care Medicine 153, 477-498.

Benarie, M.M., 1980. URBAN AIR POLLUTION MODELING. Benarie, M. M. Urban Air Pollution Modelling. Xv+405p. the Mit Press: Cambridge, Mass., USA. Illus, XV+405P.

Bennett, D.H., Margni, M.D., McKone, T.E., Jolliet, O., 2002a. Intake fraction for multimedia pollutants: A tool for life cycle analysis and comparative risk assessment. Risk Analysis 22, 905-918.

Bennett, D.H., McKone, T.E., Evans, J.S., Nazaroff, W.W., Margni, M.D., Jolliet, O., et al., 2002b. Defining intake fraction. Environmental Science & Technology 36, 207A-211A.

Bey, I., et al., 2001. Global modeling of tropospheric chemistry with assimilated meteorology: Model description and evaluation. Journal of Geophysical Research-Atmospheres 106, 23073-23095.

Bey, I., Jacob, D.J., Yantosca, R.M., Logan, J.A., Field, B.D., Fiore, A.M., Li, Q.B., Liu, H.G.Y., Mickley, L.J., Schultz, M.G., 2001. Global modeling of tropospheric chemistry with assimilated meteorology: Model description and evaluation. Journal of Geophysical Research-Atmospheres 106, 23073-23095.

Bolisani, E., Scarso, E., 1996. International manufacturing strategies: Experiences from the clothing industry. International Journal of Operations & Production Management 16, 71-&.

Borga, K., Di Guardo, A., 2005. Comparing in measured and predicted PCB concentrations Arctic seawater and marine biota. Science of the Total Environment 342, 281-300.

Boyle, P., Levin, B., International Agency for Research on Cancer., 2008. World cancer report. IARC Press, Lyon 511 p. pp.

Brand, G., Braunschweig, A., Scheidegger, A., Schwank, O., 1998. Weighting in ecobalances with the ecoscarcity method - ecofactors 1997, BUWAL (SAFEL) Environment Series No. 297, Bern.

Breivik, K., Czub, G., McLachlan, M.S., Wania, F., 2010. Towards an understanding of the link between environmental emissions and human body burdens of PCBs using CoZMoMAN. Environment International 36, 85-91.

Breivik, K., Sweetman, A., Pacyna, J.M., Jones, K.C., 2007. Towards a global historical emission inventory for selected PCB congeners - A mass balance approach-3. An update. Science of the Total Environment 377, 296-307.

Brunner, P., Rechberger, H., 2004. Practical handbook of material flow analysis. Lewis.

Buzby, 2003. International Trade and Food Safety. United States Department of Agriculture Economic Research Service, Agricultural Economic Report No. AER828.

CGRER, 2006. Emission inventory for the INTEX-B project. Center for Global and Regional Environmental Research, University of Iowa.

Chaudhary, M., Chaudhary, G., 2009. Global encyclopaedia of political geography. Global Vision Pub. House.

Collins, W.D., Bitz, C.M., Blackmon, M.L., Bonan, G.B., Bretherton, C.S., Carton, J.A., Chang, P., Doney, S.C., Hack, J.J., Henderson, T.B., Kiehl, J.T., Large, W.G., McKenna, D.S., Santer, B.D., Smith, R.D., 2006. The Community Climate System Model version 3 (CCSM3). Journal of Climate 19, 2122-2143.

Cowell, S.J., Fairman, R., Lofstedt, R.E., 2002. Use of risk assessment and life cycle assessment in decision making: A common policy research agenda. Risk Analysis 22, 879-894.

Crettaz, P., Pennington, D., Rhomberg, L., Brand, K., Jolliet, O., 2002. Assessing human health response in life cycle assessment using ED(10)s and DALYs: Part 1 - Cancer effects. Risk Analysis 22, 931-946.

De Schryver, A.M., Brakkee, K.W., Goedkoop, M.J., Huijbregts, M.A.J., 2009. Characterization Factors for Global Warming in Life Cycle Assessment Based on Damages to Humans and Ecosystems. Environmental Science & Technology 43, 1689-1695.

Dentener, F., 2008. GAINS-Asia Deliverable D03. A sectoral and spatially resolved set of emission data based on GAINS and EDGAR. Laxenburg, Austria.

Dimaranan, B.V., 2006. Global Trade, Assistance, and Production: The GTAP 6 Data Base. Center for Global Trade Analysis. Purdue University, West Lafayette, IN.

Domingo, J.L., Bocio, A., 2007. Levels of PCDD/PCDFs and PCBs in edible marine species and human intake: A literature review. Environment International 33, 397-405.

EEA, 2009. European Community emission inventory report 1990-2007 under the UNECE Convention on Long-range Transboundary Air Pollution (LRTAP).

Emmons, L.K., Walters, S., Hess, P.G., Lamarque, J.-F., Pfister, G.G.F., D. Granier, C. Guenther, A. Kinnison, D. Laepple, T. Orlando, J. Tie, X. Tyndall, G. Wiedinmyer, C. Baughcum, S. L. Kloster, S., 2010. Description and evaluation of the Model for Ozone and Related chemical Tracers, version 4 (MOZART-4). Geosci. Model Dev. 3, 43-67.

EPA, U., 2010. Estimation Programs Interface Suite™ for Microsoft® Windows, v 4.00. United States Environmental Protection Agency, Washington, DC.

Eurostat, 2001. Nameas for air emissions, Results of pilot studies.

Eurostat, 2003. NAMEA for Air Emissions Compilation Guide. Final Draft version.

FAO, 2000. Food Balance Sheets. Food and Agriculture Organization.

FAO, 2002. FAO Fishery Information, Data and Statistics Unit: Commodities 2000, Rome.

Fjeld, R., Eisenberg, N., Compton, K., 2007. Quantitative environmental risk analysis for human health. Wiley-Interscience.

Fox-Rabinovitz, M., Cote, J., Dugas, B., Deque, M., McGregor, J.L., 2006. Variable resolution general circulation models: Stretched-grid model intercomparison project (SGMIP). Journal of Geophysical Research-Atmospheres 111.

Franklin, M., Koutrakis, P., Schwartz, J., 2008. The role of particle composition on the association between PM2.5 and mortality. Epidemiology 19, 680-689.

Friot, D., 2010a. Centre énergétique et procédés, MINES ParisTech, Sophia Antipolis Cedex.

Friot, D., 2010b. PhD Thesis. Centre énergétique et procédés, MINES ParisTech, Sophia Antipolis Cedex.

Friot, D., Antille, G., 2009. Carbon tariffs & sharing scheme of de-carbonisation costs: analytical tools based on Multi-Regional Input-Output models. Ecological Economics, Submitted for publication.

GEOS, 2005. GEOS-4 2x2.5 met data, in: Yantosca, B. (Ed.). Goddard Earth Observing System, ftp://ftp.as.harvard.edu/pub/geos-chem/data/GEOS_2x2.5/GEOS_4_v4/2005/.

Gioia, R., Jones, K.C., Lohmann, R., Nizzetto, L., Dachs, J., 2010. Field-derived Henry's law constants for polychlorinated biphenyls in oceanic waters. J. Geophys. Res. 115, C05024.

Gioia, R., Lohmann, R., Dachs, J., Temme, C., Lakaschus, S., Schulz-Bull, D., Hand, I., Jones, K.C., 2008a. Polychlorinated biphenyls in air and water of the North Atlantic and Arctic Ocean. Journal of Geophysical Research-Atmospheres 113.

Gioia, R., Nizzetto, L., Lohmann, R., Dachs, J., Temme, C., Jones, K.C., 2008b. Polychlorinated Biphenyls (PCBs) in air and seawater of the Atlantic Ocean: Sources, trends and processes. Environmental Science & Technology 42, 1416-1422.

Guinee, J.B., Gorree, M., Heijungs, R., Huppes, G., Kleijn, R., de Koning, A., van Oers, L., Wegener Sleeswijk, A., Suh, S., Udo de Haes, H.A., de Bruijn, J.A., van Duin, R., Huijbregts, M.A.J., 2002. Handbook on Life Cycle Assessment: Operational Guide to the ISO Standards. Kluwer Academic Publishers, Dordrecht.

Hammami, R., Frein, Y., Hadj-Alouane, A.B., 2008. Supply chain design in the delocalization context: Relevant features and new modeling tendencies. International Journal of Production Economics 113, 641-656.

Hauck, M., Huijbregts, M.A.J., Hollander, A., Hendriks, A.J., van de Meent, D., in press. Modeled and monitored variation in space and time of PCB-153 concentrations in air, sediment, soil and aquatic biota on a European scale. Science of The Total Environment In Press, Corrected Proof.

Hauschild, M. 2010. Recommended methods for LCIA. European comission Joint Research Centre, Institute for environment and sustainability. http://lct.jrc.ec.europa.eu/pdf-directory/Recommendation%20of%20methods%20for%20LCIA%20Draft%20for%20consultation-15-10-2010.pdf

Hayward, D., Wong, J., Krynitsky, A.J., 2007. Polybrominated diphenyl ethers and polychlorinated biphenyls in commercially wild caught and farm-raised fish fillets in the United States. Environmental Research 103, 46-54.

Hellweg, S., Demou, E., et al., 2009. Integrating Human Indoor Air Pollutant Exposure within Life Cycle Impact Assessment. Environmental Science & Technology 43, 1670-1679.

Hendrickson, C.T., Lave, L.B., Matthews, H.S., 2005. Environmental Life Cycle Assessment of Goods and Services: An Input-Output Approach. Resources for the Future Press, Washington, D.C.

Hertwich, E.G., Peters, G.P., 2009. Carbon Footprint of Nations: A Global, Trade-Linked Analysis. Environmental Science & Technology 43, 6414-6420.

Hofstetter, P., 1998. Perspectives in Life Cycle ImpactAssessment. Kluwer Academic Publishers, Norwell, MA.

Hofstetter, P., Hammitt, J.K., 2002. Selecting human health metrics for environmental decision-support tools. Risk Analysis 22, 965-983.

Hong, J.L., Shaked, S., Rosenbaum, R.K., Jolliet, O., 2010. Analytical uncertainty propagation in life cycle inventory and impact assessment: application to an automobile front panel. International Journal of Life Cycle Assessment 15, 499-510.

Huijbregts, M.A.J., Lundi, S., McKone, T.E., van de Meent, D., 2003. Geographical scenario uncertainty in generic fate and exposure factors of toxic pollutants for life-cycle impact assessment. Chemosphere 51, 501-508.

Huijbregts, M.A.J., Thissen, U., Guinee, J.B., Jager, T., Kalf, D., van de Meent, D., Ragas, A.M.J., Sleeswijk, A.W., Reijnders, L., 2000. Priority assessment of toxic substances in life cycle assessment. Part I: Calculation of toxicity potentials for 181 substances with the nested multi-media fate, exposure and effects model USES-LCA. Chemosphere 41, 541-573.

Humbert, S., Manneh, R., Shaked, S., Wannaz, C., Horvath, A., Deschenes, L., Jolliet, O., Margni, M., 2009. Assessing regional intake fractions in North America. Science of the Total Environment 407, 4812-4820.

Humbert, S., Marshall, J.D., Shaked, Shanna, Spadaro, Joseph, Nishioka, Y., Preiss, P., McKone, T.E., Horvath, A., Jolliet, O., in review. **Intake fractions and characterization factors for particulate matter: review and recommendations for life cycle assessment**. Environmental Science and Technology (in review).

IEA, 2006. CO2 emissions from fuel combustion, 1971-2004.

Instituto Nacional de Ecologia, 2006. Inventario nacional de emisiones de méxico, 1999.

ISO, 2006. ISO 14040, Environmental management -- Life cycle assessment -- Principles and framework. International Organization for Standardization, Geneva.

Jolliet, O., Margni, M., Charles, R., Humbert, S., Payet, J., Rebitzer, G., Rosenbaum, R., 2003. IMPACT 2002+: A new life cycle impact assessment methodology. International Journal of Life Cycle Assessment 8, 324-330.

Jolliet, O., Soucy, G., Dettling, J., Humbert, S., Manneh, R., Deschenes, L., Margni, M., 2008. Use of Intake Fractions and Blood Half-Lives in Combination with Toxic Equivalency Factors (TEFs) to Evaluate Multi-Compound Emissions and Blood Concentrations. Epidemiology 19, S371-S371.

Juraske, R., Anton, A., Castells, F., 2008. Estimating half-lives of pesticides in/on vegetation for use in multimedia fate and exposure models. Chemosphere 70, 1748-1755.

Kalantzi, O.I., Alcock, R.E., Johnston, P.A., Santillo, D., Stringer, R.L., Thomas, G.O., Jones, K.C., 2001. The global distribution of PCBs and organochlorine pesticides in butter. Environmental Science & Technology 35, 1013-1018.

Kazerouni, N., Sinha, R., Hsu, C.H., Greenberg, A., Rothman, N., 2001. Analysis of 200 food items for benzo a pyrene and estimation of its intake in an epidemiologic study. Food and Chemical Toxicology 39, 423-436.

Klein, H., 2007. Transboundary air pollution by main pollutants (S, N, O3) and PM: Germany.

Klimont, Z., Modelling Particulate Emissions in Europe. A Framework to Estimate Reduction Potential and Control Costs. Interim Report IR-02-076. Laxenburg, Austria.

Lammel, G., Klopffer, W., Semeena, V.S., Schmidt, E., Leip, A., 2007. Multicompartmental fate of persistent substances - Comparison of predictions from multi-media box models and a multicompartment chemistry-atmospheric transport model. Environmental Science and Pollution Research 14, 153-165.

Lenzen, M., Pade, L.-L., Munksgaard, J., 2004. CO2 multipliers in Multi-region Input-Output Models. Economic Systems Research 16, 391-412.

Leontief, W., 1936. Quantitative input and output relations in the economic system of the United States. Review of economic statistics 18, 105-125.

Levy, J.I., Wilson, A.M., Evans, J.S., Spengler, J.D., 2003. Estimation of primary and secondary particulate matter intake fractions for power plants in Georgia. Environmental Science & Technology 37, 5528-5536.

Li, N.Q., Wania, F., Lei, Y.D., Daly, G.L., 2003. A comprehensive and critical compilation, evaluation, and selection of physical-chemical property data for selected polychlorinated biphenyls. Journal of Physical and Chemical Reference Data 32, 1545-1590.

Liang, Q., Jaegle, L., Hudman, R.C., Turquety, S., Jacob, D.J., Avery, M.A., Browell, E.V., Sachse, G.W., Blake, D.R., Brune, W., Ren, X., Cohen, R.C., Dibb, J.E., Fried, A., Fuelberg, H., Porter, M., Heikes, B.G., Huey, G., Singh, H.B., Wennberg, P.O., 2007. Summertime influence of Asian pollution in the free troposphere over North America. Journal of Geophysical Research-Atmospheres 112.

Liem, A.K.D., Furst, P., Rappe, C., 2000. Exposure of populations to dioxins and related compounds. Food Additives and Contaminants 17, 241-259.

Liu, J.F., Mauzerall, D.L., Horowitz, L.W., 2009a. Evaluating inter-continental transport of fine aerosols:(2) Global health impact. Atmospheric Environment 43, 4339-4347.

Liu, J.F., Mauzerall, D.L., Horowitz, L.W., Ginoux, P., Fiore, A.M., 2009b. Evaluating inter-continental transport of fine aerosols: (1) Methodology, global aerosol distribution and optical depth. Atmospheric Environment 43, 4327-4338.

Loutfy, N., Fuerhacker, M., Tundo, P., Raccanelli, S., Ahmed, M.T., 2007. Monitoring of polychlorinated dibenzo-p-dioxins and dibenzofurans, dioxin-like PCBs and polycyclic aromatic hydrocarbons in food and feed samples from Ismailia city, Egypt. Chemosphere 66, 1962-1970.

Mackay, D., 2006. Handbook of physical-chemical properties and environmental fate for organic chemicals, 2nd ed. Taylor & Francis, Boca Raton, FL.

Macleod, M., Riley, W.J., McKone, T.E., 2005. Assessing the influence of climate variability on atmospheric concentrations of polychlorinated biphenyls using a global-scale mass balance model (BETR-global). Environmental Science & Technology 39, 6749-6756.

Maddalena, R.L., McKone, T.E., Layton, D.W., Hsieh, D.P.H., 1995. COMPARISON OF MULTIMEDIA TRANSPORT AND TRANSFORMATION MODELS - REGIONAL FUGACITY MODEL VS CALTOX. Chemosphere 30, 869-889.

Manneh, R., Margni, M., Deschenes, L., 2010. Spatial Variability of Intake Fractions for Canadian Emission Scenarios: A Comparison between Three Resolution Scales. Environmental Science & Technology 44, 4217-4224.

Margni, M., 2003. Source to Intake Modeling in Life Cycle Impact Assessment. Swiss Federal Institute of Technology (EPFL), Lausanne.

Margni, M., Pennington, D.W., Amman, C., Jolliet, O., 2004. Evaluating multimedia/multipathway model intake fraction estimates using POP emission and monitoring data. Environmental Pollution 128, 263-277.

Marshall, J.D., 2007. Urban land area and population growth: A new scaling relationship for metropolitan expansion. Urban Studies 44, 1889-1904.

Marshall, J.D., Teoh, S.K., Nazaroff, W.W., 2005. Intake fraction of nonreactive vehicle emissions in US urban areas. Atmospheric Environment 39, 1363-1371.

Matthews, H.S., Lave, L., MacLean, H., 2002. Life cycle impact assessment: A challenge for risk analysts. Risk Analysis 22, 853-860.

Mattison, D.R., 2010. Environmental exposures and development. Current Opinion in Pediatrics 22, 208-218.

Meijer, S.N., Ockenden, W.A., Sweetman, A., Breivik, K., Grimalt, J.O., Jones, K.C., 2003. Global distribution and budget of PCBs and HCB in background surface soils: Implications or sources and environmental processes. Environmental Science & Technology 37, 667-672.

Miller, R.E., Blair, P.D., 1985. Input-Output analysis : foundations and extensions. Prentice-Hall, New Jersey.

NCEA, 1997. Exposure Factors Handbook. Washington, DC.

Norris, G.A., 2002. Life cycle emission distributions within the economy: Implications for life cycle impact assessment. Risk Analysis 22, 919-930.

NRC, 1994. Science and judgment in risk assessment. National Academy Press.

Ostro, B., 2004. Outdoor air pollution: Assessing the environmental burden of disease at national and local levels., Geneva.

Paasivirta, J., Sinkkonen, S.I., 2009. Environmentally Relevant Properties of All 209 Polychlorinated Biphenyl Congeners for Modeling Their Fate in Different Natural and Climatic Conditions. Journal of Chemical and Engineering Data 54, 1189-1213.

Palpacuer, F., Gibbon, P., Thomsen, L., 2005. New challenges for developing country suppliers in global clothing chains: A comparative European perspective. World Development 33, 409-430.

Pennington, D., Crettaz, P., Tauxe, A., Rhomberg, L., Brand, K., Jolliet, O., 2002. Assessing human health response in life cycle assessment using ED(10)s and DALYs: Part 2 - Noncancer effects. Risk Analysis 22, 947-963.

Pennington, D.W., Margni, M., Ammann, C., Jolliet, O., 2005. Multimedia fate and human intake modeling: Spatial versus nonspatial insights for chemical emissions in Western Europe. Environmental Science & Technology 39, 1119-1128.

Pennington, D.W., Margni, M., Payet, J., Jolliet, O., 2006. Risk and regulatory hazard-based toxicological effect indicators in life-cycle assessment (LCA). Human and Ecological Risk Assessment 12, 450-475.

Pennington, D.W., Potting, J., Finnveden, G., Lindeijer, E., Jolliet, O., Rydberg, T., Rebitzer, G., 2004. Life cycle assessment Part 2: Current impact assessment practice. Environment International 30, 721-739.

Perugini, M., Cavaliere, M., Giammarino, A., Mazzone, P., Olivieri, V., Amorena, M., 2004. Levels of polychlorinated biphenyls and organochlorine pesticides in some edible marine organisms from the Central Adriatic Sea. Chemosphere 57, 391-400.

Peters, G., Hertwich, E.G., 2007a. CO2 Embodied in International Trade with Implications for Global Climate Policy. Environmental Science & Technology 42, 1401-1407.

Peters, G., Hertwich, E.G., 2007b. The application of multi-regional input-output analysis to industrial ecology: evaluating trans-boundary environmental impacts, in: Suh, S. (ed.), Handbook of input-output analysis for industrial ecology. Springer, Dordrecht, The Netherlands.

Peters, G., Hertwich, E.G., 2008. Trading Kyoto, Nature Reports Climate Change.

Peters, G.P., Hertwich, E.G., 2006. The importance of imports for household environmental impacts. Journal of Industrial Ecology 10, 89-109.

Pope, C.A., Burnett, R.T., Thun, M.J., Calle, E.E., Krewski, D., Ito, K., Thurston, G.D., 2002. Lung cancer, cardiopulmonary mortality, and long-term exposure to fine particulate air pollution. Jama-Journal of the American Medical Association 287, 1132-1141.

Pruss-Ustun, A., 2006. Preventing disease through healthy environments. Towards an estimate of the environmental burden of disease., Geneva.

Rochat, D., Margni, M., Jolliet, O., 2006. Continent-specific characterization factors and intake fractions for toxic emissions: Does it make a difference? International Journal Of Life Cycle Assessment 11, 55-63.

Rosenbaum, R.K., Bachmann, T.M., Gold, L.S., Huijbregts, M.A.J., Jolliet, O., Juraske, R., Koehler, A., Larsen, H.F., MacLeod, M., Margni, M., McKone, T.E., Payet, J., Schuhmacher, M., van de Meent, D., Hauschild, M.Z., 2008. USEtox-the UNEP-SETAC toxicity model: recommended characterisation factors for human toxicity and freshwater ecotoxicity in life cycle impact assessment. International Journal of Life Cycle Assessment 13, 532-546.

Rosenbaum, R.K., Margni, M., Jolliet, O., 2007. A flexible matrix algebra framework for the multimedia multipathway modeling of emission to impacts. Environment International 33, 624-634.

Rosenbaum, R.K., McKone, T.E., Jolliet, O., 2009. CKow: A Dynamic Model for Chemical Transfer to Meat and Milk. Environmental Science & Technology 43, 8191-8198.

Ruchirawat, M., Autrup, H., Barregard, L., Brauer, M., Brunekreef, B., Duffus, J., Gordon, T., Htun, N., Mourato, S., Naeher, L., Navasumrit, P., Ostro, B., Settachan, D., St. Helen, G., Jin, Y., Zelikoff, J.T., 2008. Impacts of Atmospheric Brown Clouds on Human Health, Part III of Atmospheric Brown Clouds:

Regional Assessment Report with Focus on Asia. . Project Atmospheric Brown Cloud, United National Environmental Programme, Nairobi, Kenya.

Russell, A.J., 2006. Human and ecological risk assessment and life cycle assessment: Intersections, collisions, and future directions. Human and Ecological Risk Assessment 12, 427-430.

Schantz, S.L., Widholm, J.J., Rice, D.C., 2003. Effects of PCB exposure on neuropsychological function in children. Environmental Health Perspectives 111, 357-376.

Schmidt, G.A., Ruedy, R., Hansen, J.E., Aleinov, I., Bell, N., Bauer, M., Bauer, S., Cairns, B., Canuto, V., Cheng, Y., Del Genio, A., Faluvegi, G., Friend, A.D., Hall, T.M., Hu, Y.Y., Kelley, M., Kiang, N.Y., Koch, D., Lacis, A.A., Lerner, J., Lo, K.K., Miller, R.L., Nazarenko, L., Oinas, V., Perlwitz, J., Rind, D., Romanou, A., Russell, G.L., Sato, M., Shindell, D.T., Stone, P.H., Sun, S., Tausnev, N., Thresher, D., Yao, M.S., 2006. Present-day atmospheric simulations using GISS ModelE: Comparison to in situ, satellite, and reanalysis data. Journal of Climate 19, 153-192.

Schwartz, J., Coull, B., Laden, F., Ryan, L., 2008. The effect of dose and timing of dose on the association between airborne particles and survival. Environmental Health Perspectives 116, 64-69.

Schwartz, M.L., 2005. Encyclopedia of coastal science. Springer, Dordrecht.

Seinfeld, J.H., Pandis, S.N., Knovel (Firm), 2006. Atmospheric chemistry and physics

from air pollution to climate change, 2nd ed. J. Wiley, Hoboken, N.J.

Shaked, S., Jolliet, O., 2011. Global life cycle impacts of consumer products, in: Nriagu, J. (ed.), Encyclopedia of Environmental Health. Elsevier.

Sinha, R., Kulldorff, M., Gunter, M.J., Strickland, P., Rothman, N., 2005. Dietary benzo a pyrene intake and risk of colorectal adenoma. Cancer Epidemiology Biomarkers & Prevention 14, 2030-2034.

Sinkkonen, S., Paasivirta, J., 2000. Degradation half-life times of PCDDs, PCDFs and PCBs for environmental fate modeling. Chemosphere 40, 943-949.

Socolof, M.L., Geibig, J.R., 2006. Evaluating human and ecological impacts of a product life cycle: The complementary roles of life-cycle assessment and risk assessment. Human and Ecological Risk Assessment 12, 510-527.

Soucy, G., 2010. Developpement d'un indicateur d'evaluation des impacts potentiels sur la sante humaine: application aux emissions de HAP prioritaires dans la region des Grands Lacs et du St-Laurent, Chemical Engineering. Ecole Polytechnique de Montreal, Montreal.

Steinberger, J.K., Friot, D., Jolliet, O., Erkman, S., 2009. A spatially explicit life cycle inventory of the global textile chain. International Journal of Life Cycle Assessment 14, 443-455.

Stiglitz, J., 2006. Making globalization work. W.W. Norton & Co.

Stohl, A., Bonasoni, P., Cristofanelli, P., Collins, W., Feichter, J., Frank, A., Forster, C., Gerasopoulos, E., Gaggeler, H., James, P., Kentarchos, T., Kromp-Kolb, H., Kruger, B., Land, C., Meloen, J., Papayannis, A., Priller, A., Seibert, P., Sprenger, M., Roelofs, G.J., Scheel, H.E., Schnabel, C., Siegmund, P., Tobler, L., Trickl, T., Wernli, H., Wirth, V., Zanis, P., Zerefos, C., 2003. Stratosphere-troposphere exchange: A review, and what we have learned from STACCATO. Journal of Geophysical Research-Atmospheres 108, 15.

Streets, D.G., Bond, T.C., Carmichael, G.R., Fernandes, S.D., Fu, Q., He, D., Klimont, Z., Nelson, S.M., Tsai, N.Y., Wang, M.Q., Woo, J.H., Yarber, K.F., 2003. An inventory of gaseous and primary aerosol emissions in Asia in the year 2000. Journal of Geophysical Research-Atmospheres 108, 23.

Struijs, J., van Dijk, A., Slaper, H., van Wijnen, H.J., Velders, G.J.M., Chaplin, G., Huijbregts, M.A.J., 2010. Spatial- and Time-Explicit Human Damage Modeling of Ozone Depleting Substances in Life Cycle Impact Assessment. Environmental Science & Technology 44, 204-209.

Sweetman, A.J., Jones, K.C., 2000. Declining PCB concentrations in the UK atmosphere: Evidence and possible causes. Environmental Science & Technology 34, 863-869.

Tainio, M., et al., 2009. Evaluation of the European population intake fractions for European and Finnish anthropogenic primary fine particulate matter emissions. Atmospheric Environment 43, 3052-3059, doi:3010.1016/j.atmosenv.2009.3003.3030

Tainio, M., Sofiev, M., Hujo, M., Tuomisto, J.T., Loh, M., Jantunen, M.J., Karppinen, A., Kangas, L., Karvosenoja, N., Kupiainen, K., Porvari, P., Kukkonen, J., 2009. Evaluation of the European population intake fractions for European and Finnish anthropogenic primary fine particulate matter emissions. Atmospheric Environment 43, 3052-3059.

Tisdell, C., 2001. Globalisation and sustainability: environmental Kuznets curve and the WTO. Ecological Economics 39, 185-196.

Travis, C.C., Arms, A.D., 1988. BIOCONCENTRATION OF ORGANICS IN BEEF, MILK, AND VEGETATION. Environmental Science & Technology 22, 271-274.

Tukker, A., Poliakov, E., Heijungs, R., Hawkins, T., Neuwahl, F., Rueda-Cantuche, J.M., Giljum, S., Moll, S., Oosterhaven, J., Bouwmeester, M., 2009. Towards a global multi-regional environmentally extended input-output database. Ecological Economics 68, 1928-1937.

Udo de Haes, H., Sleeswijk, A.W., Heijungs, R., 2006. Similarities, differences and synergisms between HERA and LCA - An analysis at three levels. Human and Ecological Risk Assessment 12, 431-449.

UN, 1987. Report of the World Commission on Environment and Development.

UN, 2004. World Population to 2300. New York.

UN, 2008. Demographic Yearbook: Population of capital cities and cities of 100,000 or more inhabitants: latest available year, 1987-2006. New York.

UNEP, 2003. Regionally based assessment of persistent toxic substances. Chatelaine, Switzerland.

UN, Standard Country or Area Codes for Statistical Use, Revision 4, Sales No. 98.XVII.9.

Van den Berg, M., Birnbaum, L.S., Denison, M., De Vito, M., Farland, W., Feeley, M., Fiedler, H., Hakansson, H., Hanberg, A., Haws, L., Rose, M., Safe, S., Schrenk, D., Tohyama, C., Tritscher, A., Tuomisto, J., Tysklind, M., Walker, N., Peterson, R.E., 2006. The 2005 World Health Organization Reevaluation of Human and Mammalian Toxic Equivalency Factors for Dioxins and Dioxin-Like Compounds. Toxicological Sciences 93, 223-241.

van den Bergh, J., Verbruggen, H., 1999. Spatial sustainability, trade and indicators: an evaluation of the 'ecological footprint'. Ecological Economics 29, 61-72.

van Zelm, R., et al., 2008. European characterization factors for human health damage of PM10 and ozone in life cycle impact assessment. Atmospheric Environment 42, 441-453, doi:410.1016/j.atmosenv.2007.1009.1072.

van Zelm, R., Huijbregts, M.A.J., den Hollander, H.A., van Jaarsveld, H.A., Sauter, F.J., Struijs, J., van Wijnen, H.J., de Meent, D.V., 2008. European characterization factors for human health damage of PM10 and ozone in life cycle impact assessment. Atmospheric Environment 42, 441-453.

Wang, R.Y., Needham, L.L., 2007. Environmental chemicals: From the environment to food, to breast milk, to the infant. Journal of Toxicology and Environmental Health-Part B-Critical Reviews 10, 597-609.

Wania, F., Daly, G.L., 2002. Estimating the contribution of degradation in air and deposition to the deep sea to the global loss of PCBs. Atmospheric Environment 36, 5581-5593.

Wegener Sleeswijk, A., Heijungs, R., 2010. GLOBOX: A spatially differentiated global fate, intake and effect model for toxicity assessment in LCA. Science of The Total Environment 408, 2817-2832.

Authro, 2009. Code of Practice. ecoinvent report No. 2. St. Gallen.

Authro, 2008. The global burden of disease: 2004 update. Geneva, Switzerland.

Wiedmann, T., Lenzen, M., Turner, K., Barrett, J., 2007. Examining the global environmental impact of regional consumption activities -- Part 2: Review of input-output models for the assessment of environmental impacts embodied in trade. Ecological Economics 61, 15-26.

Wrisberg, N., Udo de Haes, H.A., 2002. Analytical tools for environmental design and management in a systems perspective: the combined use of analytical tools. Kluwer.

Zhang, Y.X., Tao, S., 2009. Global atmospheric emission inventory of polycyclic aromatic hydrocarbons (PAHs) for 2004. Atmospheric Environment 43, 812-819.

Zhao, X., Zheng, M., Liang, L., Zhang, Q., Wang, Y., Jiang, G., 2005. Assessment of PCBs and PCDD/Fs along the Chinese Bohai Sea coastline using mollusks as bioindicators. Archives of Environmental Contamination and Toxicology 49, 178-185.

Zhou, Y., Levy, J.I., Evans, J.S., Hammitt, J.K., 2006. The influence of geographic location on population exposure to emissions from power plants throughout China. Environment International 32, 365-373.